REPORT NO. CASD/LVP 78-078

CONTRACT NAS 3-20644

(NASA-CR-158760) ATLAS 5013 TANK CORROSION TEST Final Report (General Dynamics/Convair) 133 p HC A07/MF A01 CSCL 22B G3/18 N79-27234 Unclas 15341

ATLAS 5013 TANK CORROSION TEST

FINAL REPORT

GENERAL DYNAMICS

Convair Division

REPORT NO. CASD/LVP 78-078

ATLAS 5013 TANK CORROSION TEST

FINAL REPORT

December 1978

W. M. Sutherland
L. D. Girton
D. G. Treadway

Prepared Under
Contract NAS 3-20644
By
GENERAL DYNAMICS CONVAIR DIVISION
P.O. Box 80847
San Diego, California 92138

FOREWORD

This report presents the results of corrosion testing accomplished per Unified Test Plan No. GDC/BNZ69-007 Section 3.21.4, Ref. 2 and authorized by Sales Order TD 094-105, Ref. 1.

Specific conclusions and recommendations are provided relative to the corrosion of the Atlas 5013 tank and corrosion control for future Atlas and Centaur vehicles.

TABLE OF CONTENTS

TABLE OF CONTENTS, Contd

TABLE OF CONTENTS, Contd

LIST OF FIGURES

LIST OF FIGURES, Contd

LIST OF FIGURES, Contd

LIST OF FIGURES, Contd

LIST OF TABLES

PRECEDING PAGE BLANK NOT FILMED

PRECEDING PAGE BLANK NOT FILMED

SUMMARY

Corrosion was discovered on Atlas tank No. 5013 after it had been erected on Complex 36A at the Eastern Test Range (ETR) for 413 days. The corrosion resulted in approximately 40 small leaks in the fuel tank. As a result it was decided to use a substitute tank and submit the 5013 tank to failure analysis.

This report covers the results of tests outlined in Test Plan GDC-BNZ69-007, which was approved by General Dynamics Convair Division (GDC) and NASA-Lewis Research Center (LeRC). The major objectives of the program were:

a. Characterize the type of corrosion by x-ray and metallurgical analysis.

b. Determine the cause of the corrosion by chemical analysis.

c. Determine the degree of degradation of mechanical properties of the joints by static and fatigue tests.

d. Determine the corrosion inhibiting effectiveness of WD-40 compound and required renewal period by exposing typical joint specimens at ETR and San Diego.

It has been shown by metallurgical analysis that the corrosion is pitting and stress corrosion typically found at unprotected spotwelds in a sea-coast environment. Considerable progress was made relating x-ray defect images to metallurgical sections.

The primary corrodent was sodium chloride.

The static mechanical properties of samples taken from the 5013 tank were reduced an average of 9% and were still well within engineering requirements. The fatigue values increased 10% and were well above engineering requirements.

The corrosion tests at Point Loma, San Diego show conclusively the effectiveness of WD-40 in preventing corrosion in spotwelded joints in the sea-coast environment. The test specimens, protected or unprotected, which were exposed at ETR in the tower at Complex 36A did not corrode within the same time as the 5013 tank. This suggests that weather or other unknown factors were different during the year of the 5013 exposure. Since the ETR specimens did not corrode appreciably, no evaluation of required WD-40 renewal times could be made. The Pt. Loma data indicates that 30-day renewal is effective. After a year of 30-day renewals increasing the renewal period to 90 days resulted in no corrosion.

SECTION 1

INTRODUCTION

On 23 October 1974, a post fuel tanking inspection of the Atlas 5013 (AC-33) tank disclosed approximately 40 areas of RP-1 leakage in the fuel tank. At the time the leaks were thought to be caused by corrosion pits and stress corrosion cracks in the aft faying surface of the cylindrical skin overlap joint. The aft faying surface was open to the external environment. A subsequent investigation into the vehicle 5013 fuel tank leakage problem resulted in a recommendation to conduct a test program to obtain corrosion data from the 5013 vehicle fuel tank and to conduct a long-term test program (Reference 2). Authority to perform this activity and conduct the test is contained in TD 094-105. Table 1-1 shows a history of events.

This report documents the results, conclusions, and recommendations of the corrosion test program outlined in Test Plan GDC-BNZ69-007, (Reference 2). For reader convenience, a verbatim copy of the test objectives as they were stated in Reference 2 is given below:

"The test program is to be performed in two phases - Phase 1 will be the evaluaation of the 5013 vehicle fuel tank skin splice joints, and Phase 2 the evaluation of long term environmental exposure at ETR.

PHASE I - EVALUATION OF THE 5013 FUEL TANK SKIN SPLICE JOINTS

A. SUMMARY

Following the return of the 5013 vehicle to San Diego and removal of equipment, the fuel tank will, first, be radiographed for test specimen correlation. The tank will then be sectioned to provide corroded samples for metallographic examinations and chemical analyses. Additional tank sections will be provided from corroded areas for preparation of tensile test specimens (dog-bones) for evaluation of static and fatigue properties and of long term environmental exposure tests both with and without WD-40 protective treatments.

B. TEST OBJECTIVES

1. To provide radiographic, metallographic, and chemical analysis data of tank corrosion processes.
2. To evaluate the persistence of WD-40 in faying surfaces.
3. To evaluate static and fatigue properties of corroded weld joints.

Table 1-1. History of Events

1973	Sept	ATLAS 5013 ERECTED AT COMPLEX 36A ETR
1974	Oct	FUEL TANK LEAKAGE DISCOVERED
	Nov	PRELIMINARY REPORT AND PRESENTATION TO NASA
1975	Feb	5013 TANK RECEIVED AT SAN DIEGO
	Mar	KSC AND GDC CHEMICAL ANALYSIS REPORTS
	Apr	TEST PLAN APPROVED BY NASA
	Jun	ECP APPROVED BY NASA
	Jul	5013 TANK STRIPPED
	Aug	BEGIN TANK X-RAY AND RE-X-RAY
1976	Jan	CUT UP TANK
	Feb	INSTALL SPECIMENS AT ETR
	Apr	INSTALL SPECIMENS AT PT LOMA
	Jun	START WD-40 PRESISTANCE TEST
1977	Jan	STATUS REVIEW MEETING WITH NASA
1978	Dec	FINAL REPORT ISSUED

4. To evaluate the effectiveness of WD-40 application to faying surfaces of previously corroded weld joints in arresting further corrosion degradation.

5. To establish X-ray standards that can be used to improve inspection techniques.

PHASE II PLAN FOR "DOG-BONE" TEST TO EVALUATE CORROSION CONTROL PROCEDURES AND TANK SKIN MATERIAL AT ETR

A. TEST OBJECTIVES

1. Evaluation of the effect of undissolved grain boundary carbides in tank skin material upon the corrosion susceptibility of launch vehicle weld joints.

2. Evaluation of the effectiveness of current corrosion control procedures (WD-40 application) in preventing corrosion degradation of launch vehicles with respect to frequency and method of application.

3. Evaluation of the effectiveness of WD-40 in inhibiting further corrosion in previously corroded launch vehicles."

The results, which support the above objectives, are presented in six sections as indicated in the Table of Contents. A final discussion, conclusions, and recommendations complete the report.

SECTION 2

METALLOGRAPHIC ANALYSIS

2.1 BACKGROUND

After standing in a vertical position for 14 months at Complex 36A, ETR, Florida, Atlas tank 5013 was filled with RP-1 fuel and pressurized to 68 psig. The pressure was lowered to about 16 psig and the outer tank surface was visually inspected for leakage on 23 October 1974. Leakage was noted at approximately 40 different areas. Most of the RP-1 fuel was emanating from underneath the aft edges of the resistance welded circumferential joints. However, some of the fuel was leaking from small, V-shaped, crack-like, surface indications adjacent to the aft edge of the resistance seam welds and aft spotwelds. Typical configurations of overlap, resistance welded circumferential joints in the fuel tank are shown in Figure 2-1. Radiographs of portions of the circumferential joints on 25 October 1974 revealed many more hidden, subsurface defect indications. Essentially all of the defects were located in the aft portion of the overlap joint. The aft portion is open to the external environment. Because of the large number of defect indications, it was decided to remove the tank and use it for a long-term test program.

2.2 TEST OBJECTIVES AND REQUIREMENTS (METALLOGRAPHIC ANALYSIS)

The overall objective of the metallographic analysis was to correlate the radiographic defect images with actual physical evidence revealed by microscopic examination of metallographic sections through typical defects. Documentation of these correlations should improve the capability to interpret with greater accuracy and confidence the radiographs of resistance welded overlap joints in cold-worked 301 stainless steel sheet.

Specifically, the Unified Test Plan (Ref. 2) classified the various X-ray defect images into 10 different categories, or items, depending upon shape, type (pit, crack, or leak), location, and orientation. Details are given in Table 2-1.

2.3 PROCEDURES AND RESULTS

One of the requirements was to metallographically section into defects that were known to leak by visual observation of the outer surface. To pinpoint the location of the leaks, the following procedure was used in October 1975. The tank was pressurized with nitrogen to 10 psig while in the horizontal holding fixture at Plant 19, San Diego.

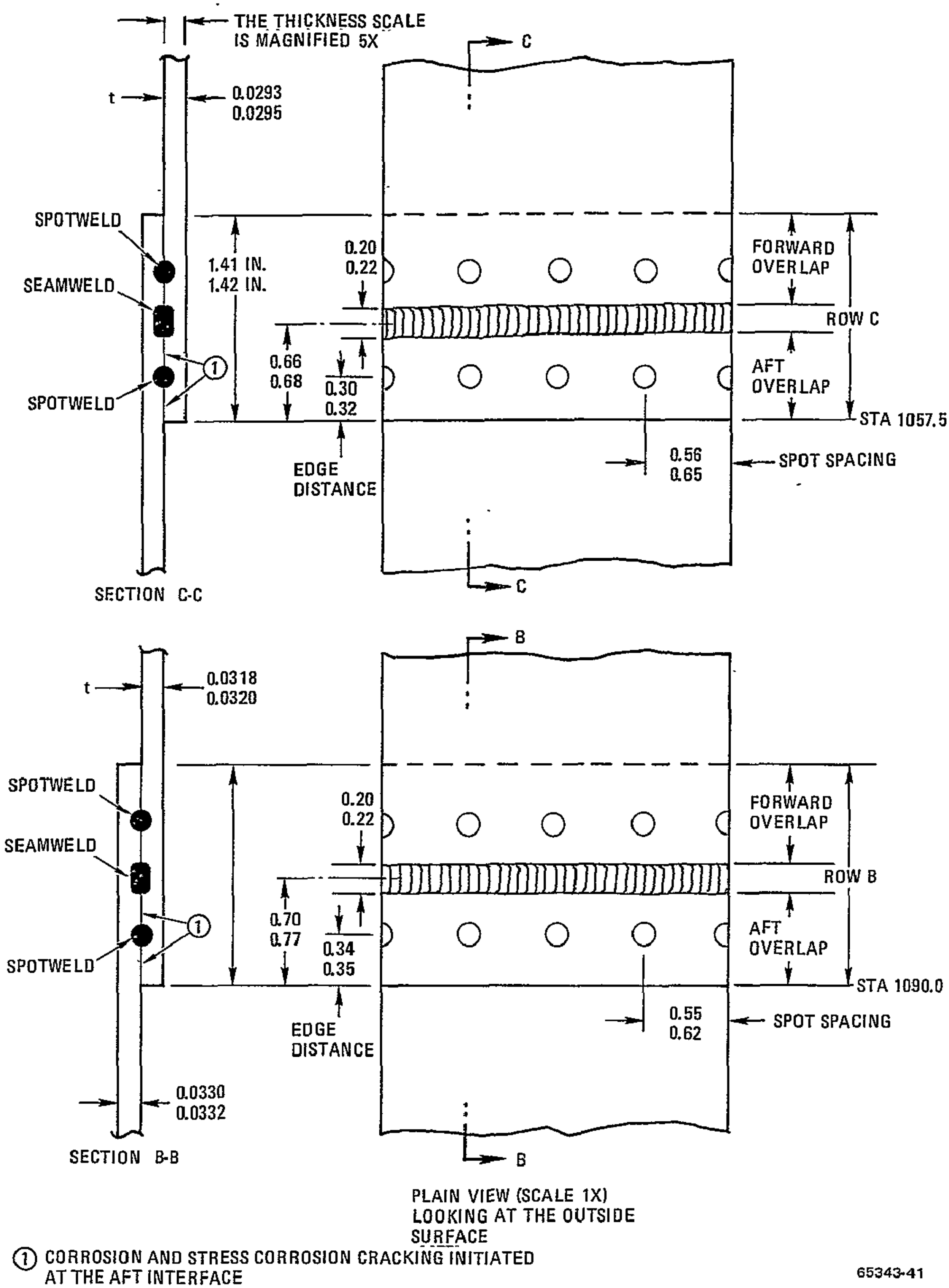

Figure 2-1. Configurations of the Resistance Welded Circumferential Joints at Sta 1057.5 and 1090, and the Actual Measured Dimensional Ranges of Metallographic Panels 1 and 2 (see Figures 2-3 and 2-4)

Table 2-1. Specific X-Ray Image Categories (Items) to be Metallographically Examined per Reference 2, page 7

Item	X-ray Indication	Type	Location	Orientation
1	round	pit	seam	—
2	round	pit	spotweld	—
3	length	crack	seam	vertical
4	length	crack	spotweld	vertical
5	length	crack	seam	horizontal
6	length	crack	spotweld	horizontal
7	—	known visual leak	seam	vertical
8	—	known visual leak	spotweld	vertical
9	—	known visual leak	seam	horizontal
10	—	known visual leak	spotweld	horizontal
11	none	—	spot-aft row	—
12	none	—	spot-fwd row	—

Measure and record:

a. nugget diameter
b. nugget penetration
c. skin chemistry
d. % carbide of specimen

Bubble leak-detection fluid was applied to the outside surface of each of the circumferential joints as the tank was slowly rotated. Visual examination for bubbles was made with a hand lens. The following leaking cracks were detected:

a. Four vertical cracks on the aft side of the seamweld in Row B (Sta 1090).

b. One vertical crack adjacent to an aft spotweld in Row B.

c. One horizontal crack on the aft side of the seamweld of Row C (Sta 1057.5).

d. No horizontal, leaking crack adjacent to a spotweld was detected (Item 10).

A metallographic test specimen panel (No. 1), 12 inches wide by 31 inches long, with the leaking defect approximately in the center, was cut from Row C. Two 12-inch wide metallographic panels (No. 2 and 3) were cut from Row B; each contained at least one leak defect. Panels 2 and 3 were 41 and 42 inches long respectively. The location of these panels in the overall fuel tank is shown in Figure 2-2.

Each of the three panels was radiographed on 17 February 1976 using the single-wall technique detailed in Table 2-2. Each film was 4-1/2 inches wide by 17 inches long. All of these radiographs, which altogether covered about a 108-inch length of the circumferential joints, were examined with hand lenses and stereomicroscopes in the

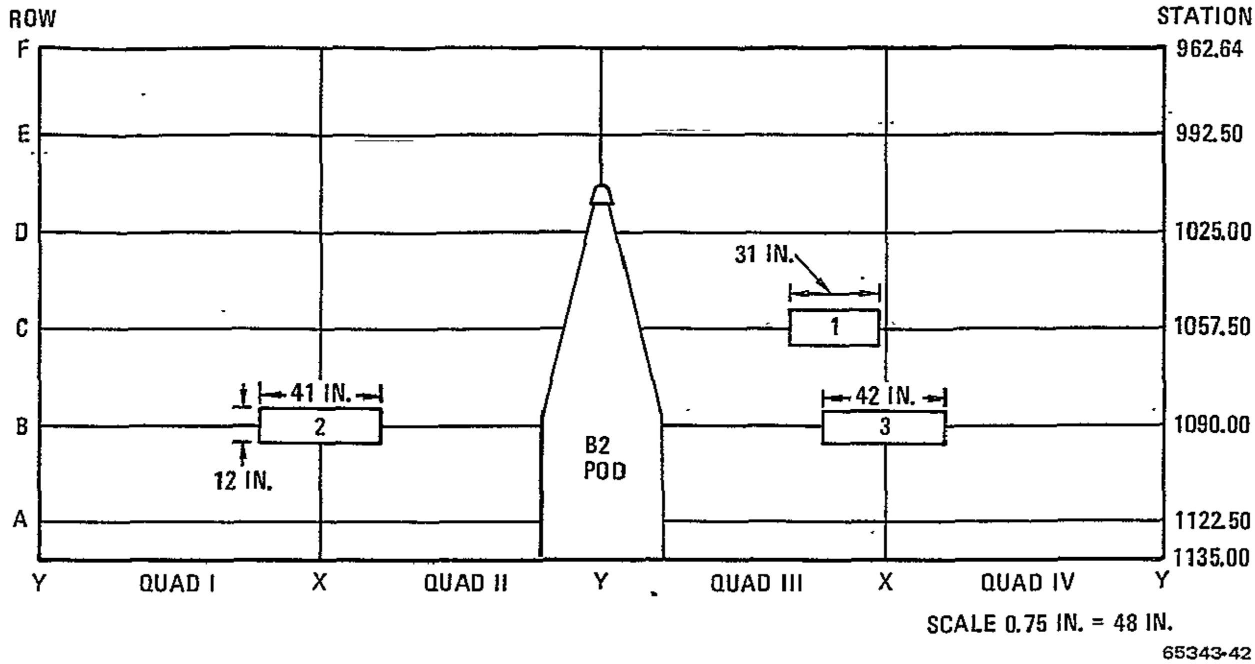

Figure 2-2. Location of Metallographic Specimen Panels 1, 2, and 3 in the 5013 Fuel Tank

3X to 30X magnification range. Images of the greatest clarity and size that appeared to best represent the categories requested (Table 2-1) were selected for sectioning. As it happened, all the selected locations were in Panels 1 and 2; consequently, Panel 3 was not used for metallographic sectioning. The as-received outside surface appearance of these two panels, aft spotweld ID numbers, and the location of the various items selected for metallographic sectioning are presented in Figures 2-3 and 2-4. Further details are listed in Table 2-3. The chemical composition and the tensile properties of the three coils that were welded together to form Row B and C are presented in Table 2-4.

The radiographic defect images were magnified to 2X and 5X and recorded on Polaroid 4 by 5 Land Film Type 52 using the setup shown in Figure 2-5. Then marker holes (0.020-inch diameter, except for Item 3) were drilled near to each defect, and each defect was radiographed again. These marker holes are needed as reference points so that the relationship between a section plane and the radiographic image can be determined accurately. The location of each metallographic section plane that was recorded photomicrographically (in most cases at 25X) is shown in a sketch adjacent to each marker-hole radiograph. In addition, both the outer and inner surface appearances of the leaking defects have been documented photographically using a conventional light macrocamera or a scanning electron microscope. The results of this effort are presented in Figure 2-6 through 2-37.

Table 2-2. Single-Wall Radiograph Technique

PART NO.	PART NAME	MATERIAL & THICKNESS	DATE	PAGE
69-73000	Sta. 1057/1090 Spec.	S.S. .063, .065	2-17-76	1 OF 1

X-RAY MACHINE & VOLTAGE RATING	FOCAL SPOT SIZE
Norelco Beryllium Window---150KVP	2.5
ISOTOPE	**SOURCE SIZE**
none	none

X-RAY LABORATORY TECHNIQUE DATA SHEET

	SPECIMEN		WELDS, VIEWS/SHOTS, OR AREAS					
	Sta. 1057	Sta. 1090						
KV	105	105						
MA	10	10						
TIME	2 min.	2 min.						
CURIES	NA	NA						
DISTANCE inches (Target/Source to Film)	60	60						
FILM (Type & Size)	M	M						
FILM (Number in Cassette)	1	1						
PENETRAMETER	.06	.06						
PENETRAMETER SHIM	NA	NA						
SCREENS (Type & Thickness)	NA	NA						
FILTER (Type & Thickness)	NA	NA						
MASKING MATERIAL	NA	NA						

REMARKS: To include filter location, details of masking, placement of film, orientation of location markers, description of the manner in whick interval markers locate areas of interest, description of or reference to welding procedure (when applicable), and for multiple film techniques requirement for single or superimposed film viewing.

Single-wall technique

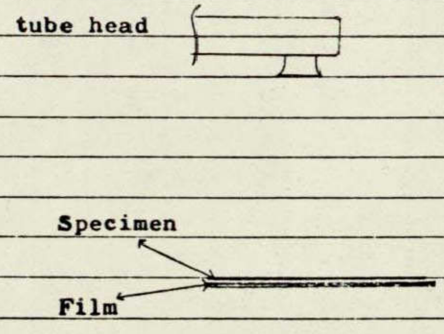

Identification and penetrameter on source side of specimen.

TECHNIQUE APPROVED BY:

James A. Auch Level II

A1876 (Rev. 3-75)

65343-50

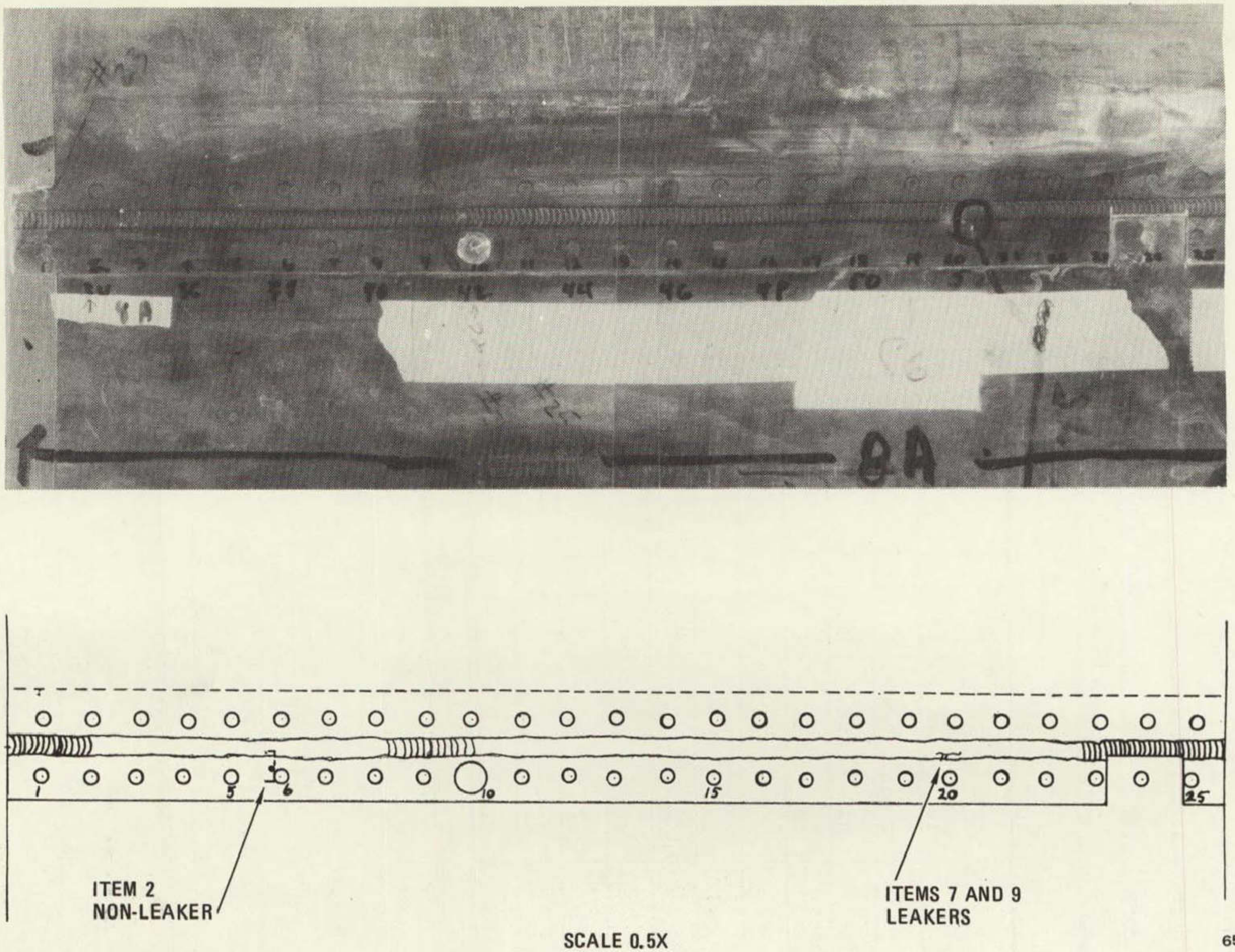

Figure 2-3. Outside Surface Appearance of Metallographic Specimen Panel No. 1 (see Figure 2-2) Aft Spotweld ID Numbers, and the Location of Items 2, 4, 7, and 9. (Sheet 1 of 2)

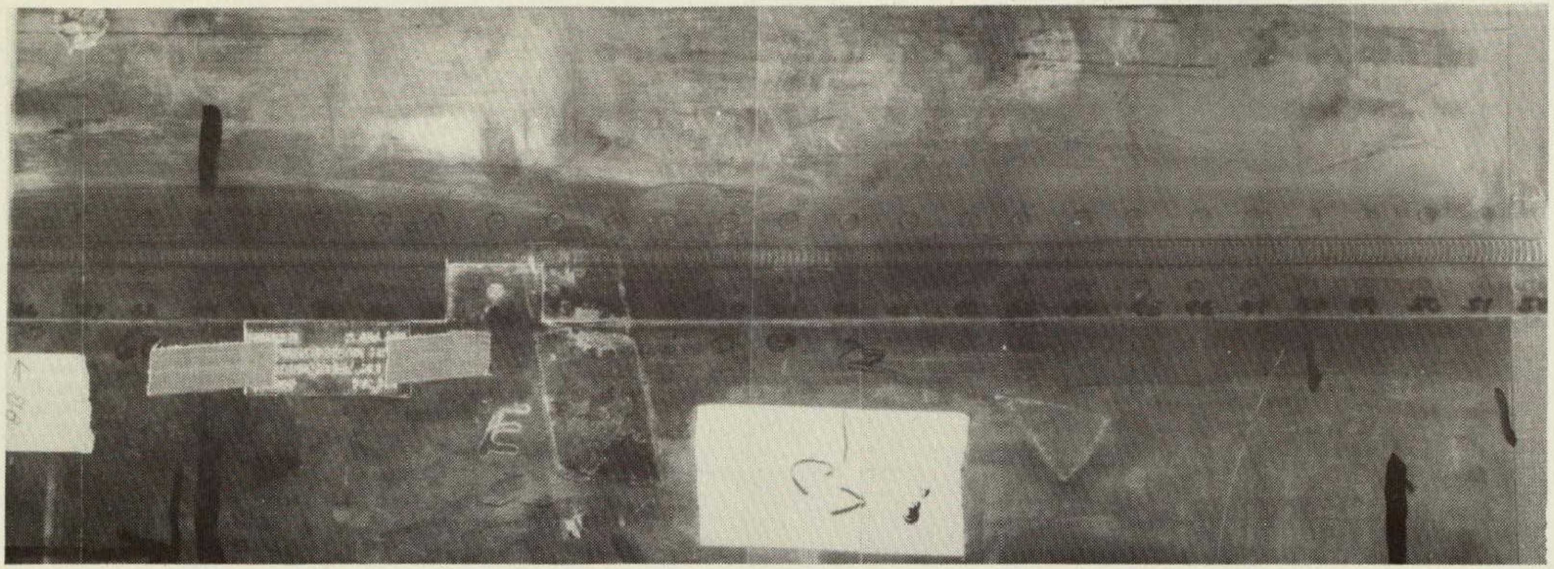

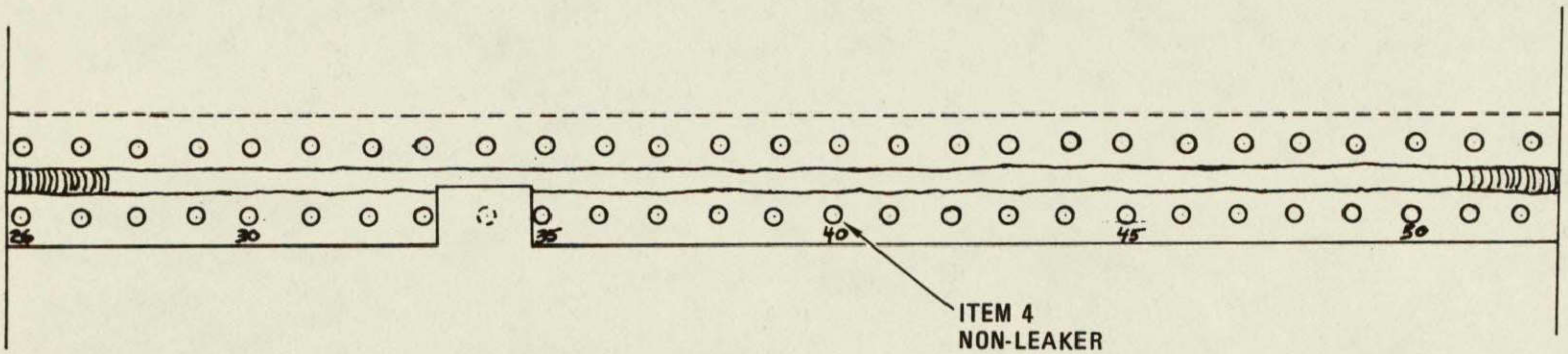

65343-43/2

Figure 2-3. Outside Surface Appearance of Metallographic Specimen Panel No. 1 (see Figure 2-2) Aft Spotweld ID Numbers, and the Location of Items 2, 4, 7, and 9. (Sheet 2 of 2)

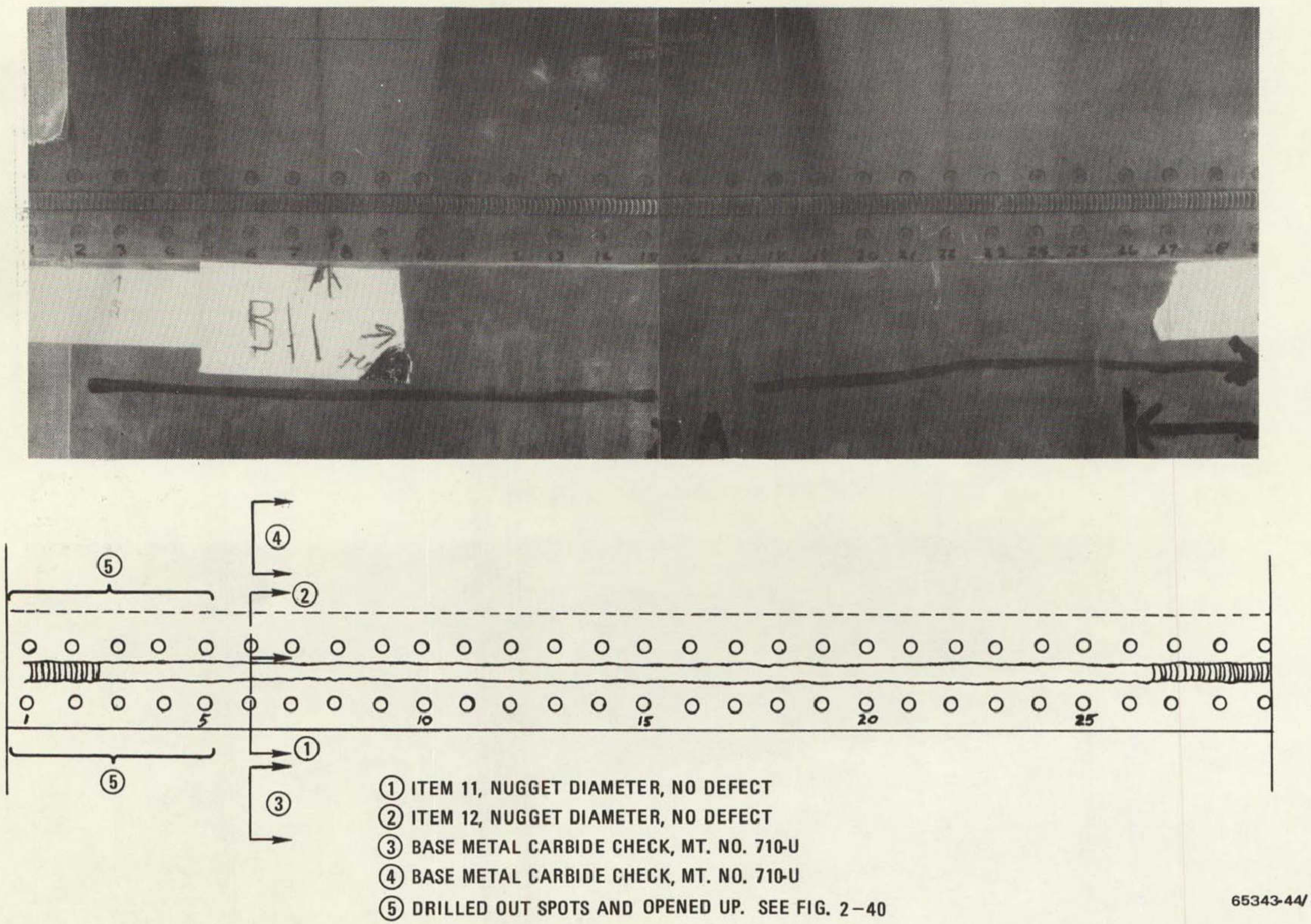

Figure 2-4. Outside Surface Appearance of Metallographic Specimen Panel No. 2 (see Figure 2-2), Aft Spotweld ID Number, the Location of Items 1, 3, 5, 6, 8, 11, and 12, and other Specimens as Noted. (Sheet 1 of 3)

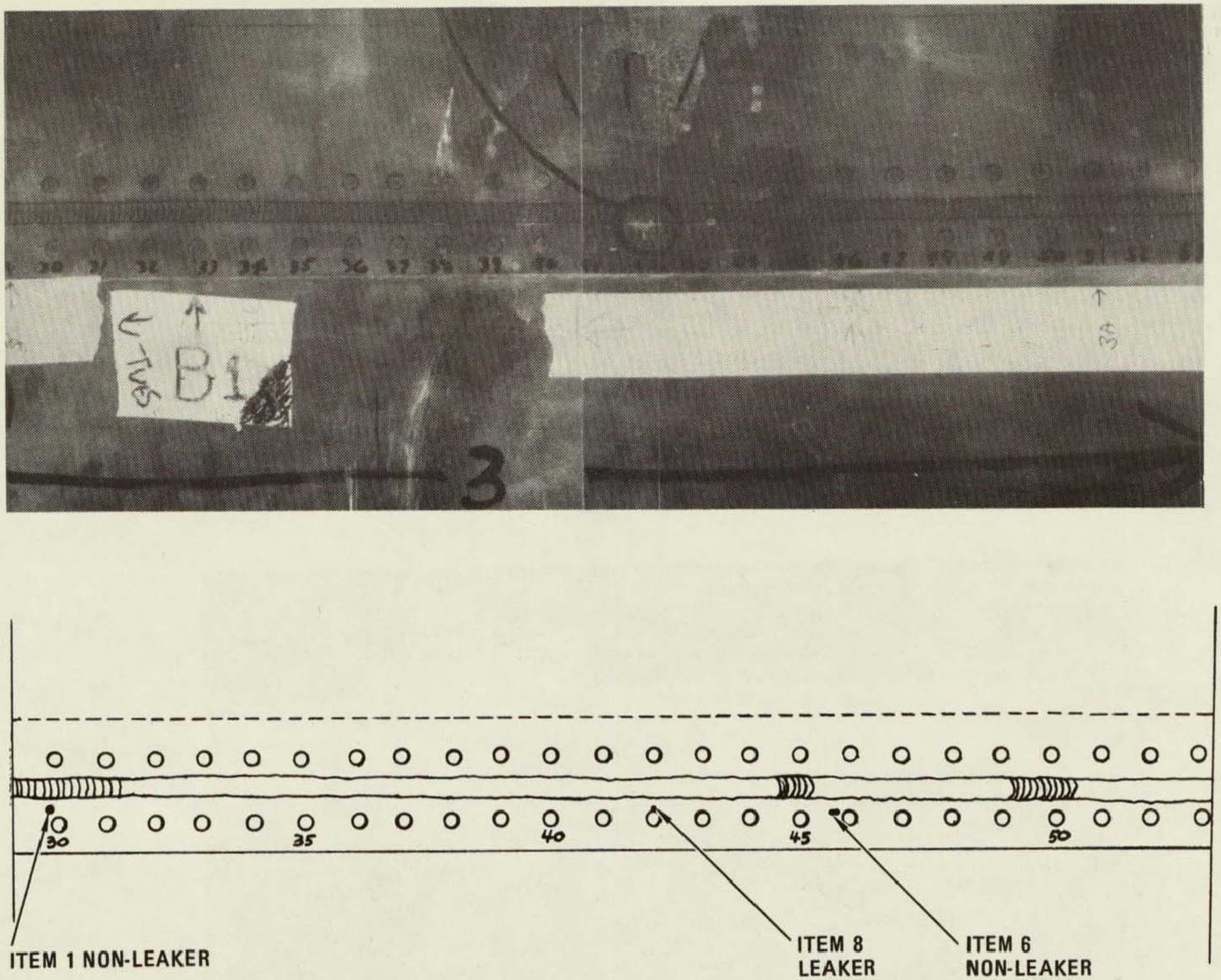

65343-44/2

Figure 2-4. Outside Surface Appearance of Metallographic Specimen Panel No. 2 (see Figure 2-2), Aft Spotweld ID Number, the Location of Items 1, 3, 5, 6, 8, 11, and 12, and other Specimens as Noted. (Sheet 2 of 3)

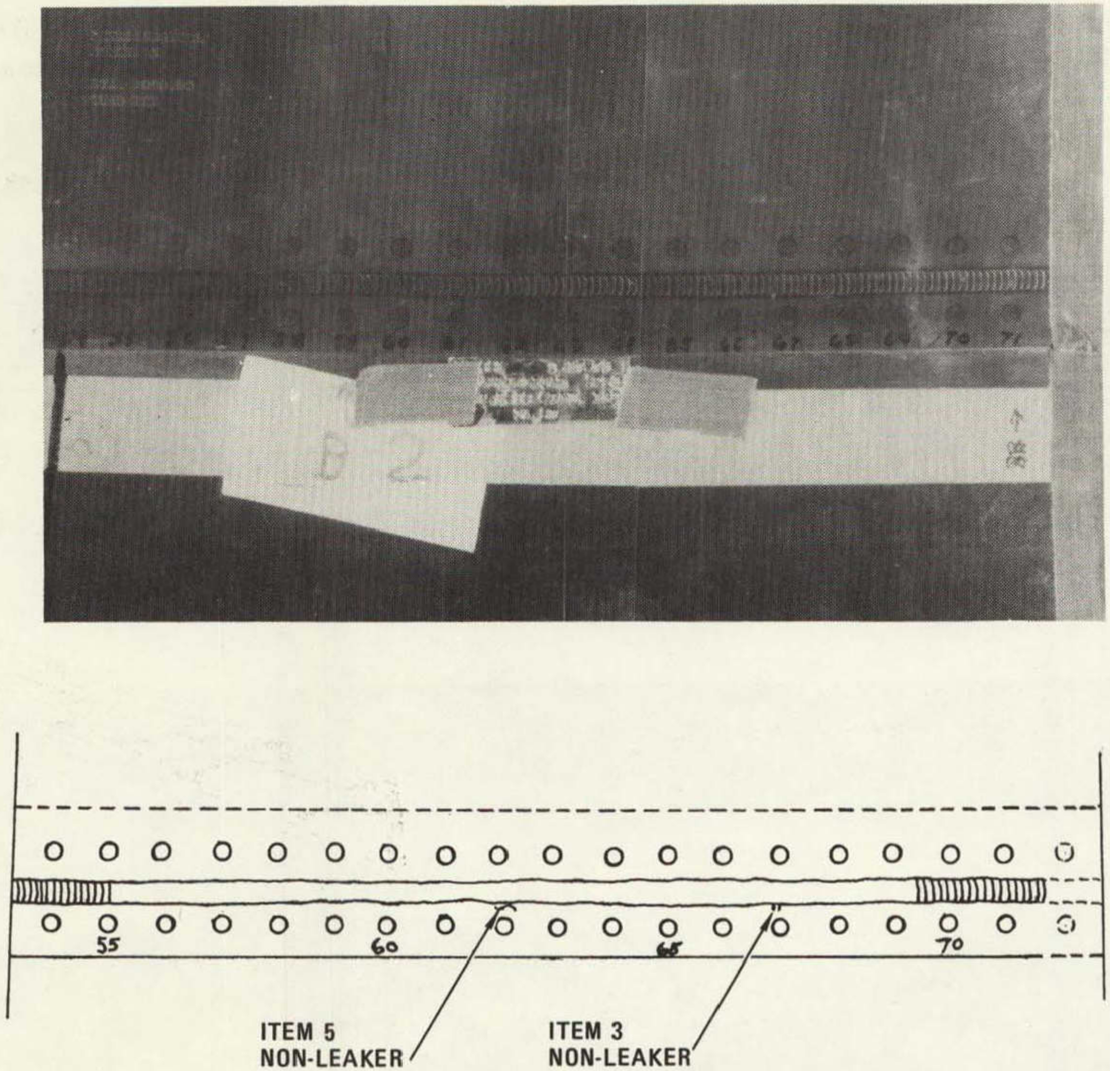

65343-44/3

Figure 2-4. Outside Surface Appearance of Metallographic Specimen Panel No. 2 (see Figure 2-2), Aft Spotweld ID Number, the Location of Items 1, 3, 5, 6, 8, 11, and 12, and other Specimens as Noted. (Sheet 3 of 3)

Table 2-3. Description and Identification of Each Defect that was Sectioned by Item No., Location, and Mount No.

Item No.	Shape of X-ray Indication	Apparent Defect Type	Orientation	Relative Location (1)	Specific Defect Location(2) Sta	(Spot)	Mount No.	Figures
1	round	pit (NVL)	—	seam	1090	(30)	360-u	2-6, 2-7, 2-8
2	round	pit (NVL)	—	spotweld	1057	(6)	361-u	2-9, 2-10
3	linear	crack (NVL)	vertical	seam	1090	(67)	222-u	2-11, 2-12, 2-13
4	linear	crack (NVL)	vertical	spotweld	1057	(45)	364-u	2-14, 2-15
5	linear	? (NVL)	horizontal	seam	1090	(63)	365-u	2-16 thru 2-21
6	linear	crack (NVL)	horizontal	spotweld	1090	(46)	366-u	2-22, 2-23
7	linear	crack (KVL)	vertical	seam	1057	(20)	677-u	2-24 thru 2-30
8	—	crack (KVL)	vertical	spotweld	1090	(42)	744-u	2-31 thru 2-35
9	—	crack (KVL)	horizontal	seam	1057	(20)	676-u	2-36, 2-37
10	(3)	crack (KVL)	horizontal	spotweld	—		—	—
11	none	—	—	spot-aft row	1090	(6)	213-u	
12	none	—	—	spot-fwd row	1090	(6)	214-u	

(1) Indicates whether the defect is adjacent to the seamweld or an aft spotweld.
(2) Location of each defect by station number and spot number, See Figures 2-3 and 2-4.
(3) No defect was observed matching this category.
NVL = No Visible Leak
KVL = Known Visible Leak.

Table 2-4. Fuel Tank Skin Chemistry and Mechanical Properties

Part Number 69-73550-42	Chemical Analysis (Washington Steel Co.)		Mechanical Properties (General Dynamics, Convair)				
			Sample*	Thickness (inch)	T.S (ksi)	Y.S (ksi)	EL (%)
	C	0.074					
Coil No.	Mn	1.04					
76946-2	P	0.022	A1L	0.0295	229.0	217.0	5.0
	S	0.005	A2L	0.0295	229.1	216.9	5.0
Heat No.	Si	0.67	B1L	0.0297	233.1	219.2	5.0
11522-5	Cr	17.23	B2L	0.0300	-	216.0	5.0
	Ni	6.93	A1T	0.0300	241.6	199.1	5.5
Nominal Gauge	Cu	0.21	A2T	0.0299	241.6	200.7	5.5
0.030 Inch	N_2	0.039	B1T	0.0301	239.8	200.9	5.5
	Mo	0.23	B2T	0.0302	239.7	198.7	5.5

Part Number 69-73550-43	Chemical Analysis		Mechanical Properties				
			Sample*	Thickness (inch)	T.S (ksi)	Y.S. (ksi)	EL (%)
	C	0.092					
Coil No.	Mn	0.96					
70222-A1	P	0.017	A1L	0.0315	247.4	238.4	3.0
	S	0.006	A2L	0.0317	246.6	235.4	3.5
Heat No.	Si	0.64	B1L	0.0317	243.1	232.2	3.0
20439-6	Cr	17.27	B2L	0.0317	241.8	231.0	4.0
	Ni	7.02	A1T	0.0318	251.4	220.3	5.0
Nominal Gauge	Cu	0/15	A2T	0.0318	250.5	216.5	5.0
0.032 Inch	N_2	0.037	B1T	0.0317	247.7	213.6	5.0
	Mo	0.16	B2T	0.0317	246.1	213.1	5.0

Part No. 69-73550-44	Chemical Analysis		Mechanical Properties				
			Sample*	Thickness (inch)	T.S. (ksi)	Y.S. (ksi)	EL (%)
	C	0.092					
Coil No.	Mn	0.96					
70210-A1	P	0.017	A1L	0.0336	242.5	233.4	4.0
	S	0.006	A2L	0.0338	244.1	226.1	4.0
Heat No.	Si	0.64	B1L	0.0330	240.5	232.1	6.0
20439-2	Cr	17.27	B2L	0.0330	242.0	230.9	5.5
	Ni	7.02	A1T	0.0337	249.7	222.4	6.0
Nominal Gauge	Cu	0.15	A2T	0.0338	248.2	217.4	5.0
0.033 Inch	N_2	0.037	B1T	0.0331	245.0	215.4	5.0
	Mo	0.16	B2T	0.0332	245.8	220.4	5.0

*Sample code designates coupon 1 or 2 from location A or B in the longitudinal (L) or transverse (T) orientation.

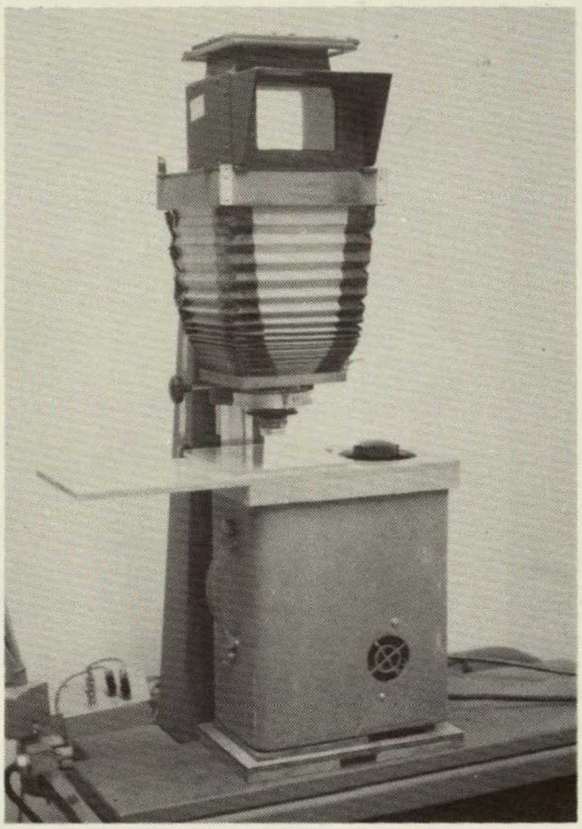

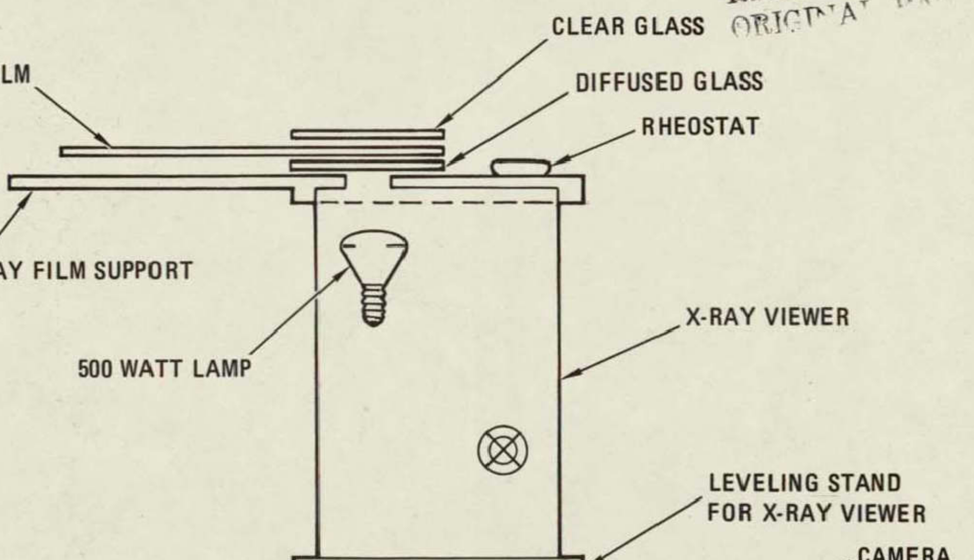

65343-45

Figure 2-5. Setup Used to Magnify and Record the Radiographic Images on Polaroid 4 x 5 Land Film Type 52.

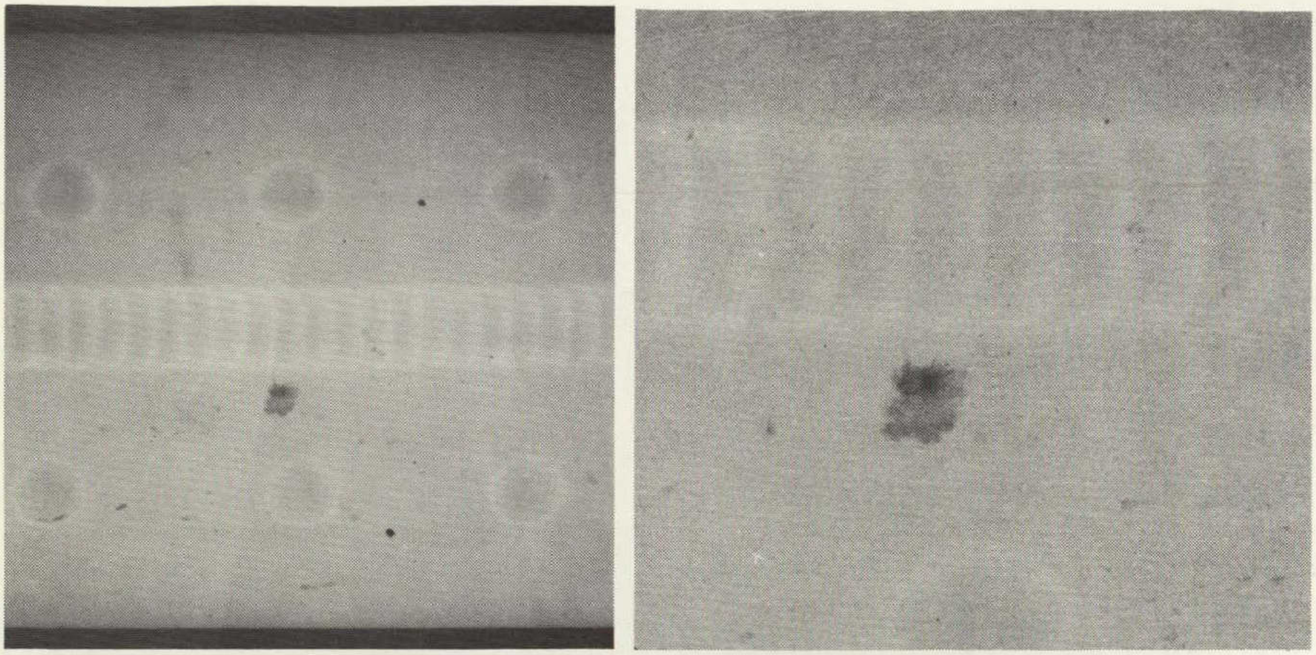

2X 5X

ABOVE – X-RAY IMAGE OF THE "ROUND" DEFECT AT 2X AND 5X MAGNIFICATIONS
– X-RAY FILM 5X5001, 3-3A, 2-17-76, DENSITY 2.41

BELOW – SAME DEFECT WITH FOUR 0.020 IN. DIA MARKER HOLES ADDED
– X-RAY FILM M1, MAY 1976, DENSITY 2.15

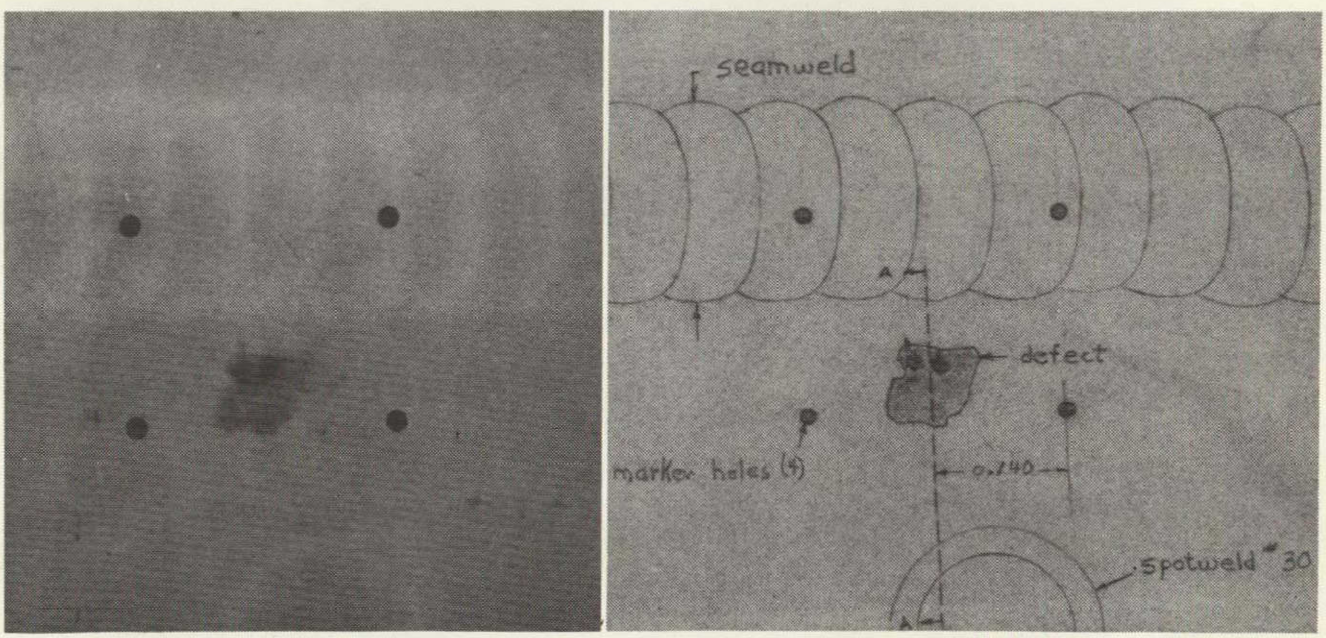

65343-46 5X STA 1090 SPOTWELD 30

Figure 2-6. X-ray Appearance of a Round Defect Indication Near the Seamweld (Item 1) and the Location of a Section (A-A) Through the Defect (see Figure 2-7).

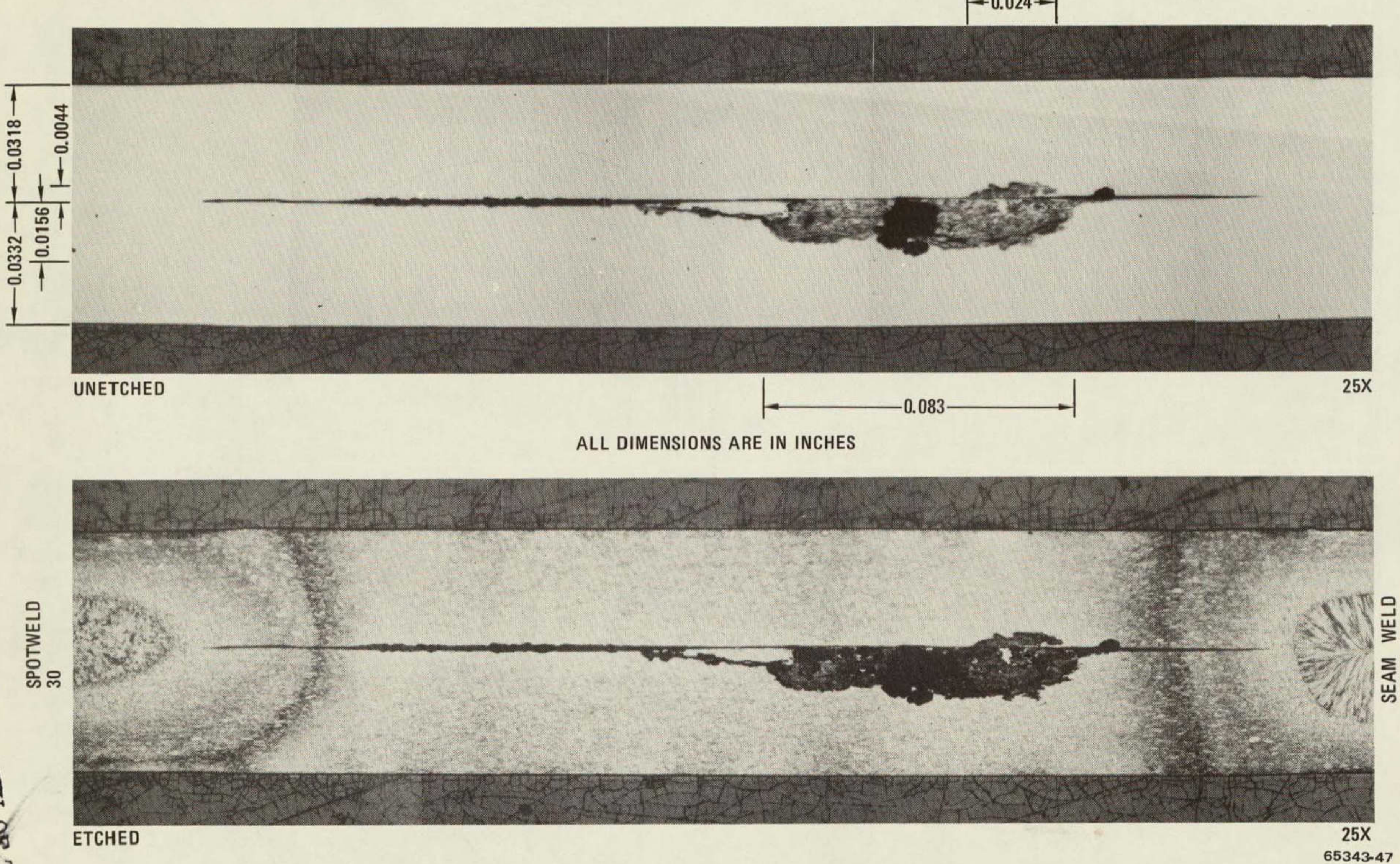

Figure 2-7. Appearance of Section A-A Through the Round, Pit-type Defect Indication Shown in Figure 2-6. A Portion of the Unetched Defect is Shown at 500X in Figure 2-8.

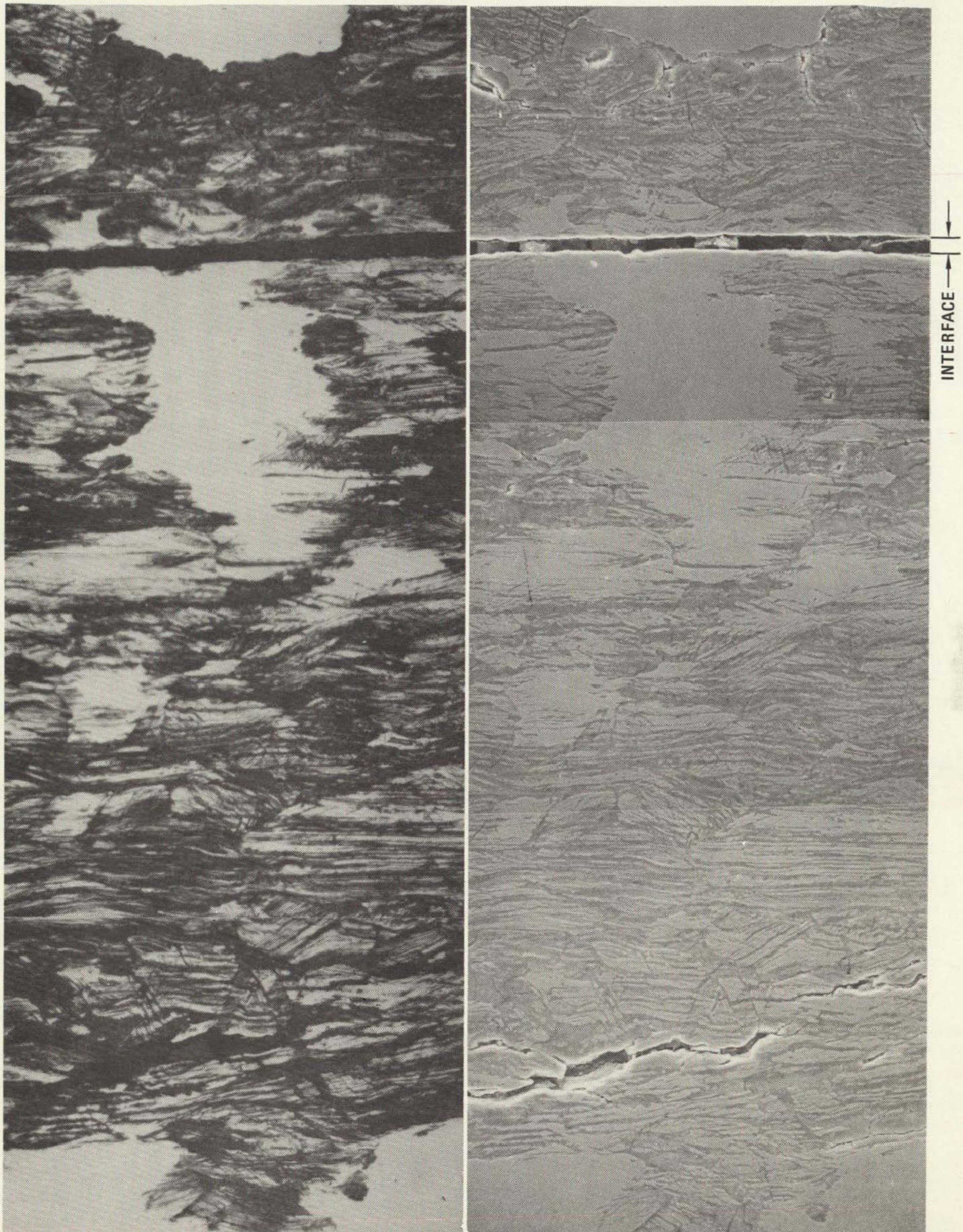

Figure 2-8. Portion of Unetched Defect Shown in Figure 2-7 at 500X Magnification

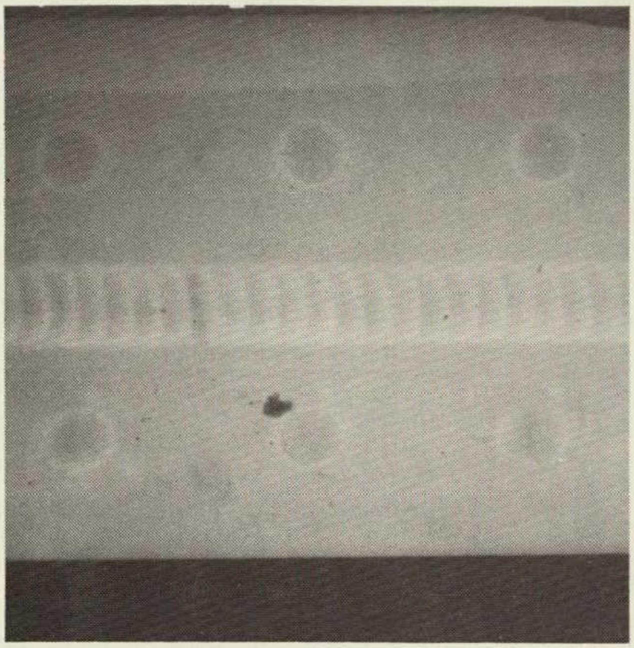

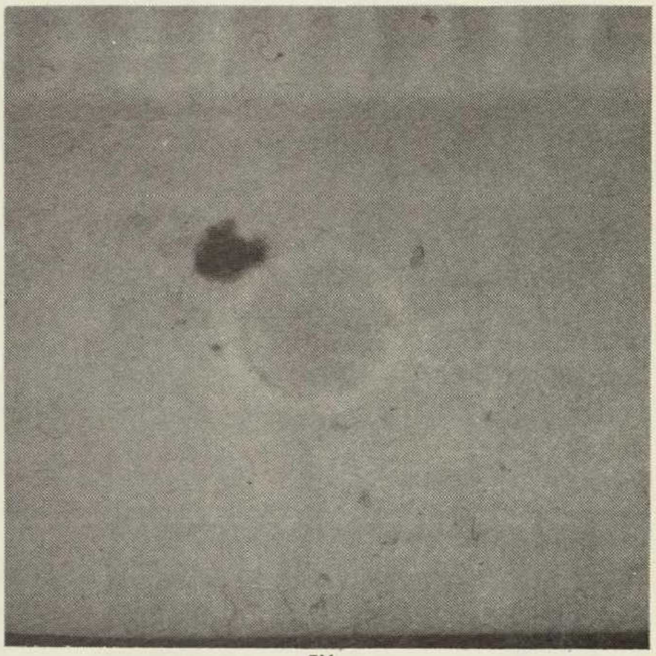

2X

5X

ABOVE – X-RAY IMAGE OF THE "ROUND" DEFECT MAGNIFIED 2 AND 5X
– X-RAY FILM 5X5001, 8A-8B, 2-17-76, DENSITY 2.14

BELOW – SAME DEFECT WITH FOUR MARKER HOLES ADDED
– X-RAY FILM M2, 5-12-76, DENSITY 3.38

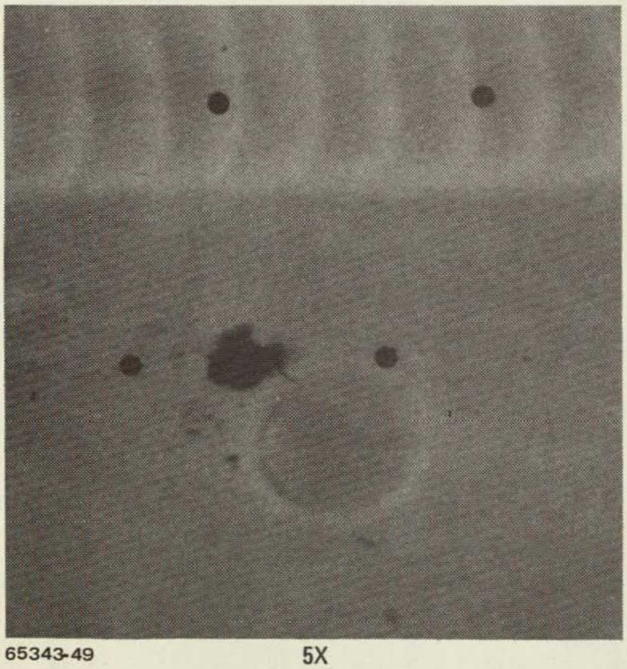

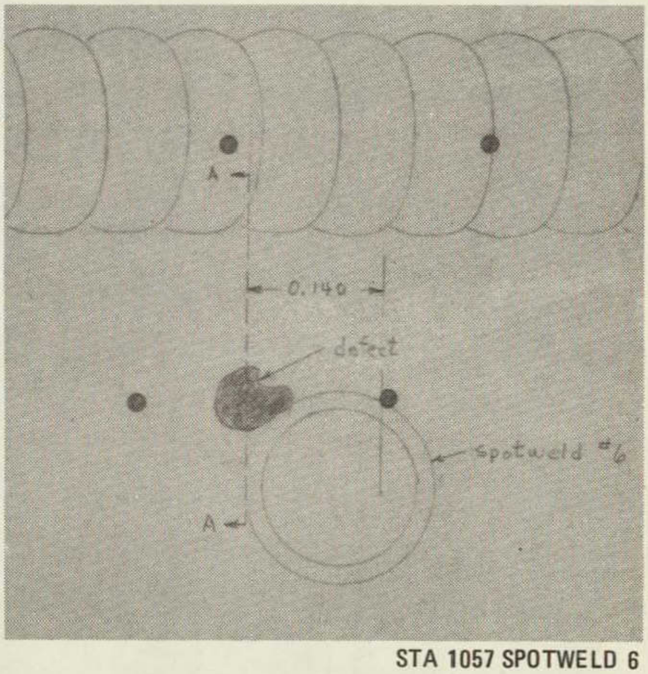

65343-49

5X

STA 1057 SPOTWELD 6

Figure 2-9. X-ray Appearance of a Round Defect Indication Near a Spotweld (Item 2) and the Location of a Section (A-A) Through the Defect (See Figure 2-10)

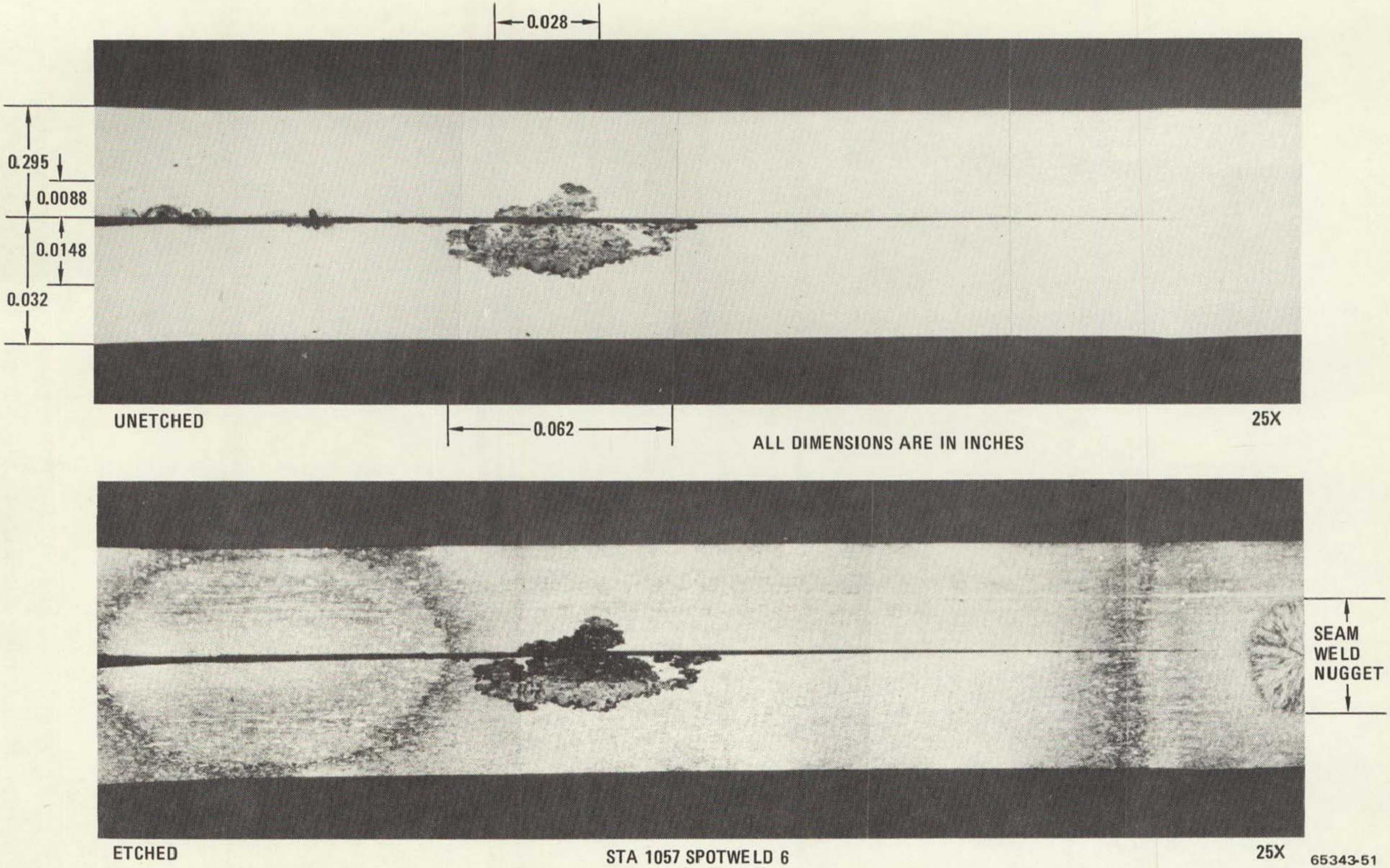

Figure 2-10. Appearance of Section (A-A) Through the Round, Pit-type Defect Indication Shown in Figure 2-9.

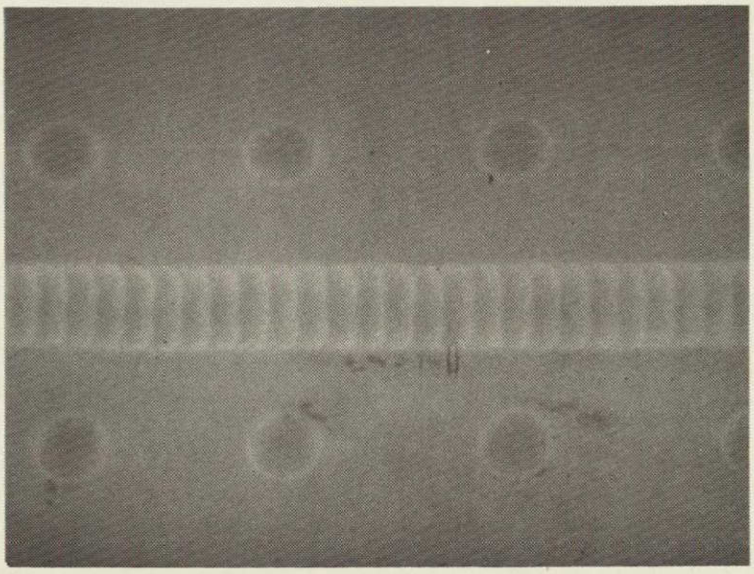

2X

ABOVE – X-RAY IMAGE OF THE DEFECTS MAGNIFIED 2X
– X-RAY FILM 5X5001, 3A-3B, 2-17-76

BELOW – SAME DEFECTS MAGNIFIED 5X WITH 4 MARKER HOLES ADDED
– X-RAY FILM 3K6031, 3-2-76

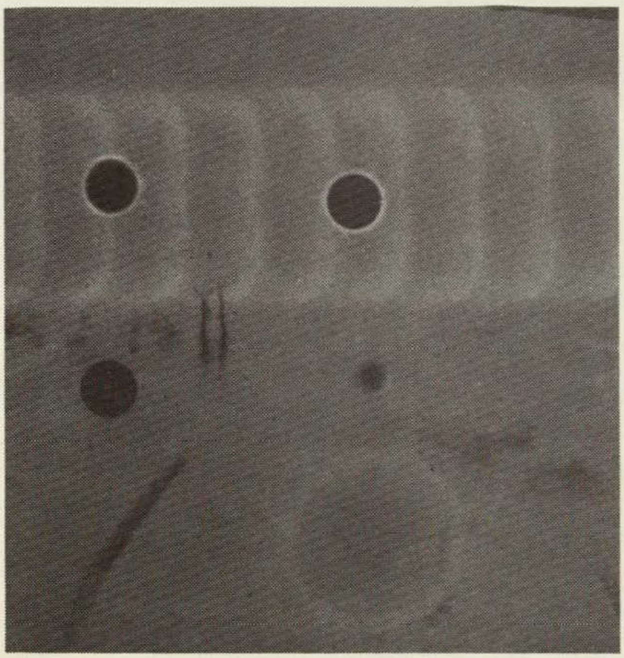

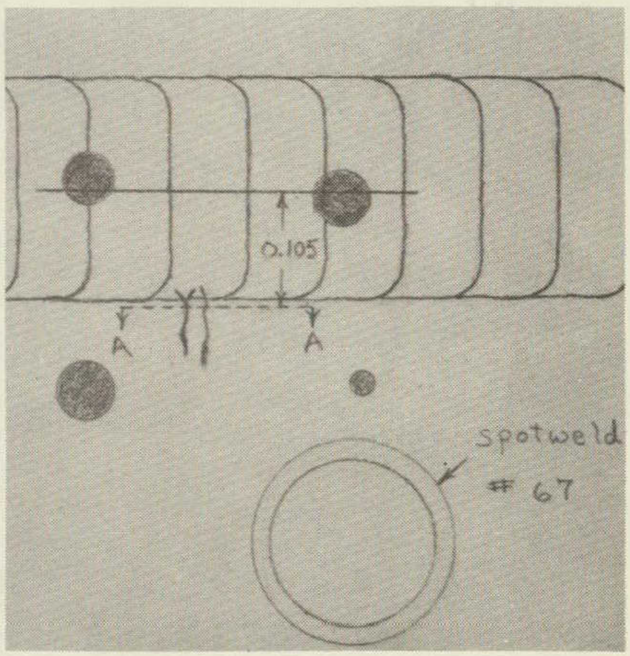

5X 5X

STA 1090 SPOTWELD 67

65343-52

Figure 2-11. X-ray Appearance of a Vertical, Crack-type Defect Indications at the Seamweld (Item 3), and the Location of a Section (A-A) through the Defects (see Figures 2-12 and 2-13)

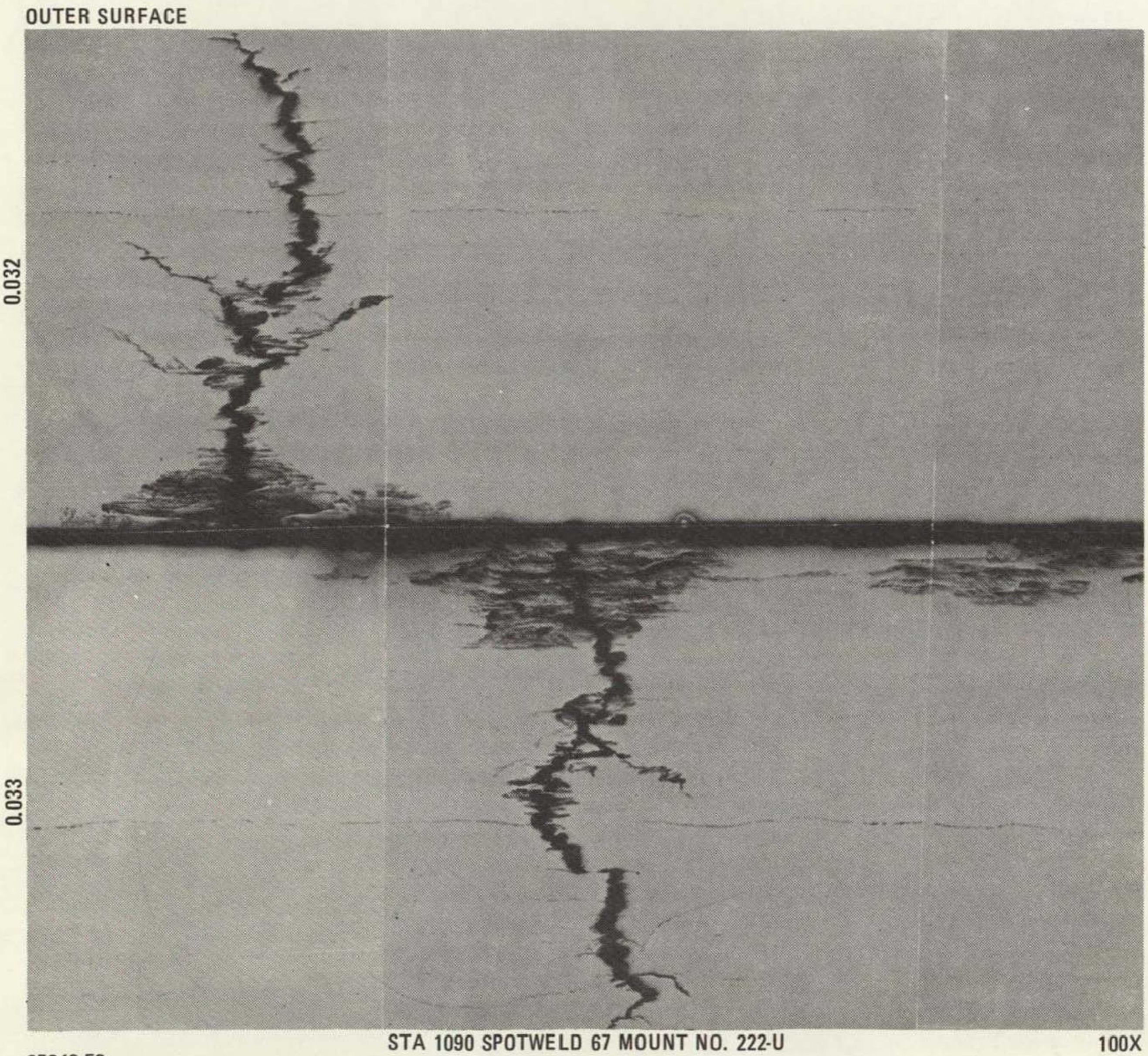

Figure 2-12. Unetched Appearance of Section A-A Through the Crack-type Defect Indications Shown in Figure 2-11

OUTER SURFACE

0.032

0.033

STA 1090 SPOTWELD 67 MOUNT NO. 222-U 100X

65343-54

Figure 2-13. Etched Appearance of Section A-A Through the Crack-type Defect Indications Shown in Figure 2-11

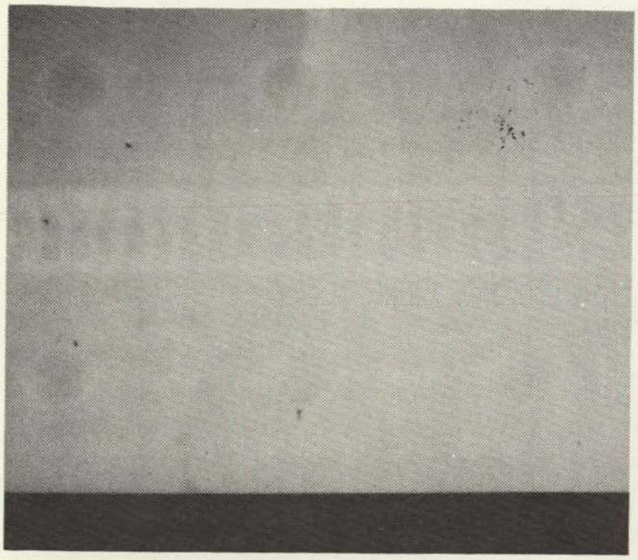

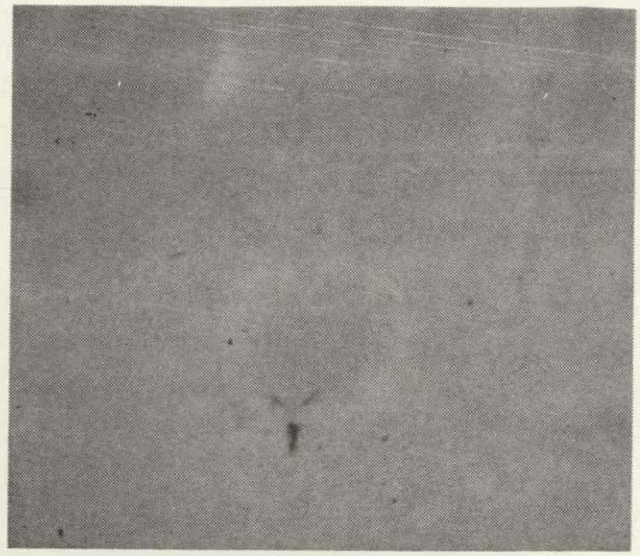

2X 5X

ABOVE – X-RAY IMAGE OF THE DEFECT MAGNIFIED 2 AND 5X
– X-RAY FILM 5X5001, 8B-9, 2-17-76, DENSITY 2.04

BELOW – SAME DEFECT WITH 4 MARKER HOLES ADDED
– X-RAY FILM M4, 5-12-76, DENSITY 3.35

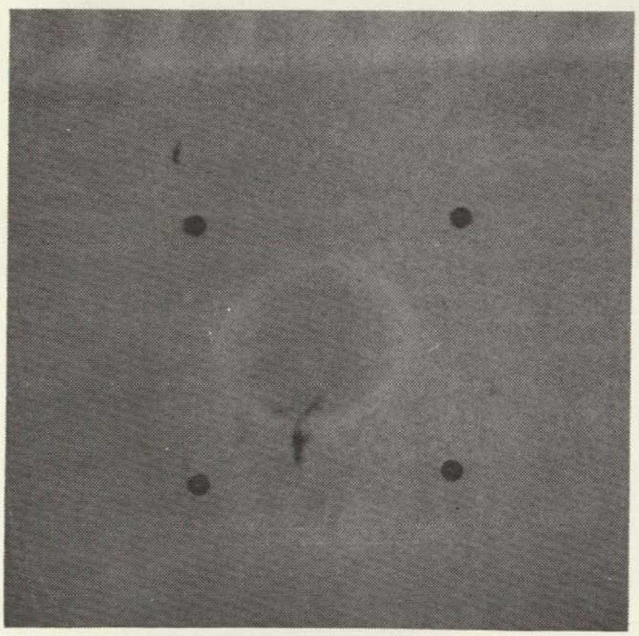

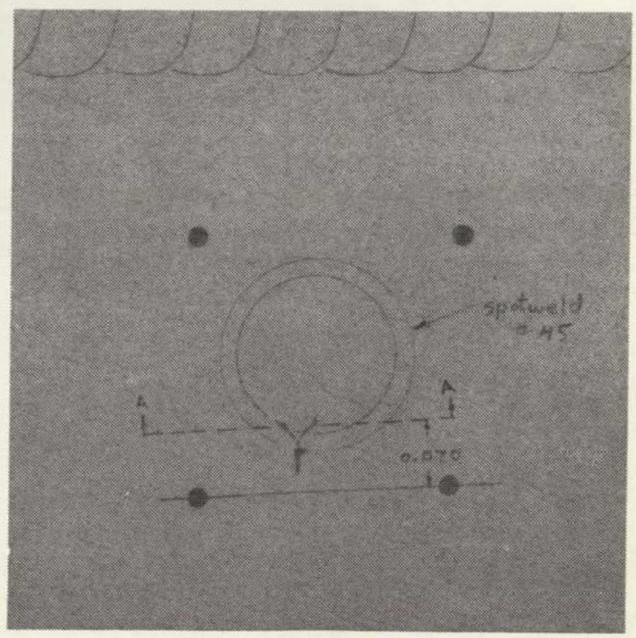

5X 5X

STA 2057 SPOTWELD 45

65343-55

Figure 2-14. X-ray Apperance of a Vertical, Crack-type Defect Indication Near a Spotweld (Item 4), and the Location of a Section (A-A) Through the Defect (see Figure 2-15)

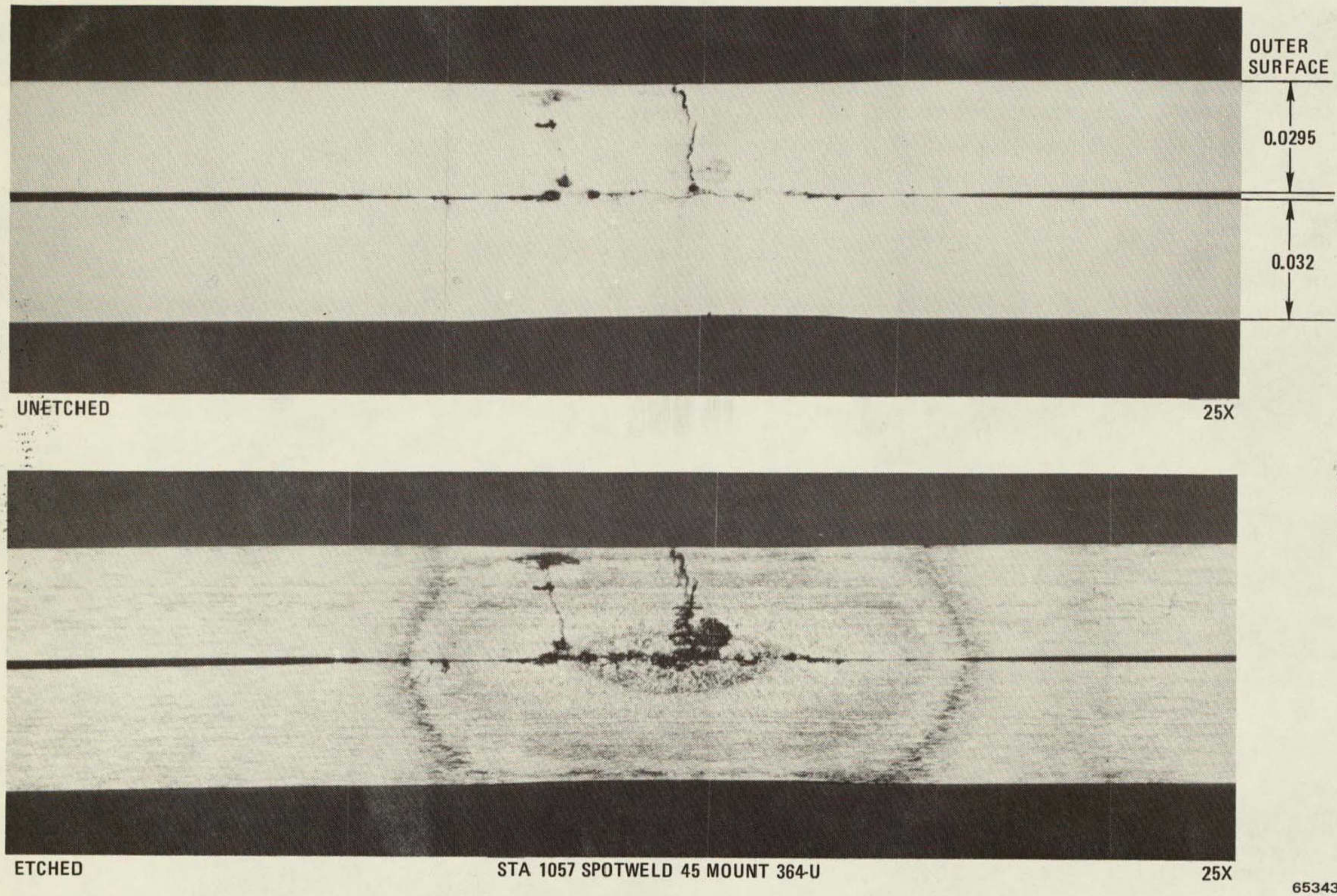

Figure 2-15. Appearance of Section A-A Through the Crack-type Defect Indication Shown in Figure 2-14

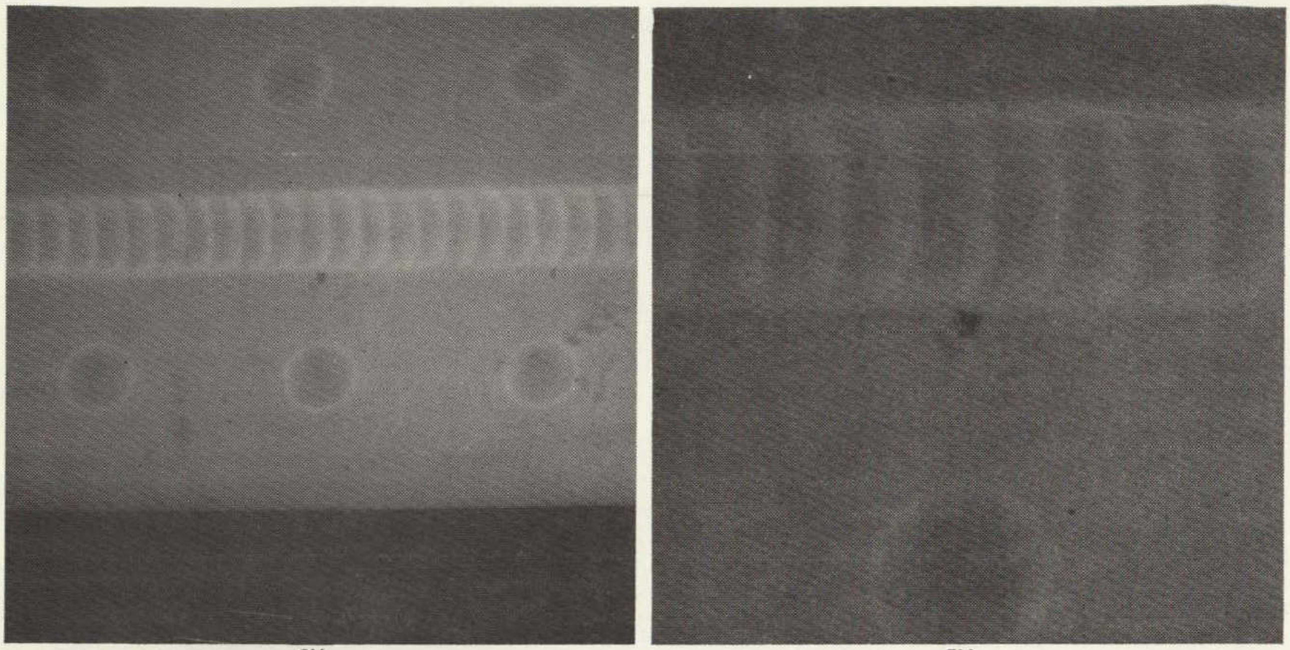

2X 5X

ABOVE – X-RAY IMAGE OF THE DEFECT MAGNIFIED 2 AND 5X
– X-RAY FILM 5X5001, 3A-3B, 2-17-76, DENSITY 2.78

BELOW – SAME DEFECT WITH 4 MARKER HOLES ADDED
– X-RAY FILM M5, 5-12-76, DENSITY 2.14

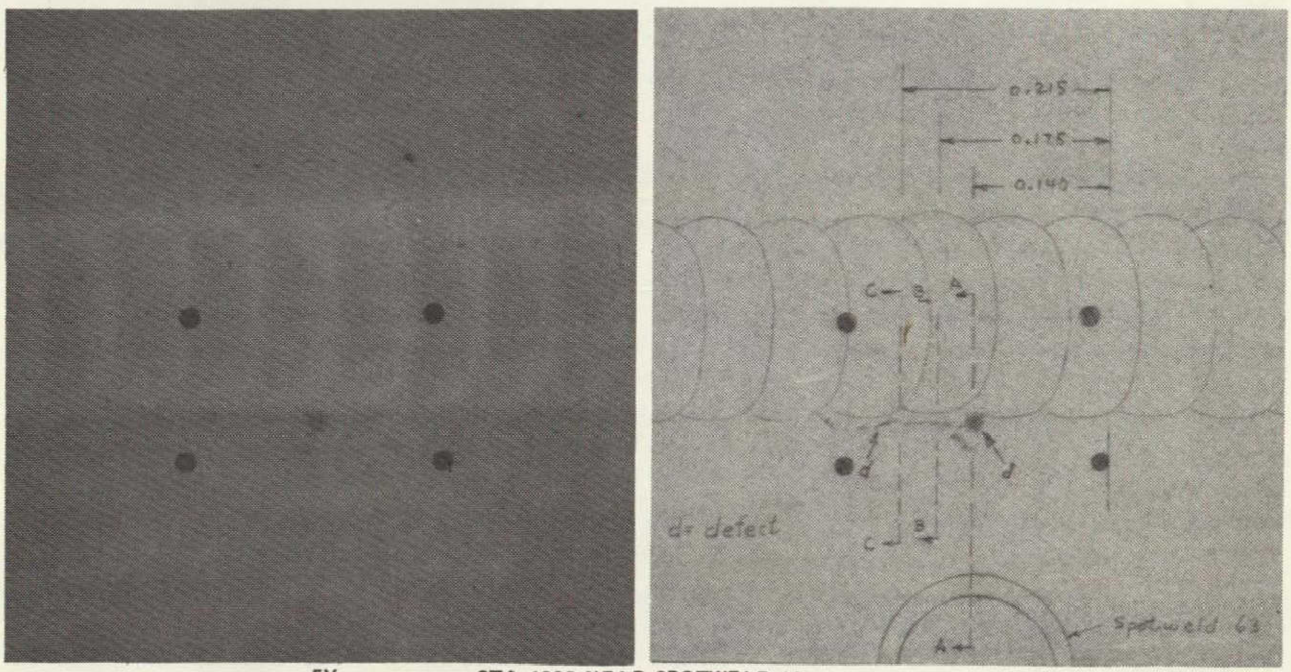

5X STA 1090 NEAR SPOTWELD 63

65343-57

Figure 2-16. X-ray Appearance of a Horizontal, "Length" Defect Indication Adjacent to the Seamweld (Item 5) and the Locations of Three Sections (A-A, B-B, and C-C) Through the Defect (see Figures 2-17 through 2-21)

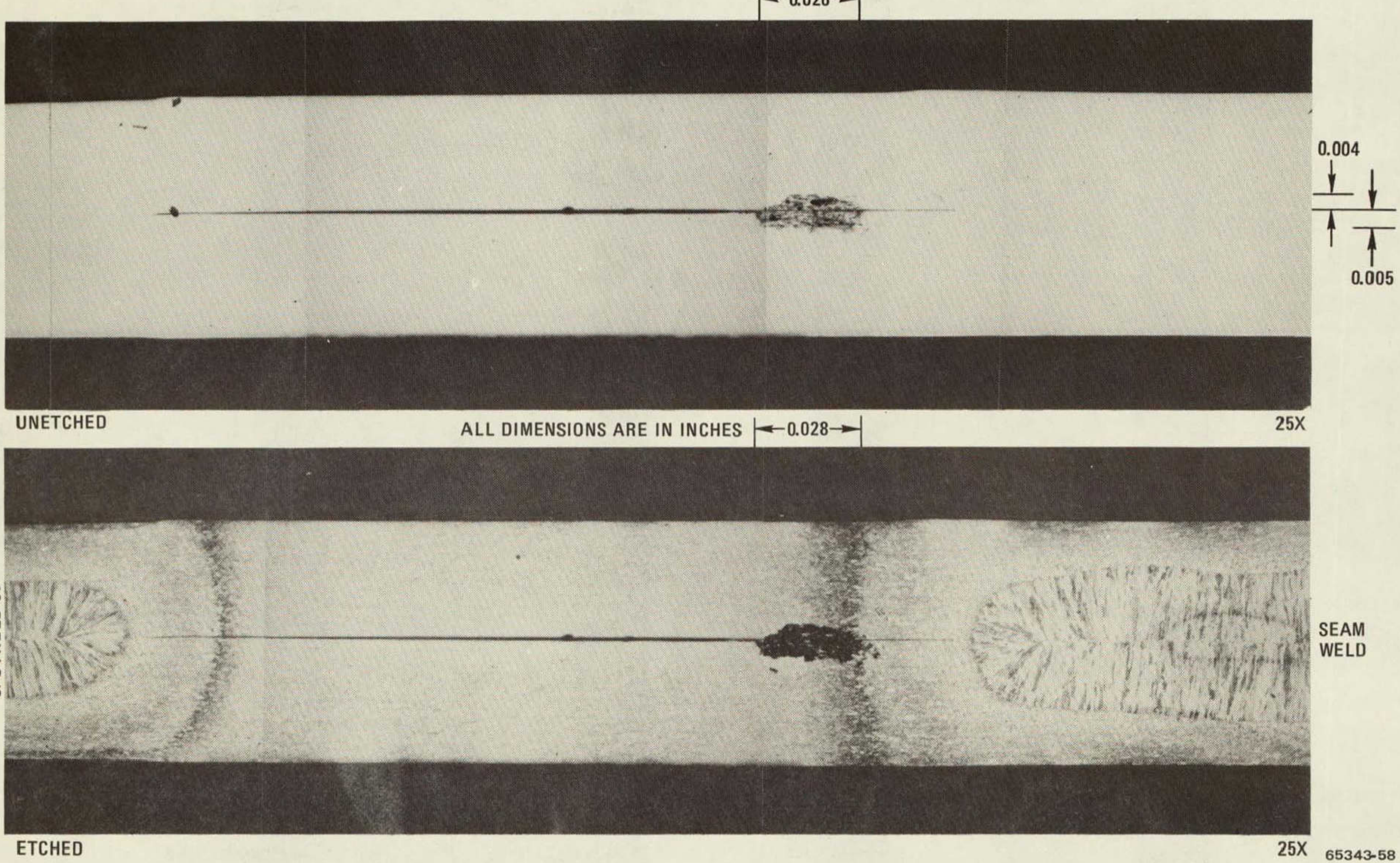

Figure 2-17. Appearance of Section A-A Through the Horizontal, "Length" Defect Indication Shown in Figure 2-16. The Magnification Reveals that the X-ray Indication was Produced by Interface Pitting-type Corrosion Attack Near and in the Weld-Carbide-Precipitation Zone

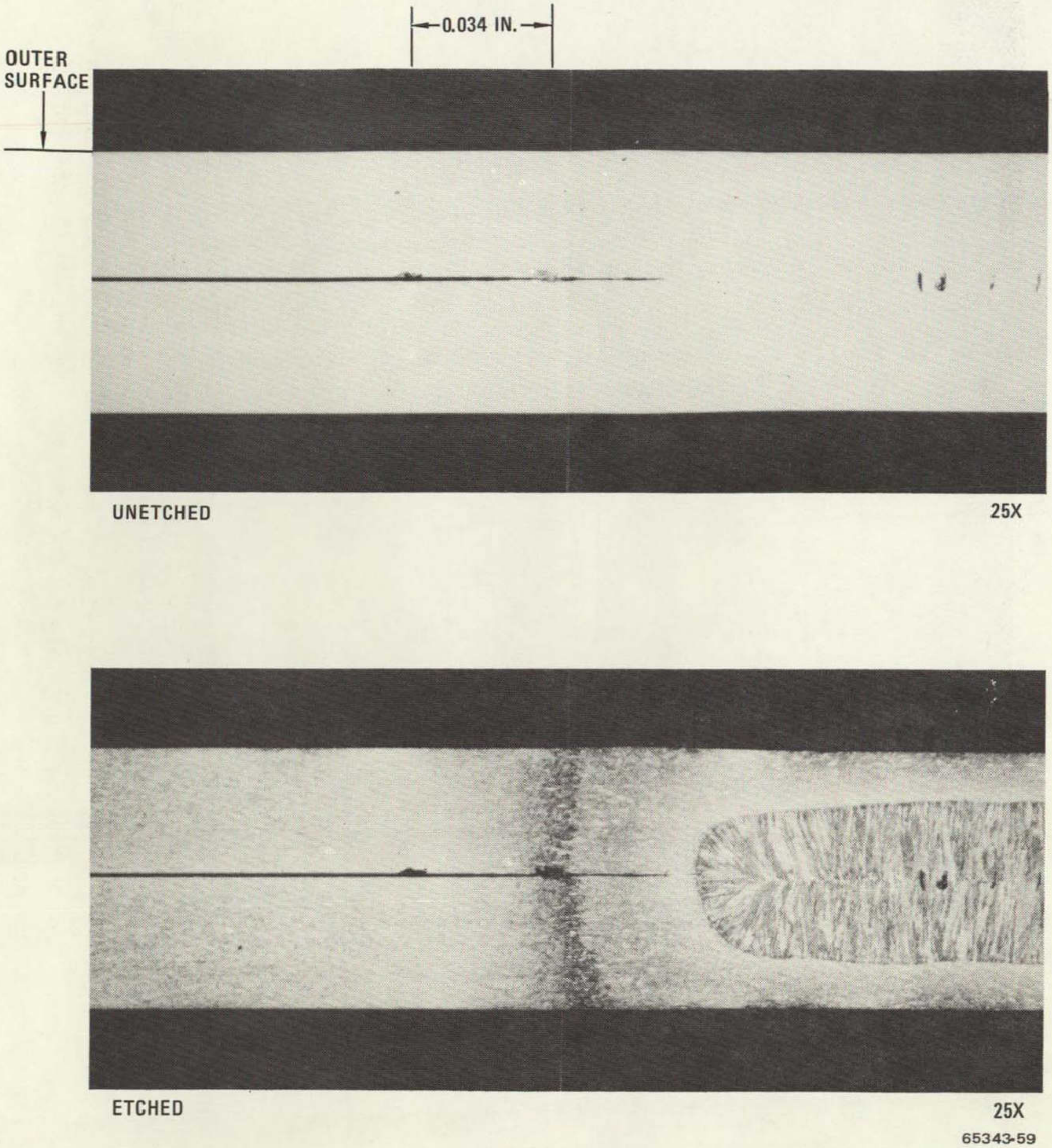

Figure 2-18. Appearance of Section B-B Through the Horizontal, "Length" Defect Indication Shown in Figure 2-16. The Defect in the Weld-Carbide-Precipitation Zone is Shown at Higher Magnification (300X) in Figure 2-19. This Section is 0.035 Inch from Section A-A

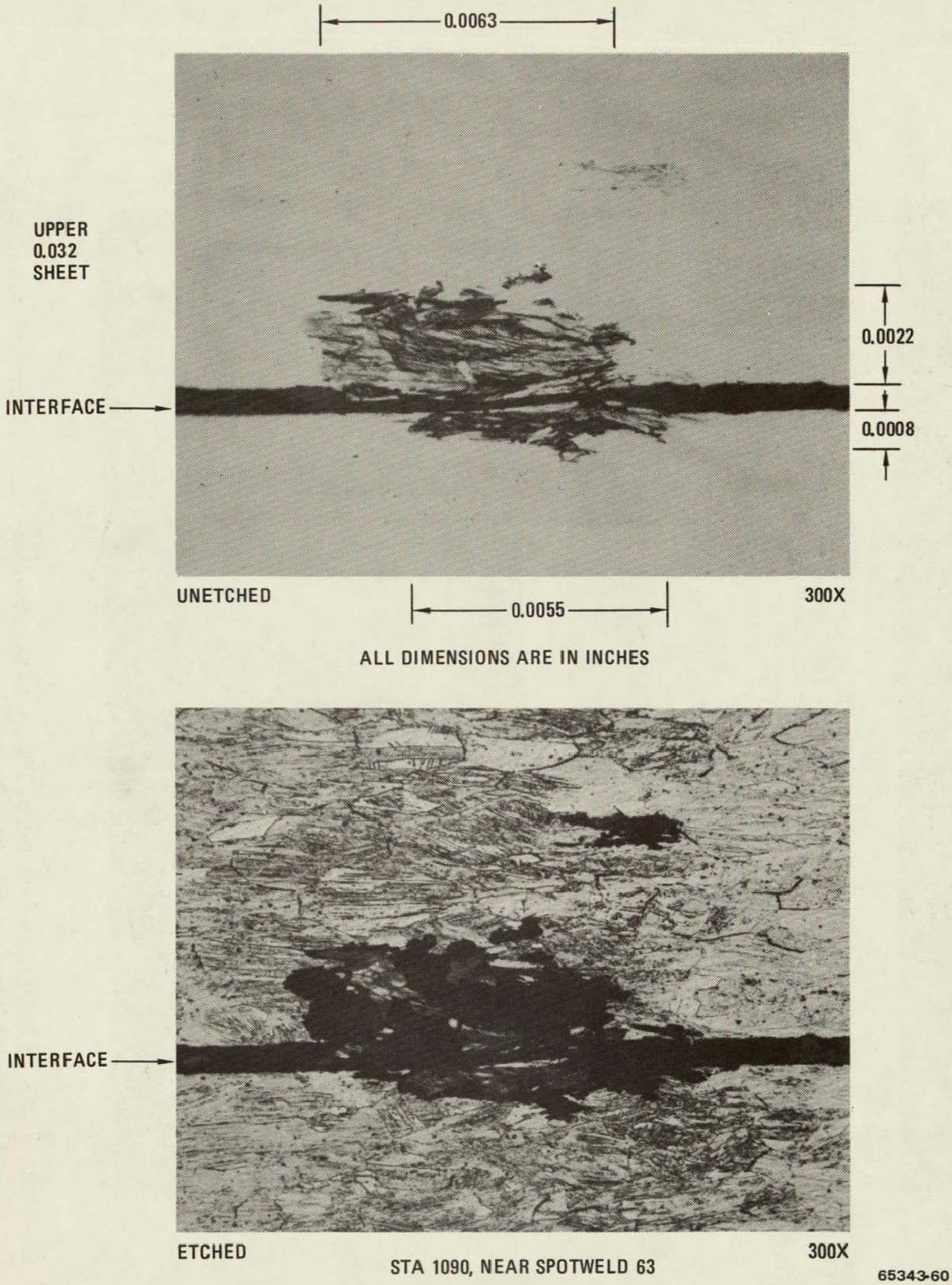

Figure 2-19. Portion of Figure 2-18 (B-B) at Higher Magnification (300X) Showing in Greater Detail the Appearance of the Corrosion Produced "Length" Defect in the Weld Carbide Zone. Dimensions of the Defect Prior to Etching are also Given

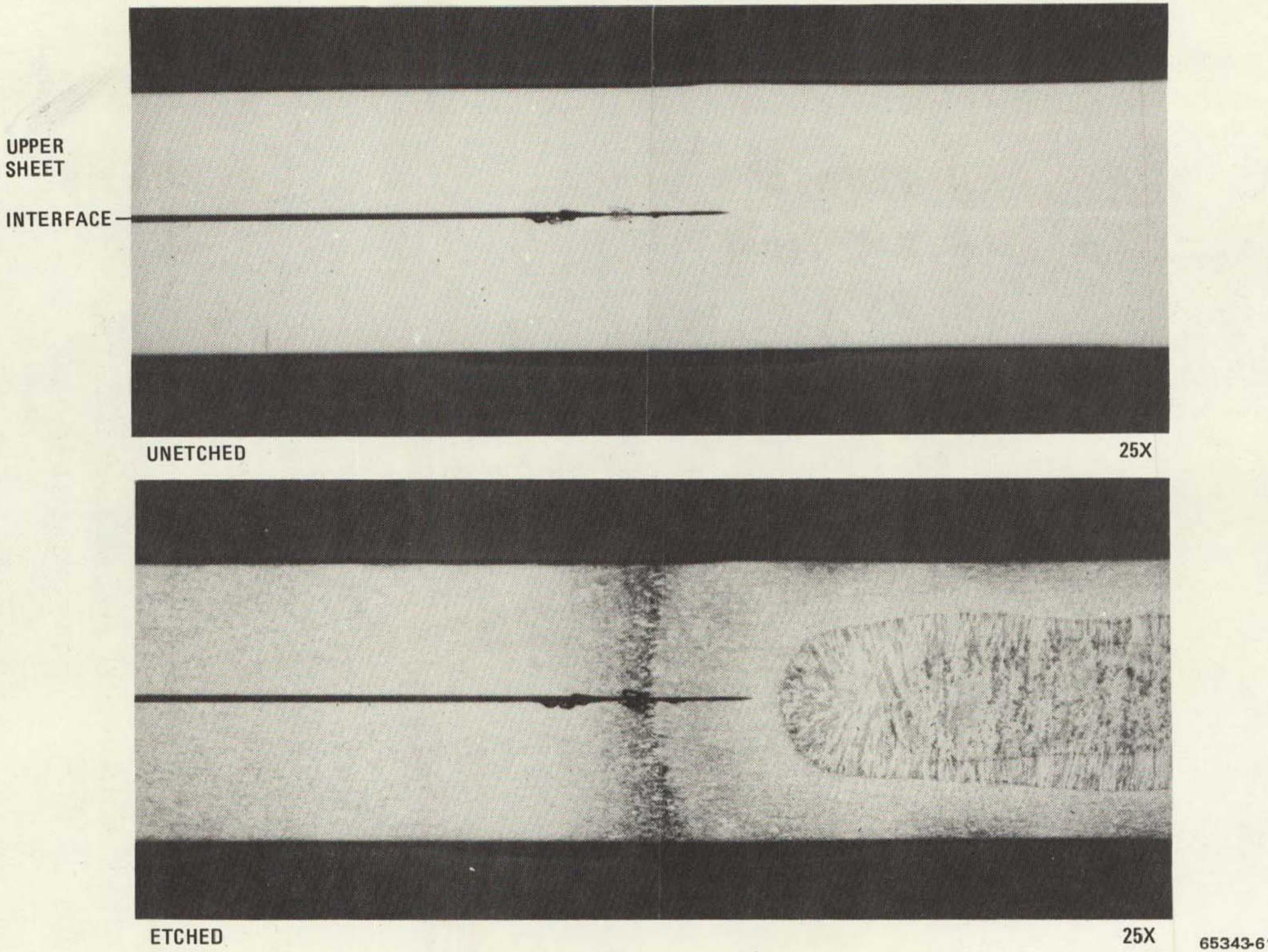

Figure 2-20. Appearance of Section C-C Shown in Figure 2-16. The Interface Defects are Shown at Higher Magnification in Figure 2-21. This Section is 0.040 Inch from Section B-B

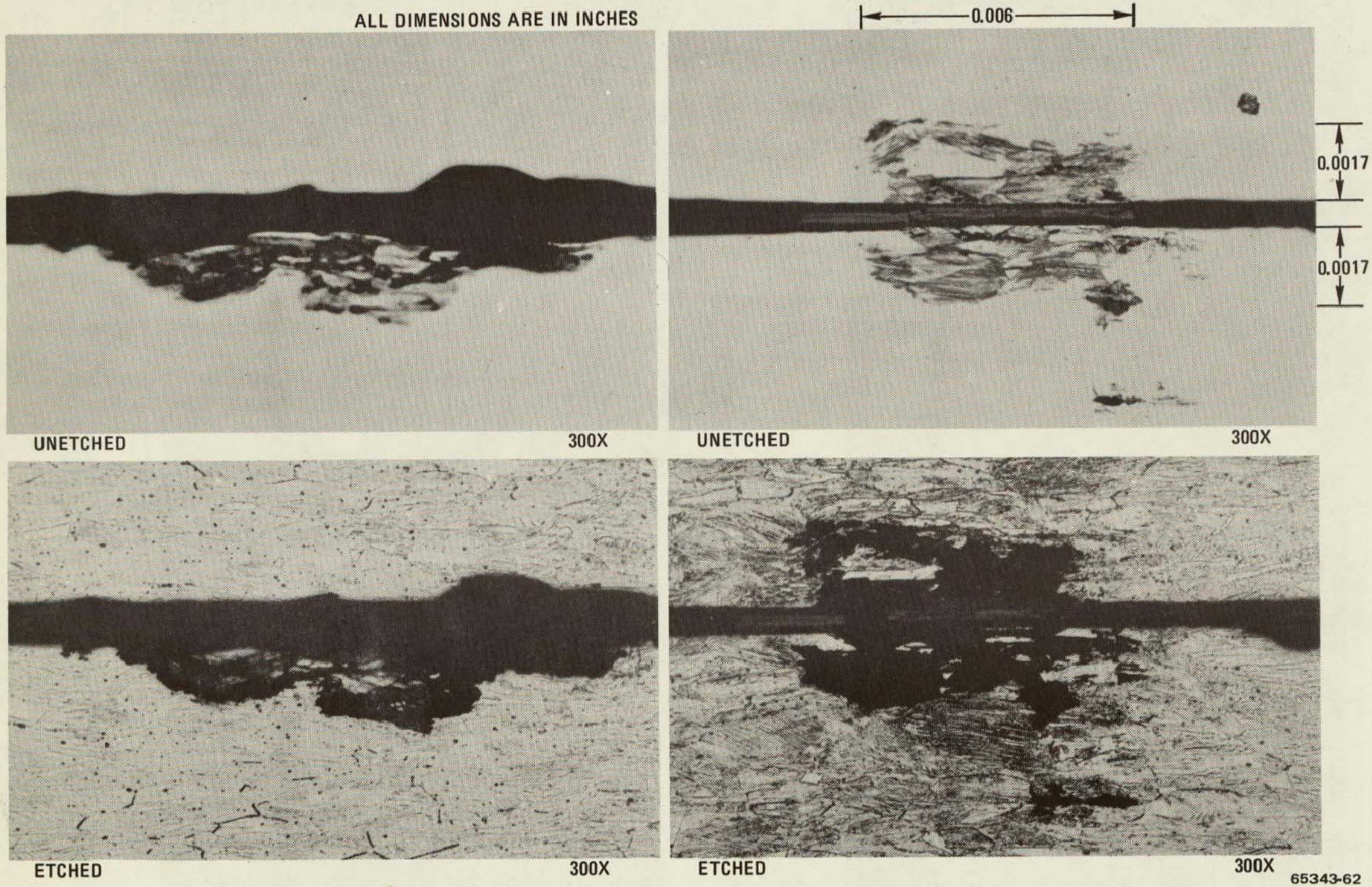

Figure 2-21. Portions of Figure 2-20 (C-C) at Higher Magnification (300X) Showing in Greater Detail the Appearance of the Corrosion Produced Defects at the Interface

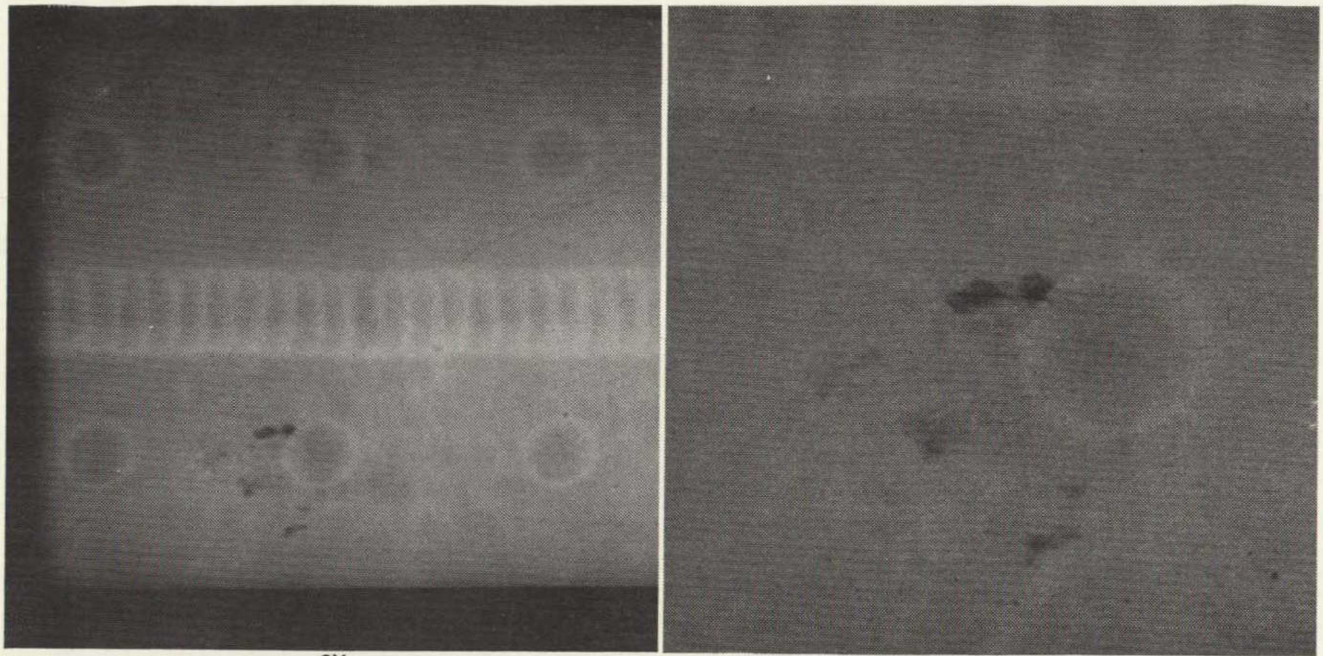

2X

5X

ABOVE – X-RAY IMAGE OF THE DEFECT MAGNIFIED 2 AND 5 TIMES
X-RAY FILM 5X5001, 3-3A, 2-17-76, DENSITY 2.47

BELOW – SAME DEFECT WITH 6 MARKER HOLES ADDED
X-RAY FILM M6, 5-12-76, DENSITY 3.22

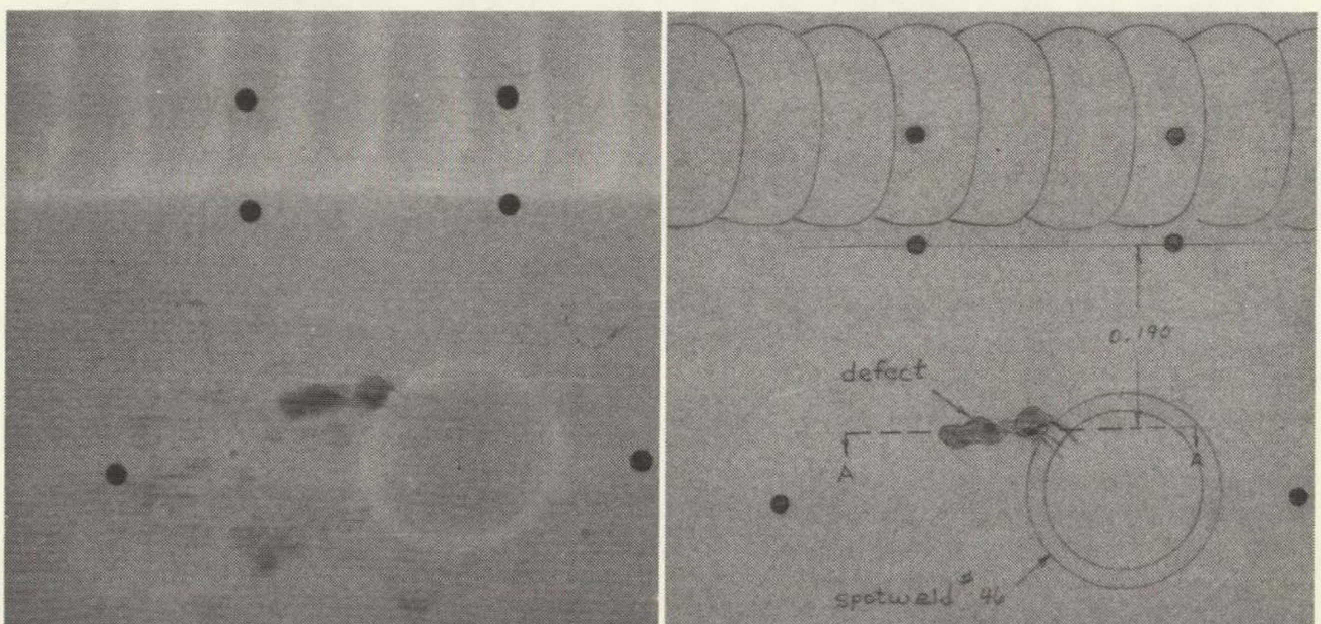

5X

STA 1090 SPOTWELD 46

65343-63

Figure 2-22. Appearance of a Horizontal, "Length" Defect Indication Adjacent to a Spotweld (Item 6), and the Location of a Section (A-A) Through the Defect (see Figure 2-23)

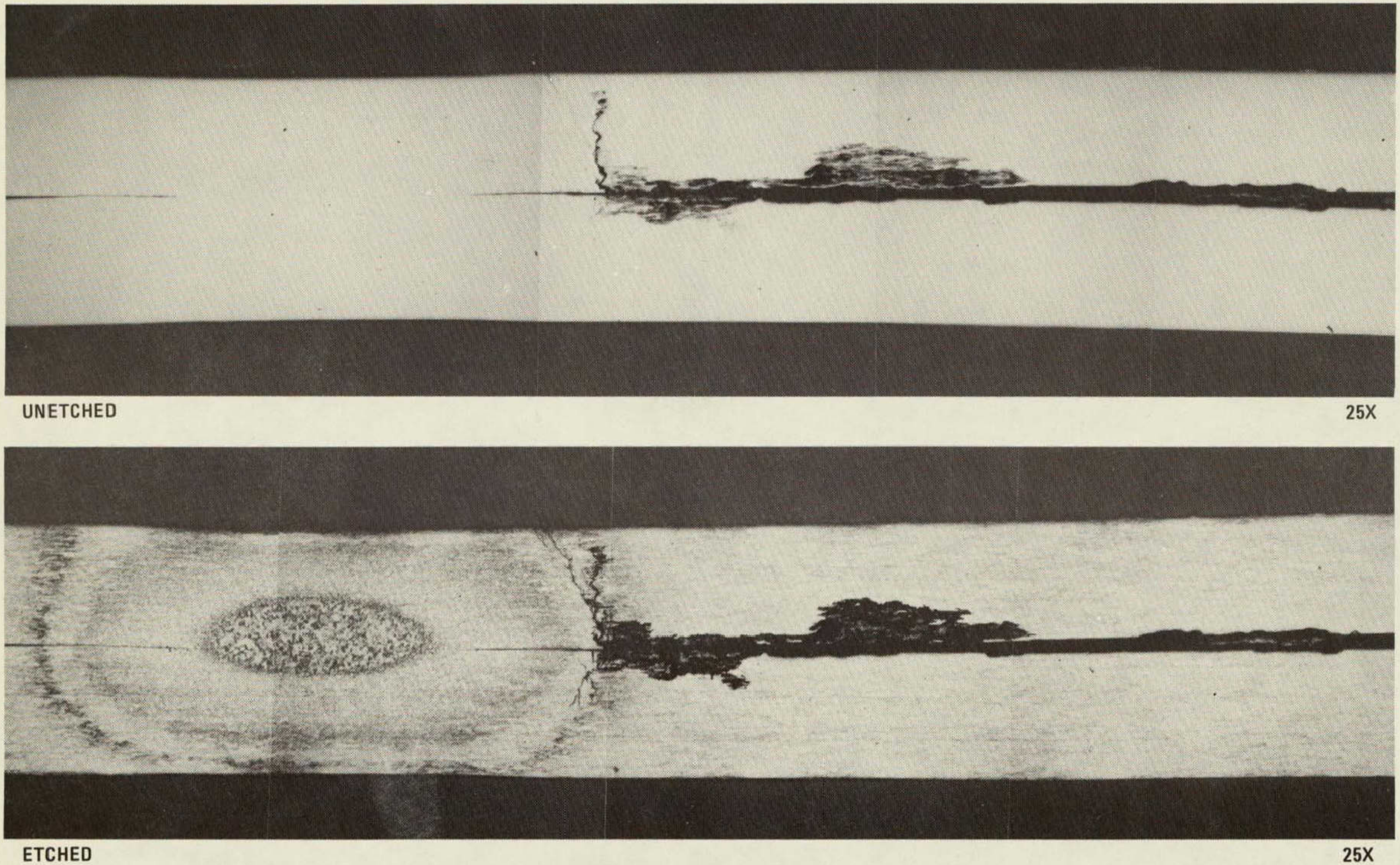

65343-64

Figure 2-23. Appearance of Section (A-A) Through the Horizontal, "Length" Defect Indication Shown in Figure 2-22. Note the Stress Corrosion Cracks in the Heat-Affected Zone of the Spotweld

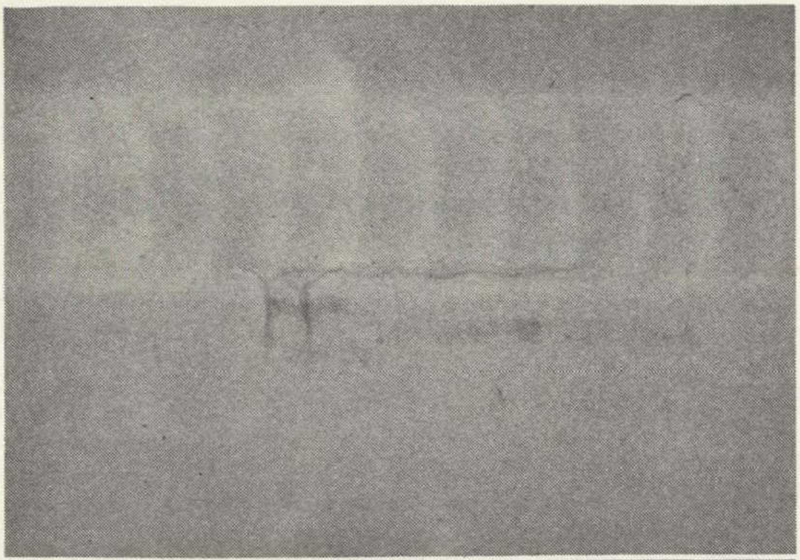

DOUBLE WALL, CONTRACTOR
FILM DATE 10-25-74
DENSITY 2.24
5X

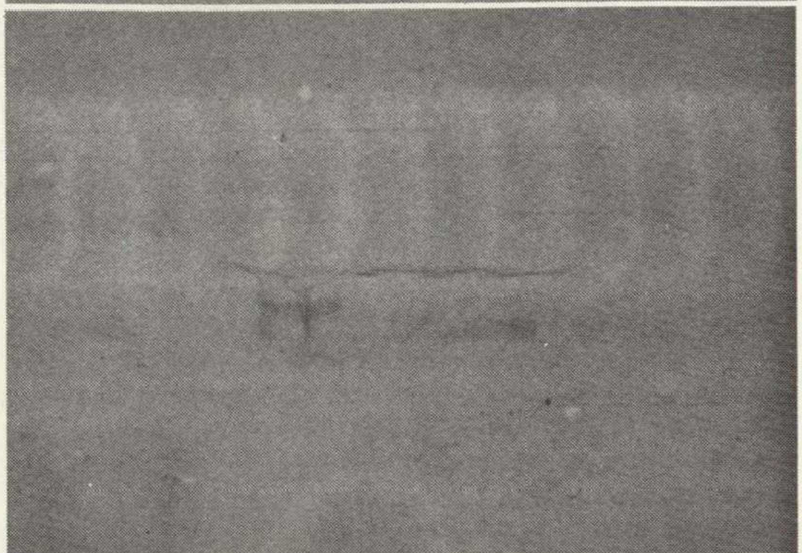

DOUBLE WALL, GD/CONVAIR
FILM DATE 9-5-75
DENSITY 2.72
5X

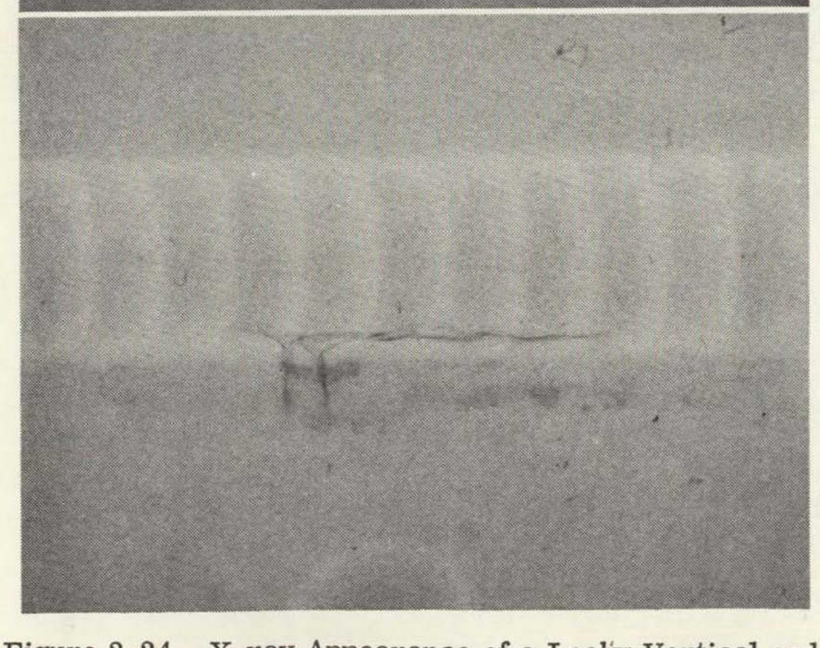

SINGLE WALL, GD/CONVAIR
FILM DATE 2-17-76
DENSITY 2.72
5X

STA 1057, NEAR SPOTWELD 20

65343-65

Figure 2-24. X-ray Appearance of a Leaky Vertical and a Leaky Horizontal Defect (Items 7 and 9) Associated with a Seamweld as Revealed by Three Different Films

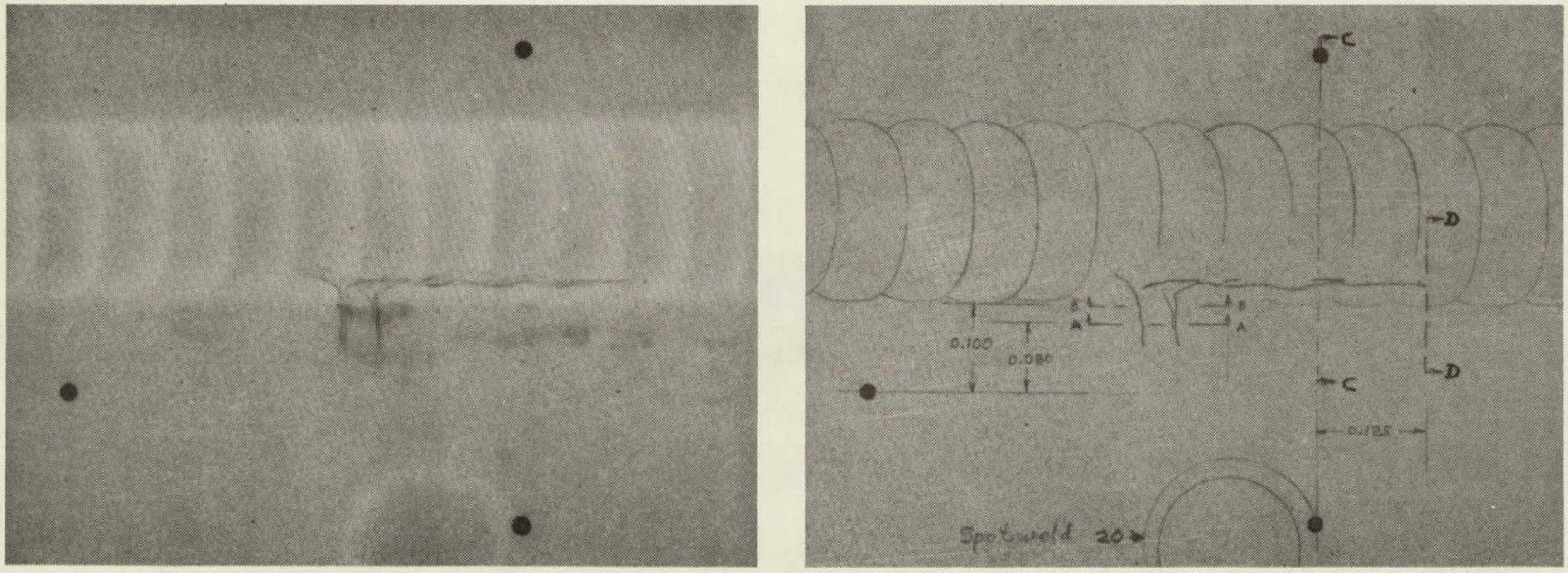

5X

SKETCH

STA 1057, NEAR SPOTWELD 20

65343-66

Figure 2-25. Same Defect Image as Shown in Figure 2-24 with 0.020-inch-diameter Marker Holes Added, X-ray Film M7, 8-16-76. The Sketch Shows the Locations of Two Sections (A-A and B-B) Through the Vertical Defects (Item 7) and Two Sections (C-C and D-D) Through the Horizontal Defect (Item 9)

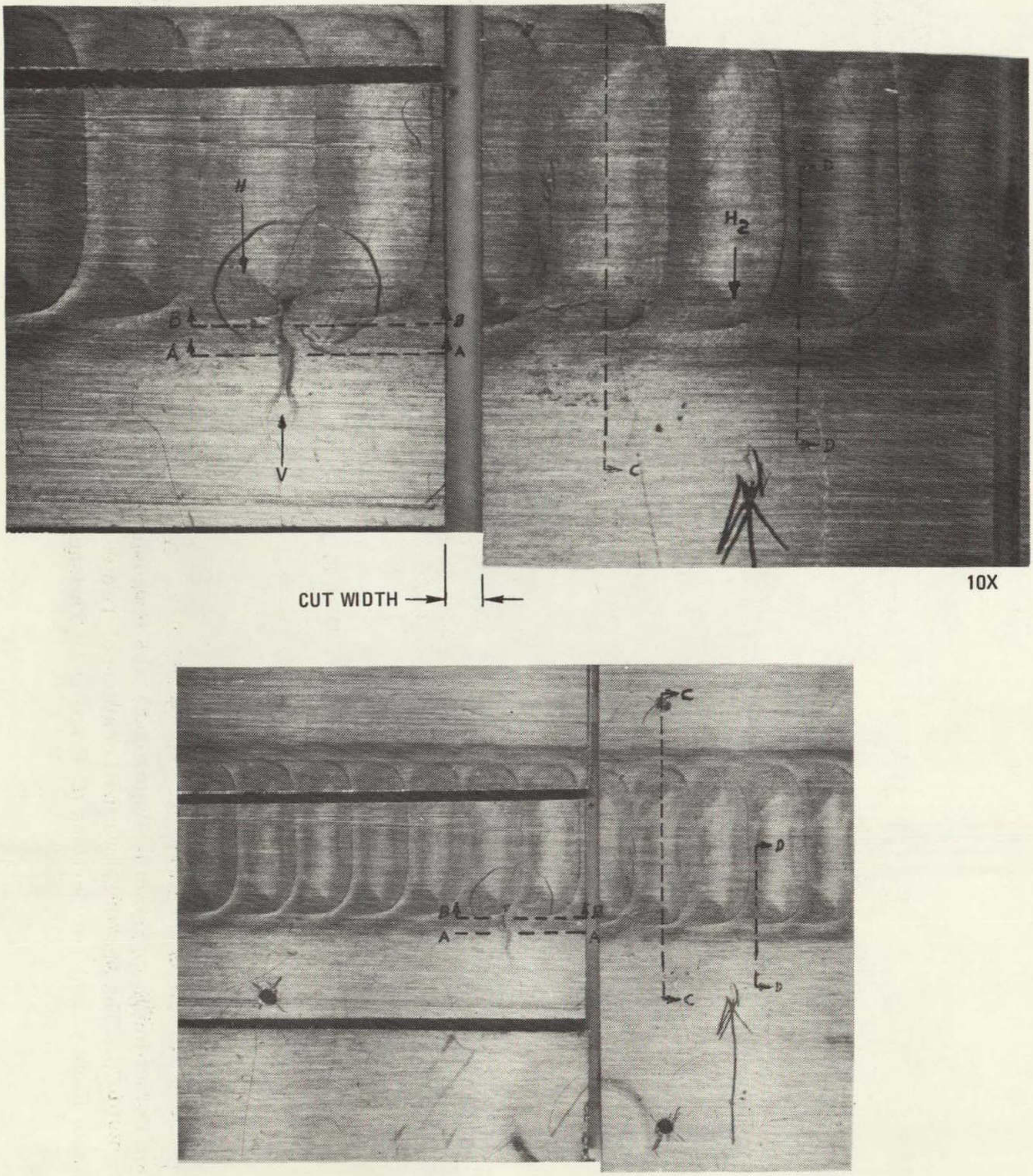

OPTICAL (LIGHT) PHOTOS
STA 2057, NEAR SPOTWELD 20

65343-67

Figure 2-26. Outside Surface Appearance of a Leaky Vertical Defect, Arrow V (Item 7) and a Leaky Horizontal Defect, from Arrow H to H_2 (Item 9) Associated with a Seamweld. Also Shown are Three 0.020-inch-diameter Marker Holes, and the Location of Four Metallographic Sections

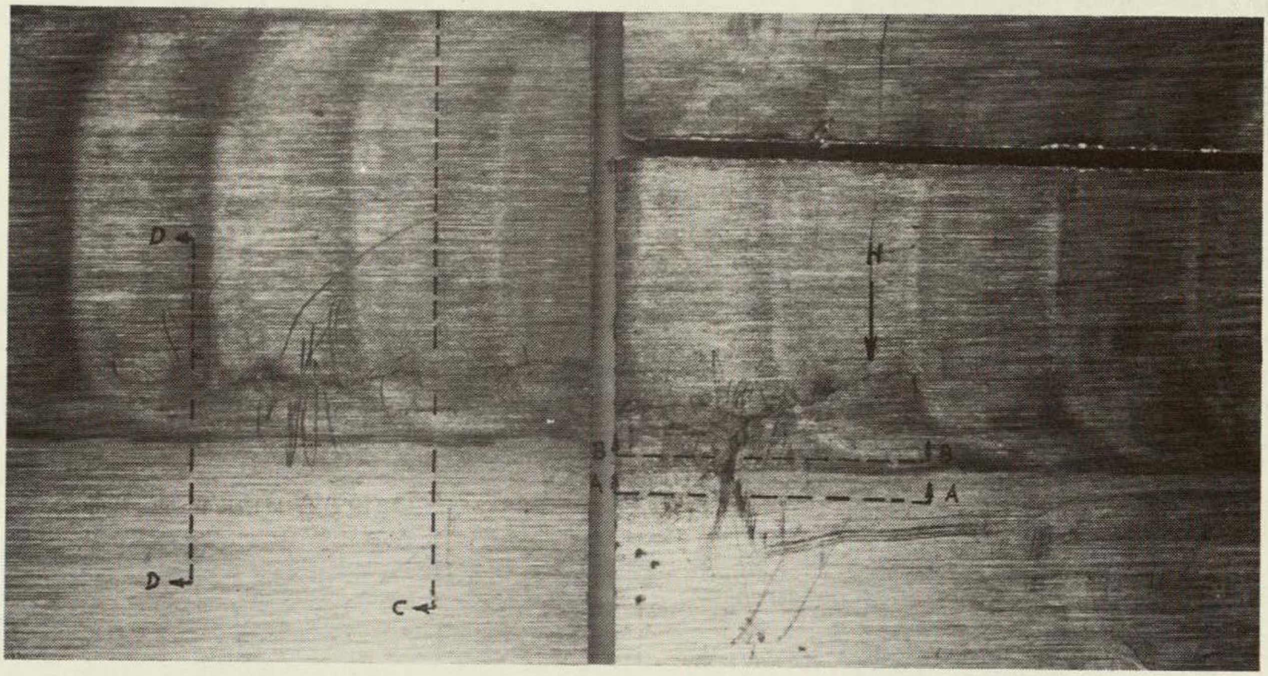

10X

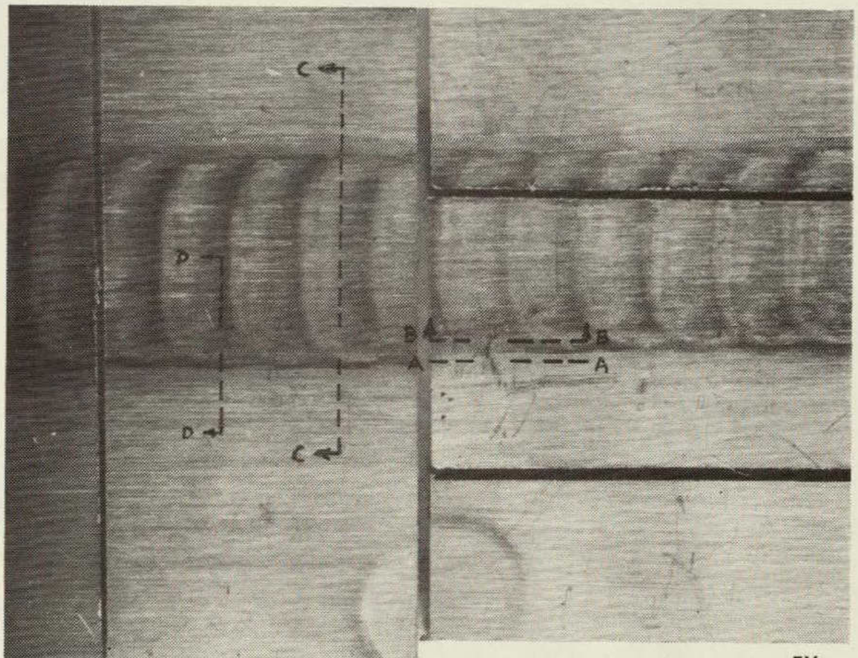

5X

SPOT 20

OPTICAL (LIGHT) PHOTOS
STA 1057, NEAR SPOTWELD 20

65343-68

Figure 2-27. Inside Surface Appearance of the Leaky Defect Shown in Figure 2-25, and the Location of the Four Sections. The Horizontal Surface Crack Extends from the D-D Section Line to Arrow H

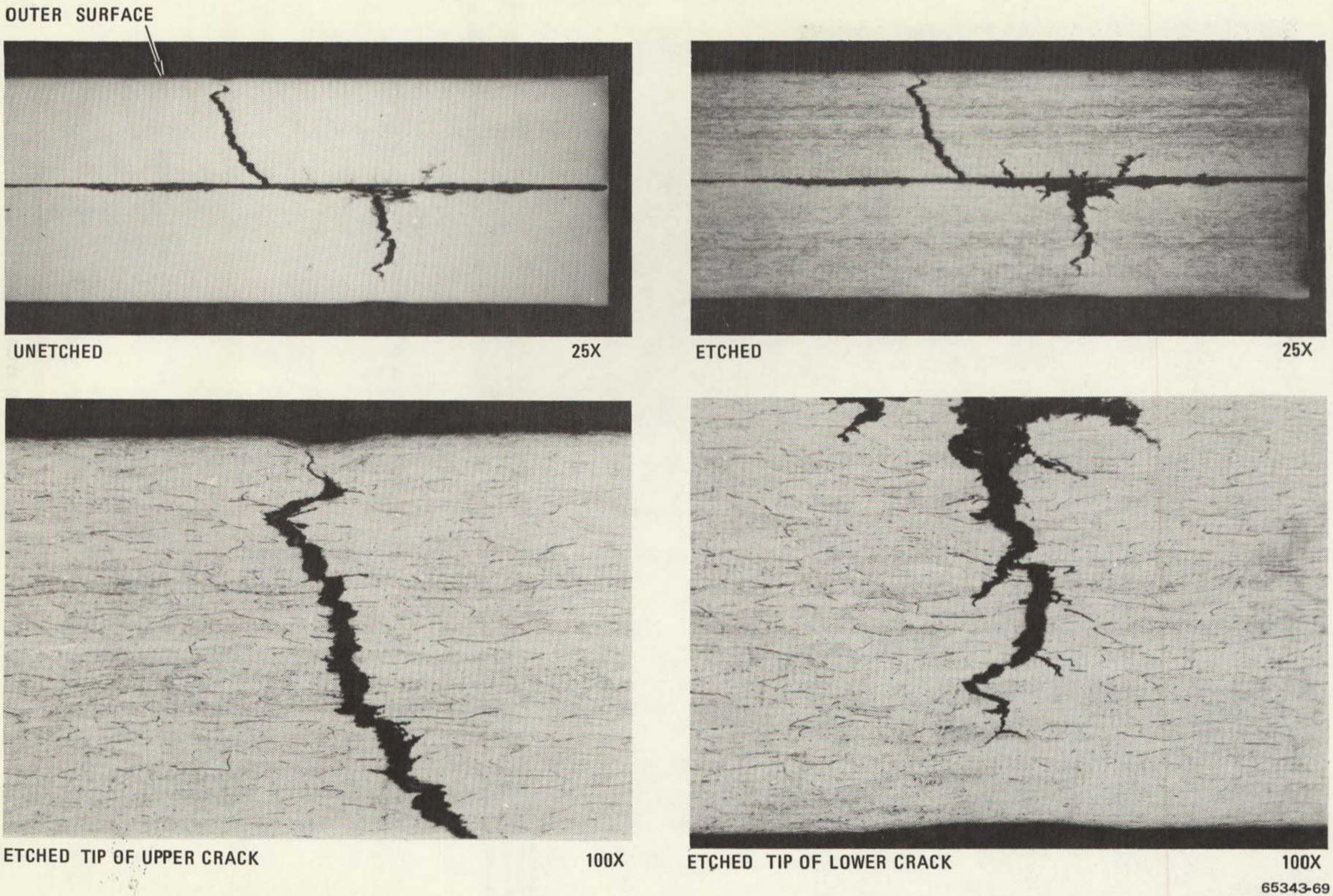

Figure 2-28. The Appearance of Section A-A Through the Vertical Defects Indications (see Figures 2-25, 2-26, and 2-27) is Shown Above. The Upper and Lower Crack Tips are Shown Below at Higher Magnification

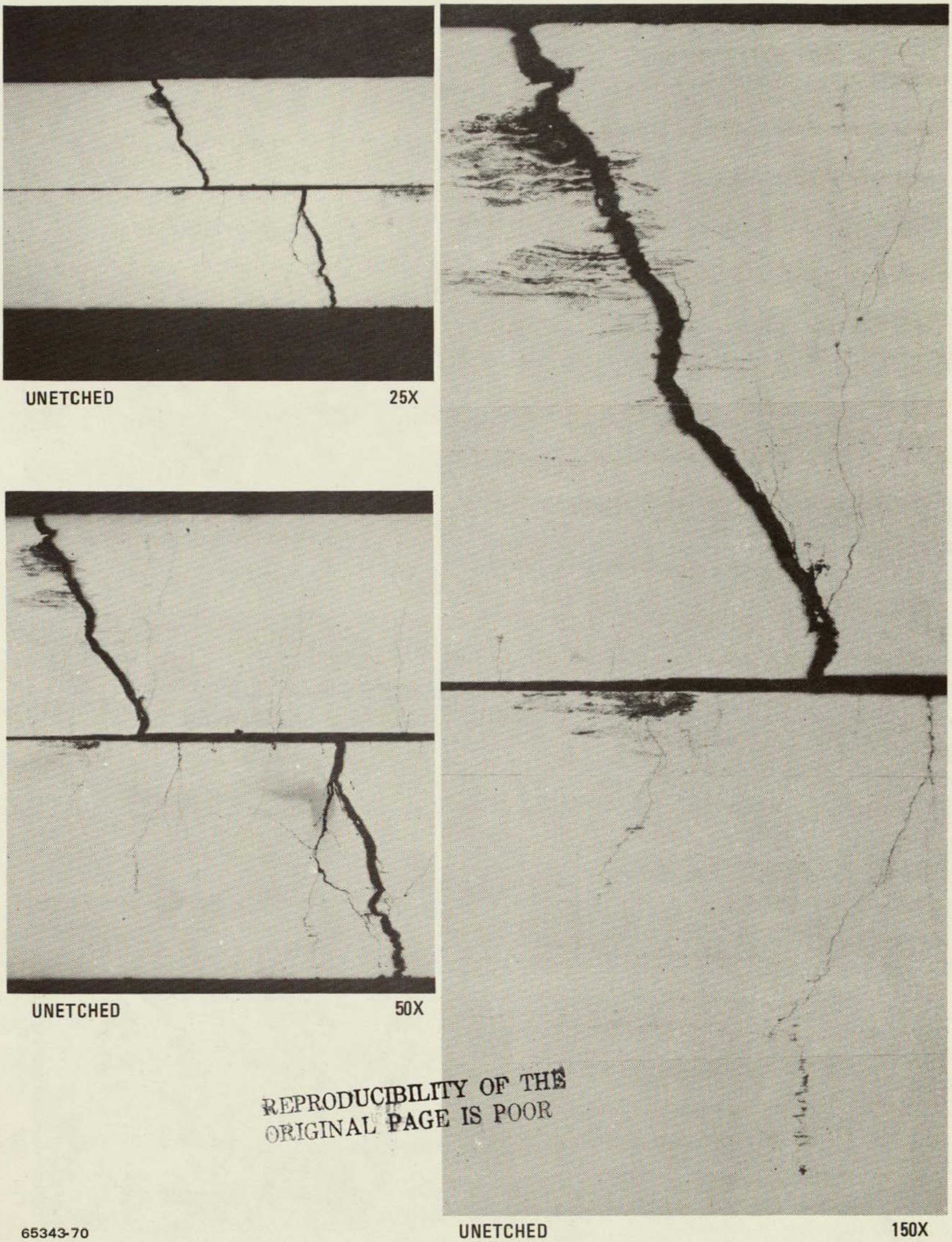

65343-70

Figure 2-29. Section Level B-B (Figure 2-25). Portions of this Section, Above and to the Right, Reveal Many Fine Stress Corrosion Cracks Propagating from the Faying Surface Toward the Exterior Surfaces

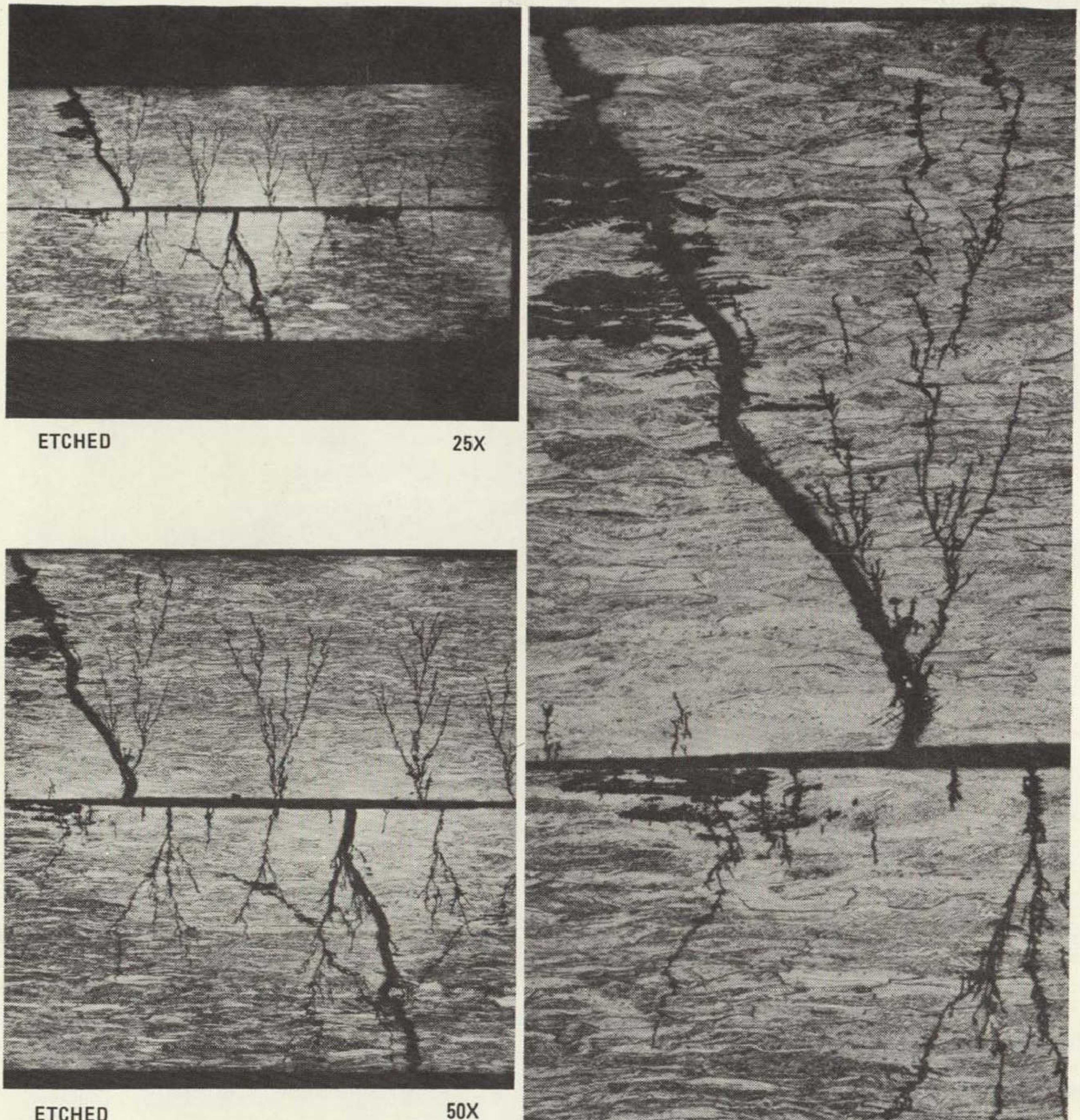

Figure 2-30. Same Areas Shown in Figure 2-29 after Etching. The Etching Broadens and Accentuates the Branching Stress Corrosion Cracks Emanating from the Faying Surface

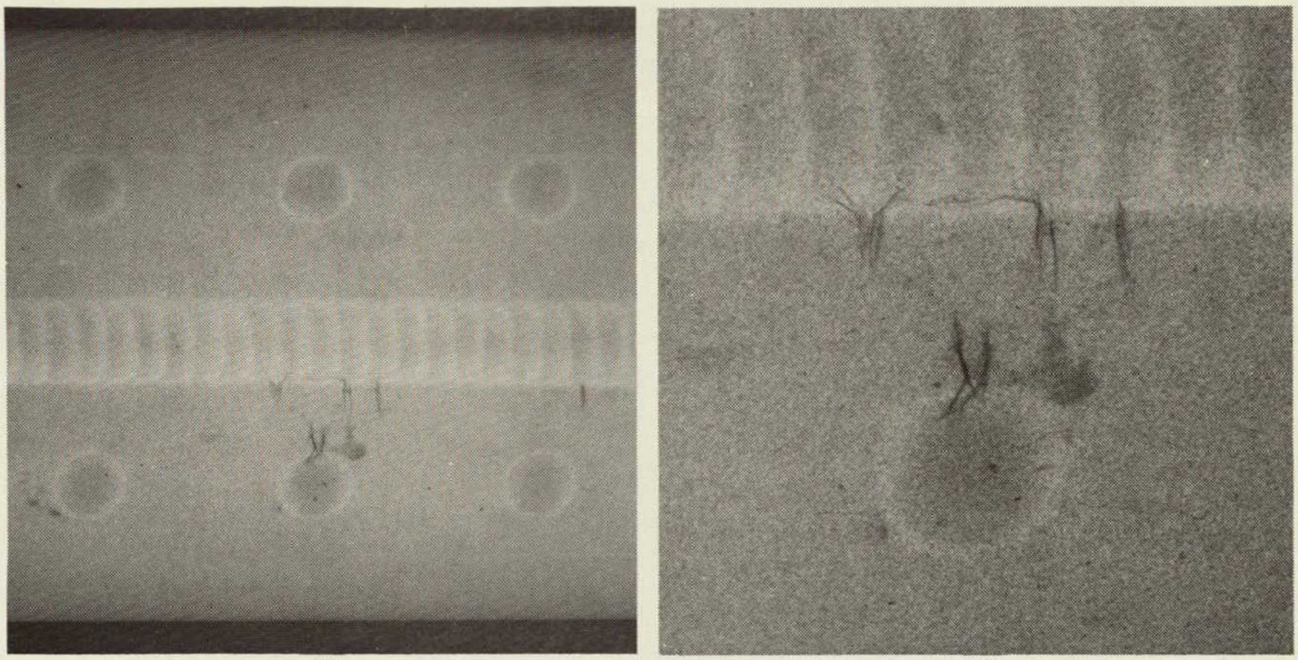

2X 5X

ABOVE – X-RAY IMAGE OF THE DEFECT MAGNIFIED 2 AND 5X
X-RAY FILM 5X5001, 3-3A, 2-17-76, DENSITY 2.47

BELOW – SAME DEFECT WITH FOUR 0.021-IN. DIAMETER
COMPLETELY THROUGH MARKER HOLES ADDED
X-RAY FILM M8, 10-11-76, DENSITY 2.52

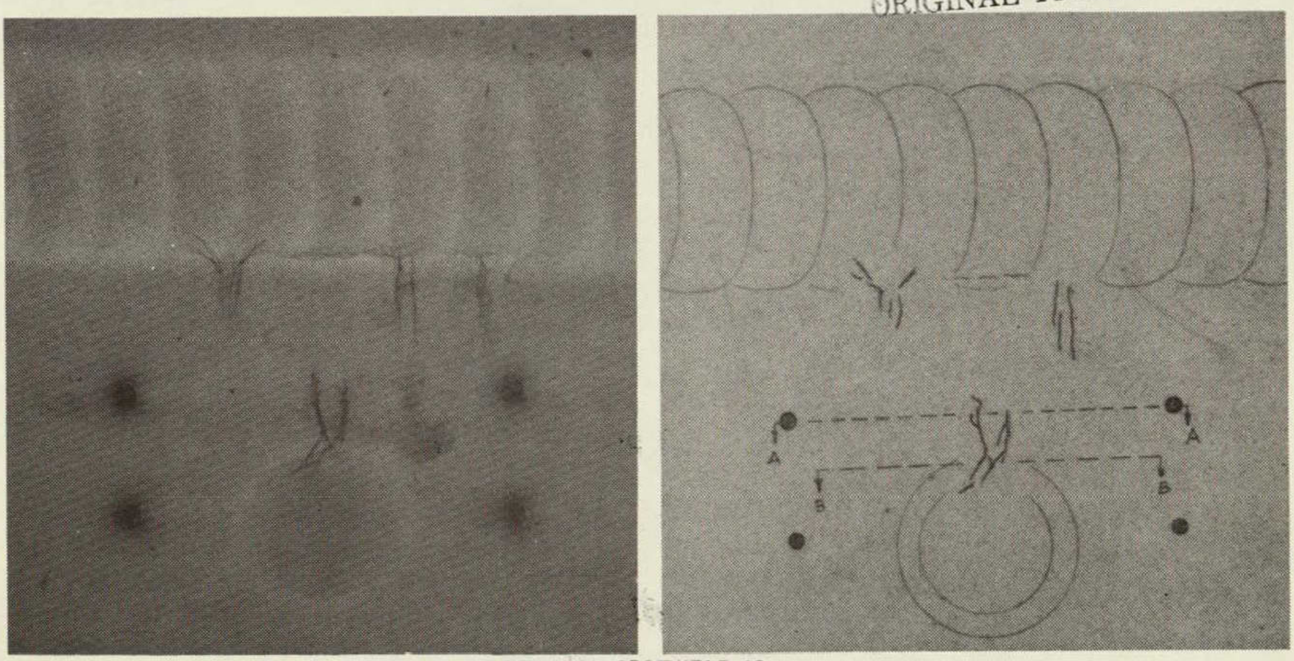

5X STA 1090 SPOTWELD 42

65343-72

Figure 2-31. X-ray Appearance of a Leaky Vertical Defect Associated with a Spotweld (Item 8) and the Locations of Two Sections (A-A and B-B) Through the Defect (see Figures 2-34 and 2-35)

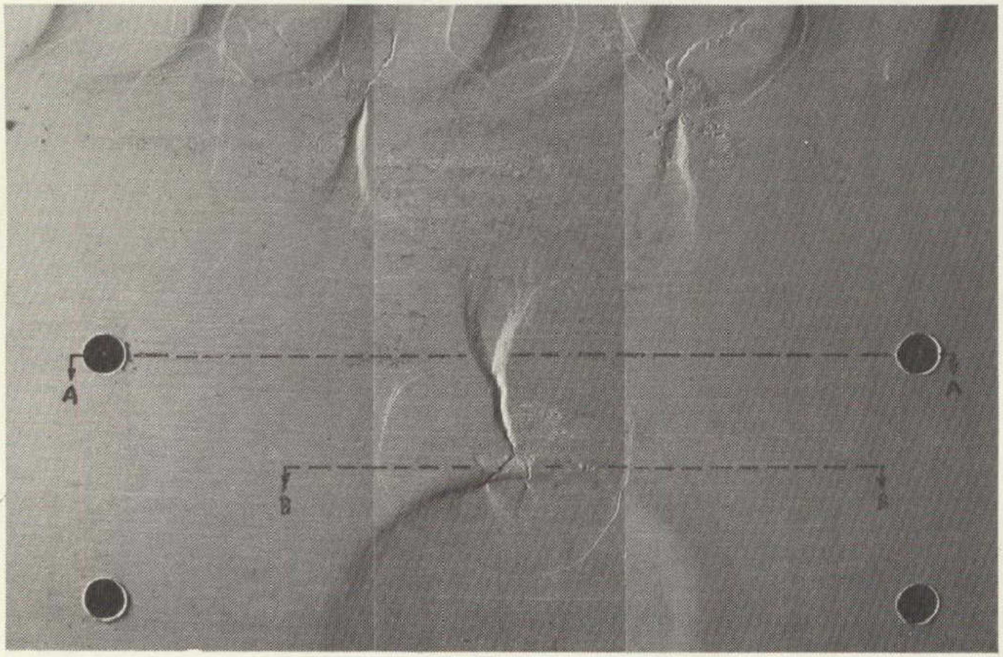

STA 1090, SPOTWELD 42 10.4X

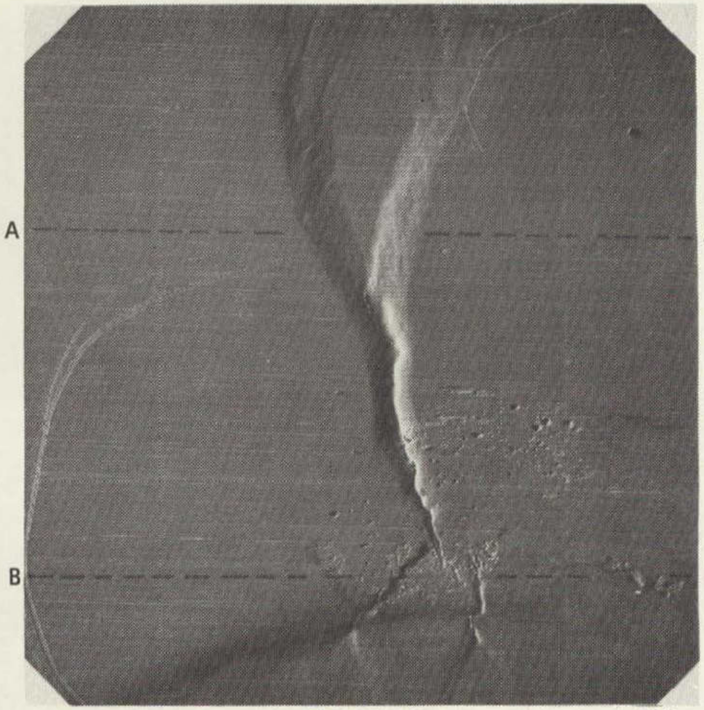

SEM PHOTOS 32X

65343-73

Figure 2-32. Outside Surface Appearance of a Leaky Vertical Defect Associated with a Spotweld (Item 8). Also Shown are Four 0.021-inch-diameter Marker Holes, and the Location of Two Metallographic Sections (see Figures 2-34 and 2-35). Note the V-shaped Depressions, Characteristic of Localized Yielding (Plastic Flow) at the Tip of a Crack (S.E.M. Photos)

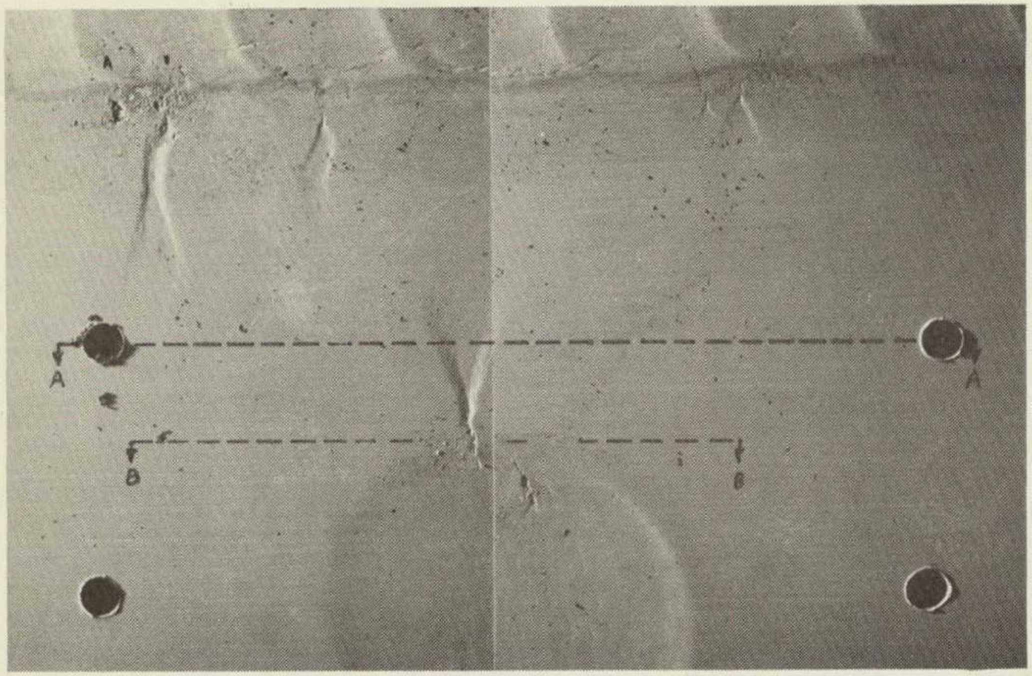

SEM PHOTOS STA 1090, SPOTWELD 42 10.6X

A A

B B

65343-74

64.5X

Figure 2-33. Inside Surface Appearance of a Leaky Vertical Defect Associated with the Same Spotweld Shown in Figure 2-31, and the Location of Two Metallographic Sections (see Figures 2-34 and 2-35) S.E.M. Photos

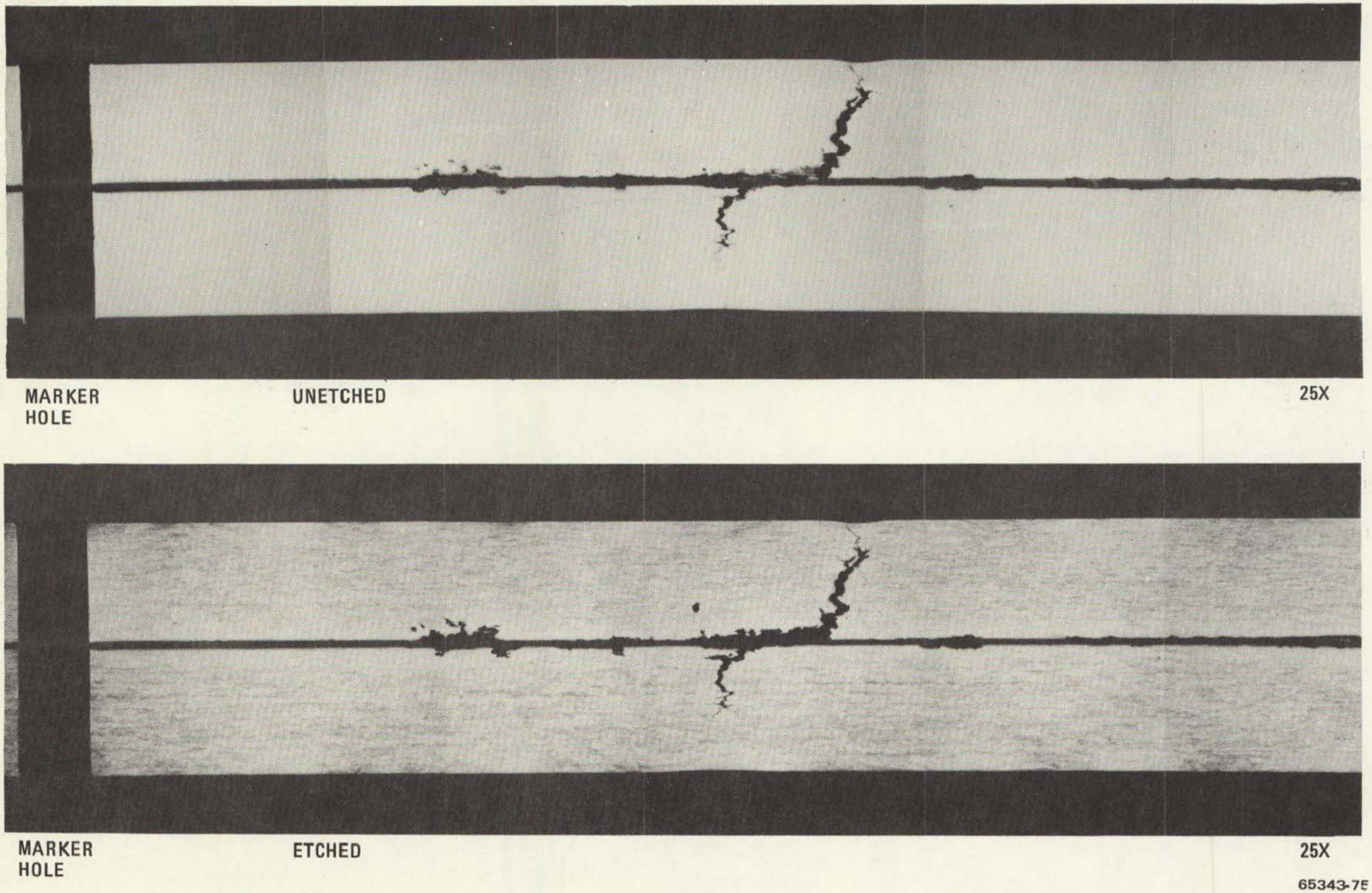

Figure 2-34. Appearance of Section A-A, described in Figures 2-31, 2-32, and 2-33, Showing Internal Cracking Beneath the Localized Surface Yielding Indications

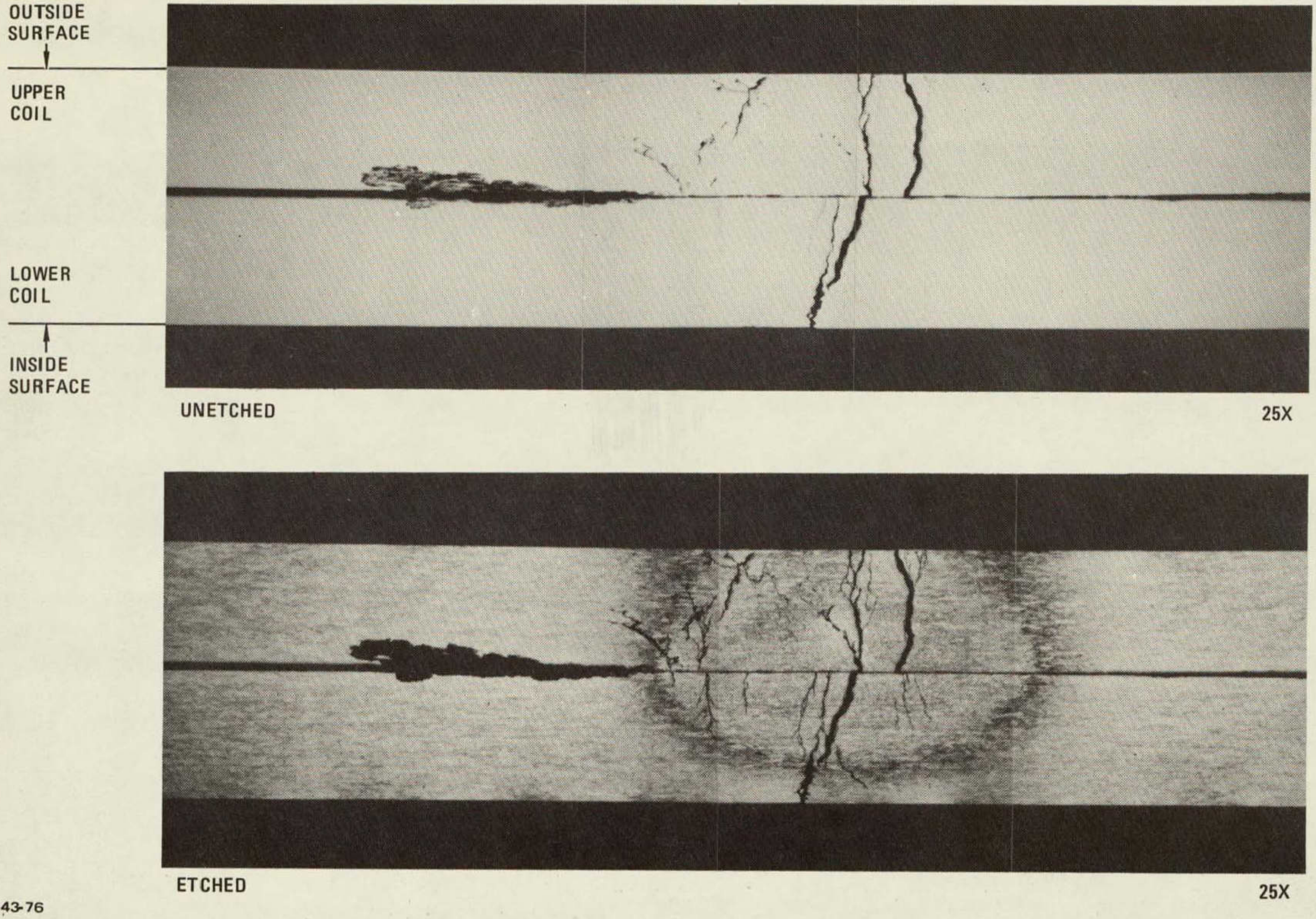

Figure 2-35. Appearance of Section B-B, Described in Figures 2-32 and 2-33, Showing Complex Stress Corrosion Cracking and a Continuous Leak Path from the Inside Surface to the Outside Surface

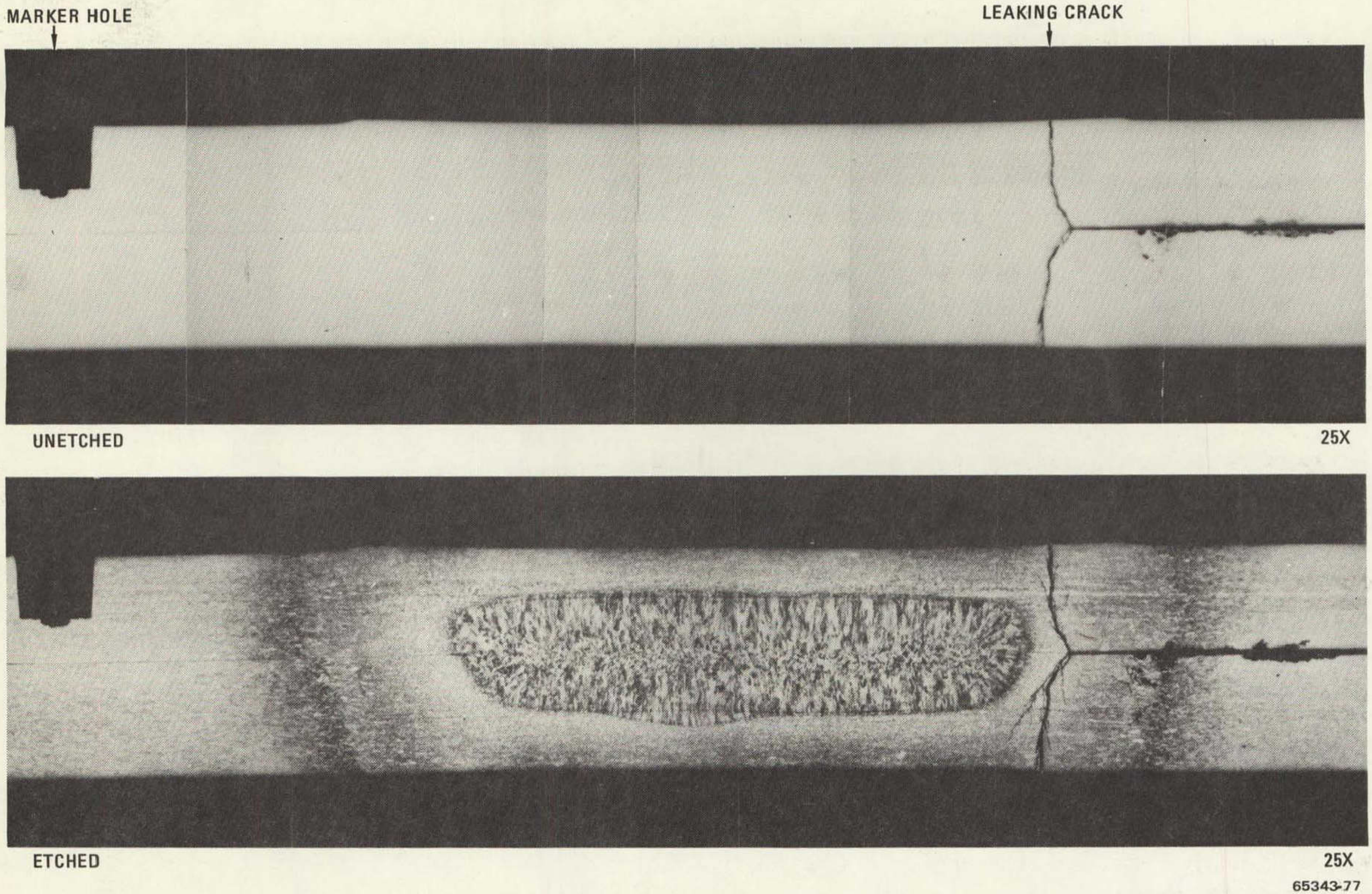

Figure 2-36. Appearance of a Section C-C Through a Visually Leaking Horizontal Defect Indication (Item 9) Shown in Figure 2-24

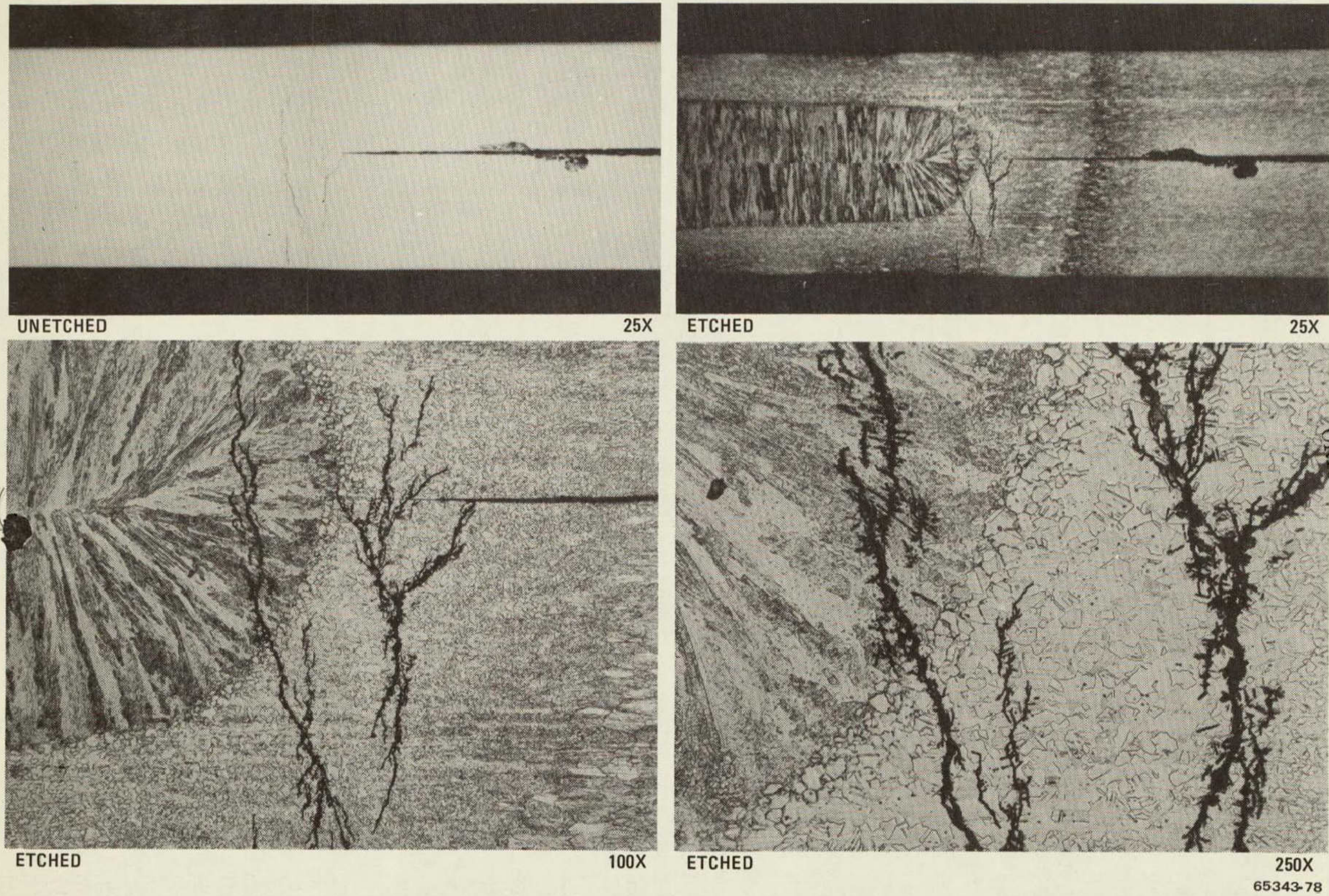

Figure 2-37. Section Level D-D, 0.125 Inch from Level C-C, Showing Stress Corrosion Cracks in Both the Soft Cast and Recrystallized Microstructures

2.3.1 DEFECT-FREE SPOTWELDS, DIAMETER AND PENETRATION. It was requested (Table 2-1, Items 11 and 12) that metallographic sections be made through a spotweld in the aft row and a spotweld in the forward row that showed no evidence of X-ray image defects. Spotweld 6 (aft) and spotweld 6 (forward) in Panel 2 (Row B, Sta. 1090) were selected, see Figure 2-4. The section plane was positioned in the center of each spotweld so that these specimens could be used for nugget diameter and penetration measurements also. In addition the overlapping spotweld row (seamweld) was sectioned. The etched appearance of each of these three sections is shown in Figure 2-38 at 25X. No defect indications were observed in any of the sections. The nugget diameters and penetrations are:

	Diameter (in.)	Penetration (%)	
Forward spotweld	0.131	55	Top (0.032)
		57	Bottom (0.033)
Aft spotweld	0.139	51	Top (0.032)
		44	Bottom (0.033)

GD/Convair specification 0-75173 requires the penetration to be in the 20 - 90% range and the nugget diameters to be 0.14 - 0.17 and 0.14 - 0.18 inch for the 0.032 and 0.033 gauge 301 XFH CRES material respectively. As may be seen, the subject spotweld nuggets meet the penetration requirements but are slightly smaller than the 0.14-inch minimum diameter requirement.

2.3.2 301 XH BASE MATERIAL, CHEMICAL AND TENSILE PROPERTIES. The chemical composition and the tensile properties of the three 301 XH CRES coils that were welded together to form Row B and C are presented in Table 2-4. The chemical composition and the mechanical property requirements of the GD/Convair specification, and also the chemical limits and aims set by the producer are listed in Table 2-5.

As may be seen from Table 2-4, the chemical and tensile properties of the three 301 XFH CRES coils meet the requirements of GD/Convair procurement specification. The carbon content (0.092%) of the 0.032 and 0.033-inch-thick coils was slightly higher than the limit of 0.09% set by the producer.

2.3.3 GRAIN BOUNDARY CARBIDES, PERCENT. In the GD/Convair procurement specification 0-71004 for the 301 XH CRES fuel tank skins, the following requirements and testing procedures for grain boundary carbides are specified:

a. Metallographic structure. The steel shall be free of grain boundary carbide network structures of either a continuous or discontinuous type in excess of 20% of the total grain boundary length.

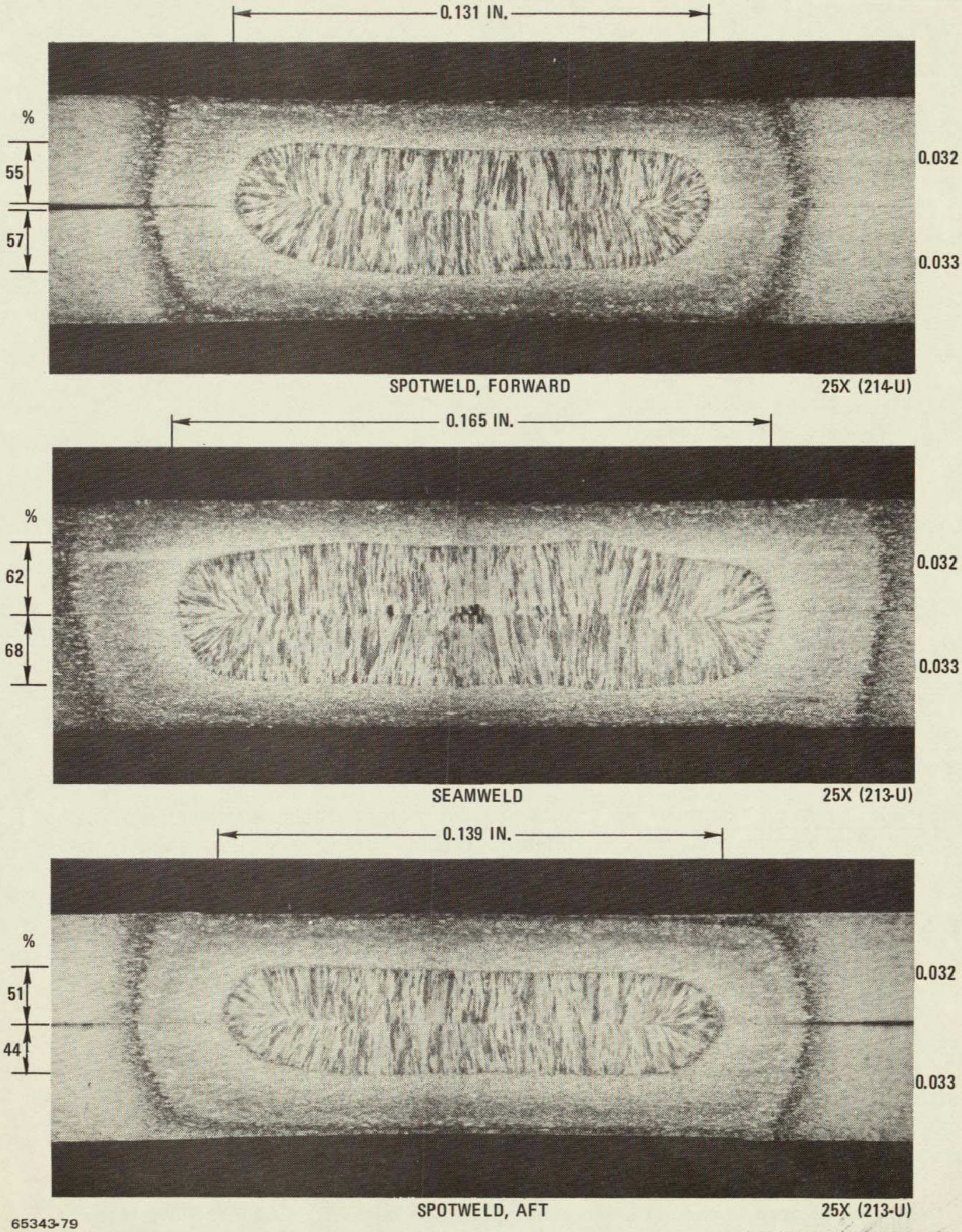

Figure 2-38. Defect-free Spot and Seamwelds

Table 2-5. Chemical and Mechanical Property Requirements

GD/Convair Spec 0-71004		Washington Steel, PA Limits	Aim
C	0.10 max	0.07 - 0.09	0.08
Mn	2.0 max	1.00 - 1.10	1.05
P	0.04 max	- 0.030 max	(1)
S	0.03 max	- 0.025 max	(1)
Si	1.0 max	0.30 - 0.70	0.45
Cr	17.0 min	17.00 - 17.50	17.25
Ni	6.5 min	6.70 - 7.10	6.85
Cu	0.50 max	-	-
N_2	0.06 max	-	-
Mo	0.50 max	-	-

(1) As low as possible. S is typically ≤0.010.
P is hard to keep low because of its presence in the scrap material. The aim is for 0.025 max.

Tensile Properties

Ftu, ksi	200 min
Fty, ksi	160 min
Elong. in 2 in. %	2 min

b. Metallographic examination. One sample for metallographic examination shall be cut from each end of each coil. Metallographic specimens shall be suitably prepared and etched in accordance with the requirements of ASTM E3-62 using sodium cyanide solution number 34 at six volts for five minutes (minimum), with the voltage maintained constant under load. The specimens shall be examined at a magnification of 250 or 500 diameters for the presence of grain boundary carbides. The results shall be compared to the requirements of (a.) for conformance.

The requirement controlling the amount of grain boundary carbide precipitation was introduced many years ago (mid '60s) into all of the GD/Convair procurement specifications concerned with cold-worked 301 CRES coils (1/2H, 3/4H, XFH, etc.) to control cryogenic notched tensile properties, not corrosion resistance.

The specimens used to check for the amount of grain boundary carbides were transverse sections cut from the cold-worked base metal near spotweld 5 in Panel 1 and near spotweld 6 in Panel 2 (see Figure 2-3 and 2-4). The summed total length of grain boundary carbide precipitation (black lines) in a 0.0045-by 0.009-inch area,

located in the center of each section, was determined. This is the normal receiving-inspection-type procedure that was used, and is being used, to check incoming material. However, in this particular problem, of interest are microstructural characteristics that may affect the surface corrosion resistance, not cryogenic notched tensile properties.

As may be seen in Figure 2-39, there was a region (layer) of material extending from each surface inward about 0.002 to 0.003 inch that contained no evidence of grain boundary carbides. This is logical, because these carbides form just after a coil comes out of the 2050°F annealing furnace in the 1600 to 800°F segment of the steam-quench cool-down cycle. The cooling rate will be slower in the center of the 0.072-inch-thick coil as compared to the surface. This metallographic evidence indicates, therefore, that the internal carbides formed during the cool-down after the final anneal cannot be a factor in the initial stages of surface corrosion attack.

The results of the grain boundary carbide measurements are listed in Table 2-6.

2.3.4 <u>FAYING SURFACE APPEARANCE</u>. To compare the appearance of a portion of the aft faying surface with the forward faying surface, spotwelds 1 through 5 of Panel 2 (Row B, Sta 1090) were drilled out. This allowed a 0.65-inch-wide by 2.95-inch-long portion of each faying surface to be opened up by appropriate cutting of the seamweld. As shown in Figure 2-40, a considerable amount of rust-colored foreign material (apparently a corrosion product) was present in the aft faying surface. Only a slight amount of staining was observed in the forward faying surface.

2.3.5 <u>ELEMENT ANALYSES, COMPARISON</u>. To obtain some information on the chemical nature of the laminated mixture of materials discovered in the low-density defect indications of Items 1 and 2 (Figures 2-6 and 2-9), semi-quantitative analyses for elements greater than atomic number 12 (Mg) were made in the defect area and, for comparison, on a similar sized area on the base metal (301 CRES) using the X-ray energy dispersive accessory on the scanning electron microscope. The results are presented in Figure 2-41. The white material (see Figure 2-8) in this laminated mixture was determined to be 301 CRES base metal.

2.3.6 <u>ETCHING</u>. In most cases the appearance of each section plane is documented photomicrographically in both the as-polished and etched condition. Electrolytic 10% oxalic acid etchant was used in all cases except for the carbide checks.

2.3.7 <u>EXPOSED DOGBONE TENSILE SPECIMEN, DEFECT IMAGES</u>. Radiographs of some of the corrosion-exposed tensile specimens had long, dark defect-type images extending in from the outer edge of the tensile specimen. These images ran parallel to the grain direction. The radiographic image appearance of three of these defects (labeled A, B, and C) is shown in Figure 2-42 for Pt. Loma specimen "Q". Defect A was first sectioned in the plan-view direction to about 0.003 inch beneath the surface (see Figure 2-43). The remaining material was then sectioned in the transverse

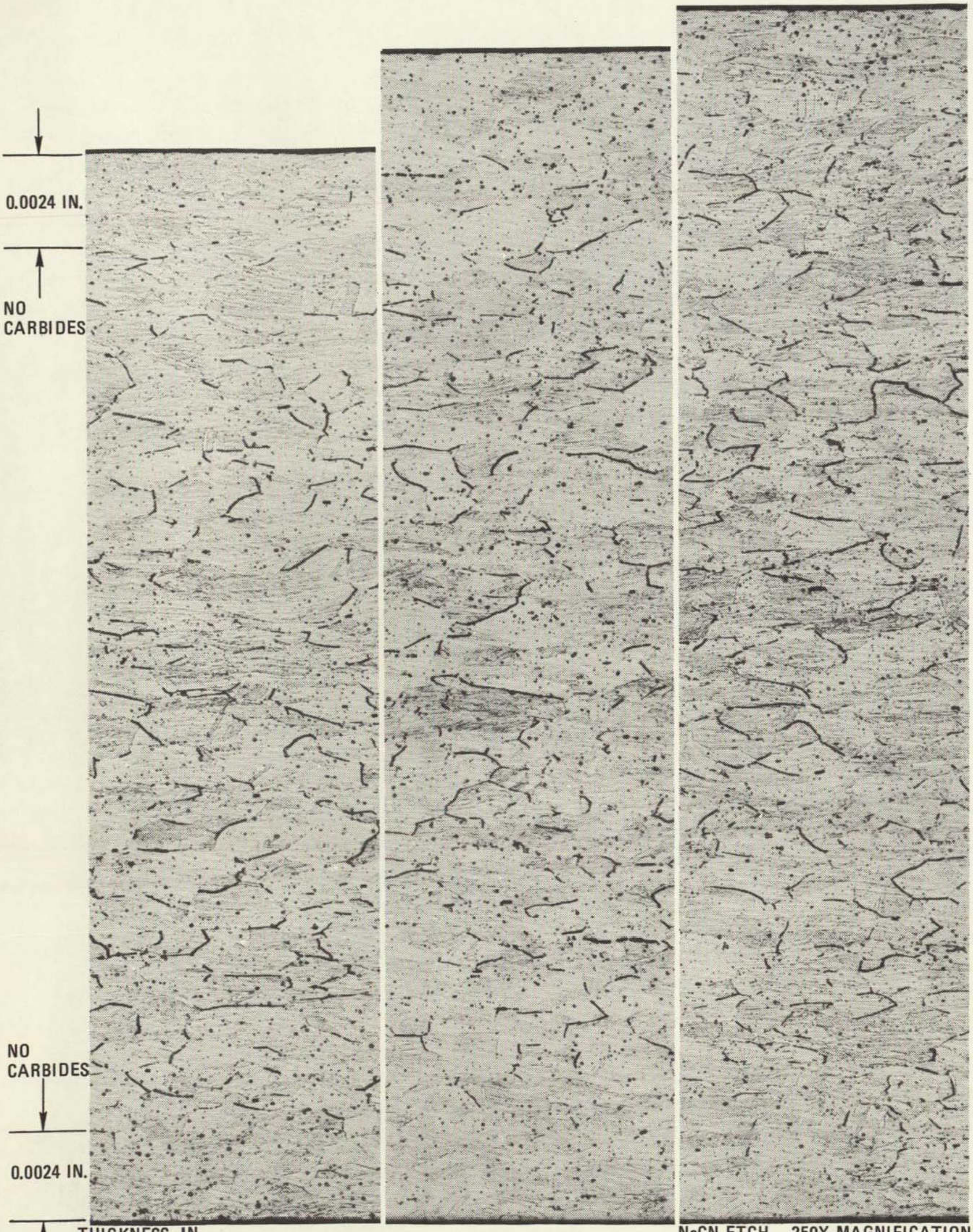

NaCN ETCH 250X MAGNIFICATION

THICKNESS, IN.			
NOMINAL	0.030	0.032	0.033
MEASURED	0.0293	0.0320	0.0331
CARBIDES, %	19	20	24

65343-80

Figure 2-39. Grain Boundary Carbide Distribution

Table 2-6. Grain Boundary Carbide Measurements

Nominal 301 XFH CRES Thickness (inch)	Carbides (%)	Section Location and ID		
		Panel	Spot	Mt. No.
0.030	19	1	5 (fwd)	709-u
0.032	20	1	5 (aft)	709-u
0.032	25	2	6 (fwd)	710-u
0.033	24	2	6 (aft)	710-u

direction at a level 0.106 inch from the outer edge (see Figure 2-44). Defects B and C were progressively sectioned to a total depth of 0.033 inch. The appearance of eight of the section levels is shown in Figure 2-45.

The sectioning revealed that the defect images were caused by long, corrosion pits or tunnels running parallel to the grain direction.

2.4 INTERPRETATION AND DISCUSSION

To accurately and fully interpret radiographic images of resistance-spotwelded, overlap joints in cold-worked 301 CRES, some understanding is needed of the material, the joining process, and the interrelationship between the two. Accordingly, a short discussion is presented here on the metallurgy and microstructure of 301 XFH CRES, and the effects of resistance spot and seam welding.

The three subject 301 XFH CRES coils were work-hardened to high tensile strength by cold-rolling annealed material. A 50 to 55% reduction in thickness is usually required to produce the extra full hard (XFH) temper. Relative to the microstructure, this work-hardening-by-rolling operation transforms the soft, single-phased, austenitic microstructure into a hard, multi-phased, microstructure consisting primarily of cold-worked martensite and cold-worked austenite. The typical etched, microstructural appearance of cold-worked 301 is shown in Figure 2-13 at 100X. The heat of the spotwelding operation transforms the hard (about 200 ksi Fty) multi-phased microstructure back into soft (about 60 ksi Fty) single-phased austenite in the heat-affected zone (HAZ) around the weld nugget. The weld nugget itself has a cast microstructure because the temperatures were high enough to melt the alloy in this localized, ellipsoidal-shaped volume. In addition, during the spotwelding process the alloy actually yielded (upset), forming a ring-shaped region about 0.001 to 0.002 inch thicker than the sum of the original thicknesses. Although this does not appear to be very much, it is 1.5 to 3.5% of the original total thickness (0.032 + 0.033 = 0.065). Since the currently used X-ray equipment consistently produces radiographs having a sensitivity better than 2%, these thicker, ring-shaped regions appear as white (actually lighter grey) ring-shaped images

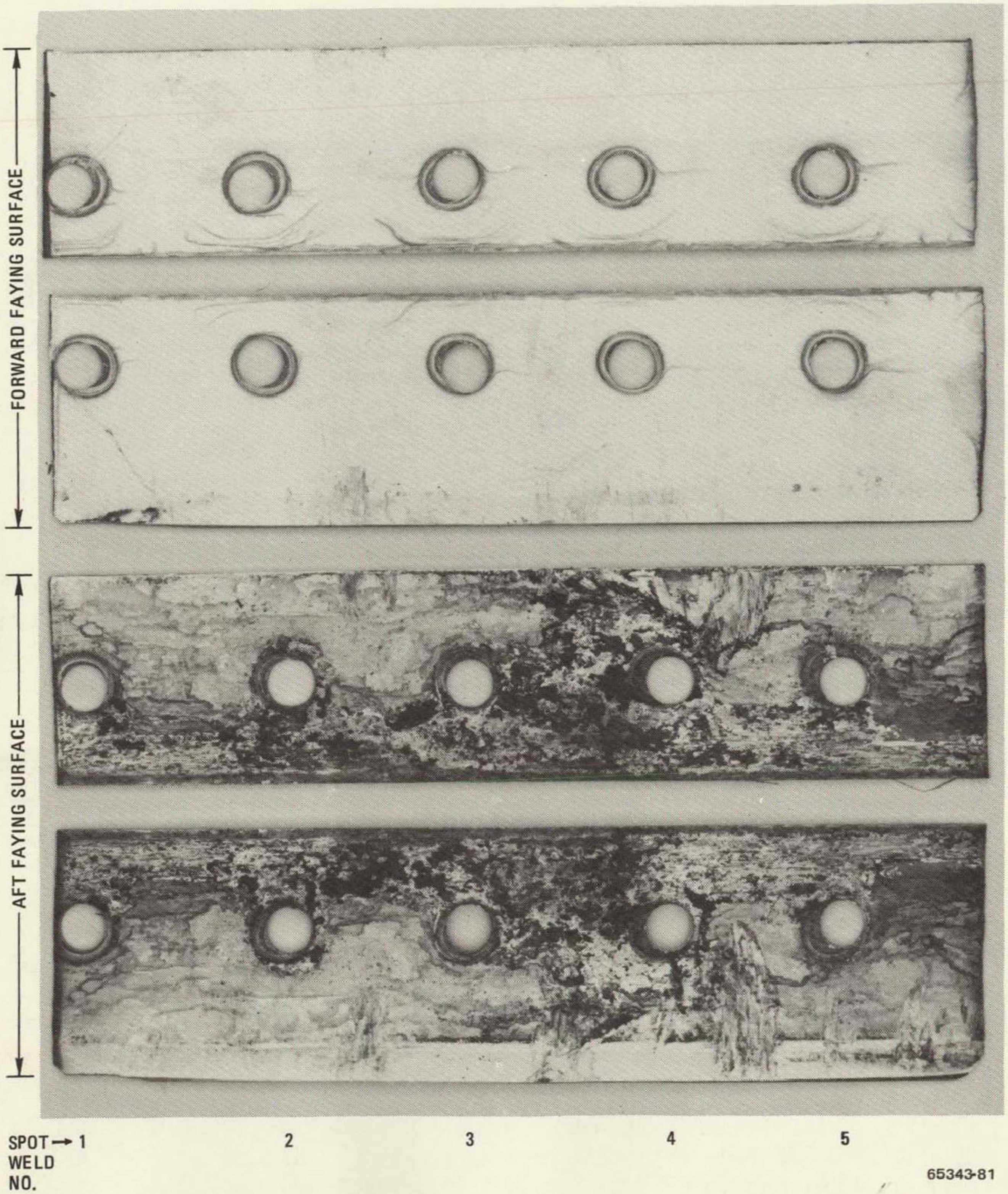

Figure 2-40. Appearance of Opened-up Aft and Forward Faying Surfaces

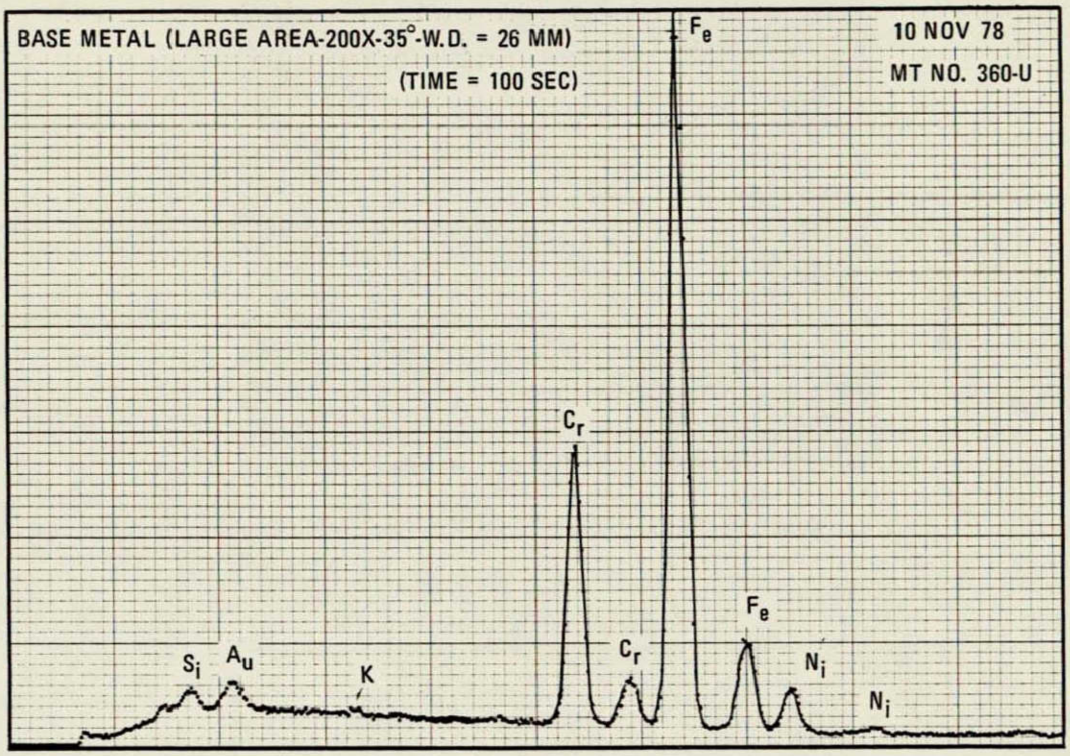

301 XFH CRES BASE METAL

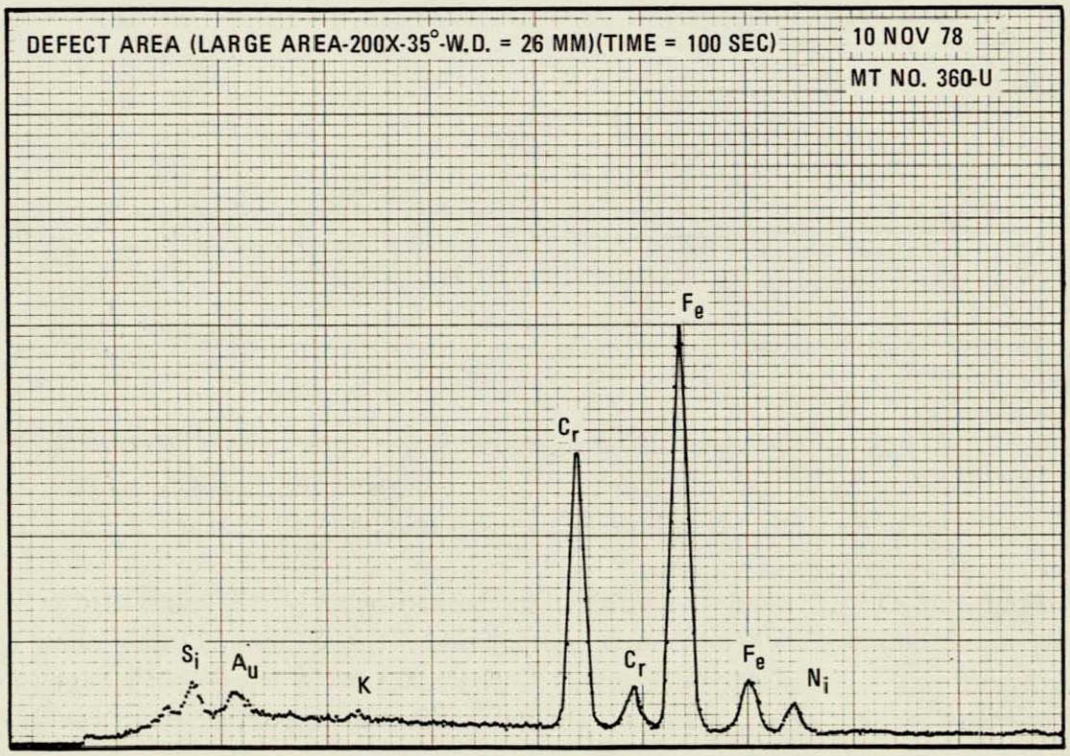

LAMINATED MIXTURE OF 301 AND LOW-DENSITY MATERIAL

65343-82

Figure 2-41. Energy Dispersive X-ray Analysis Results

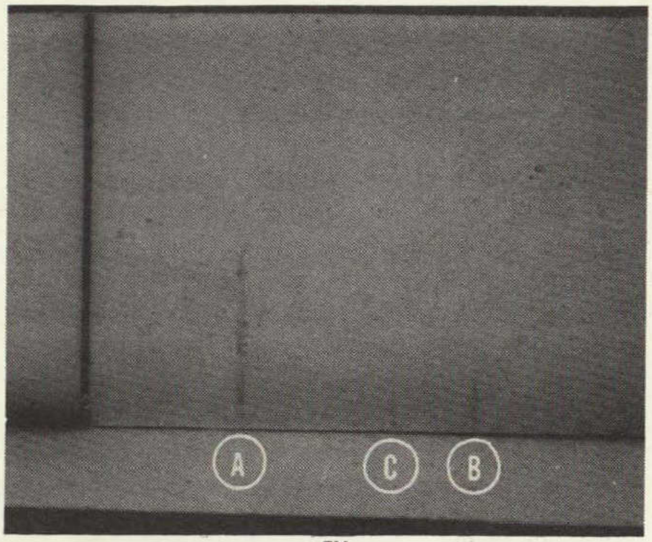

5X

X-RAY IMAGE OF THE EDGE DEFECTS A, B, AND C

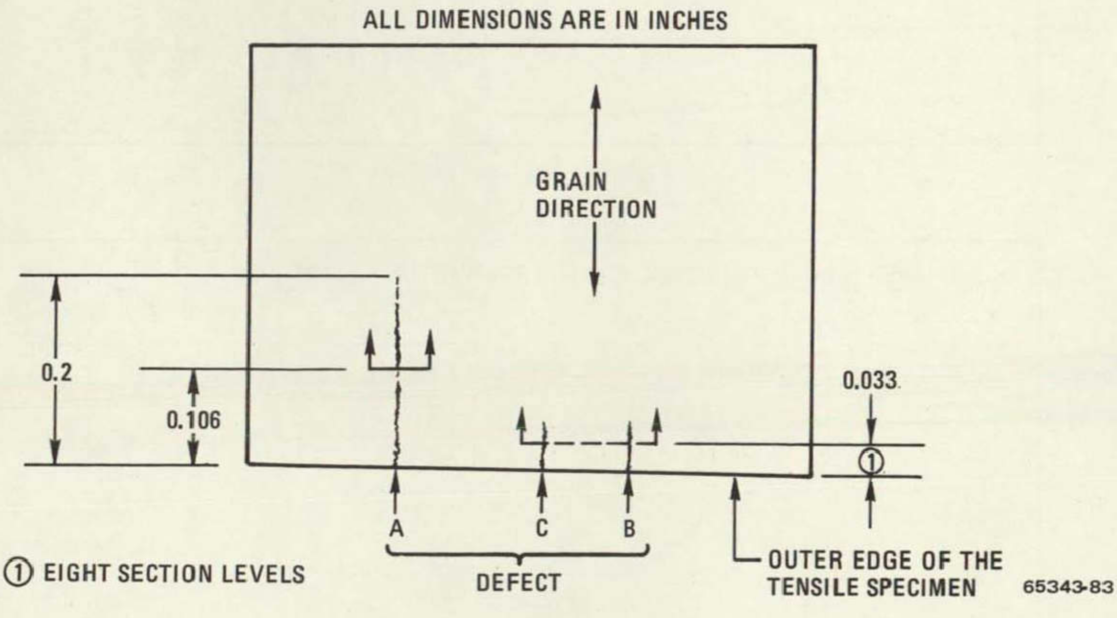

Figure 2-42. X-ray Appearance of Defect Indications A, B, and C Extending Inward from the Edge of a Tensile Specimen, and the Location of the Metallographic Sections Shown in Figures 2-43 through 2-45

in the radiographs of individual spotwelds. In the radiograph of a seamweld (which is actually a continuous row of overlapping spotwelds) the thicker regions show up as a series of white, interconnected crescents. The location of the defect images (dark) relative to these white ring or crescent-shaped images is important evidence in the interpretation of radiographs.

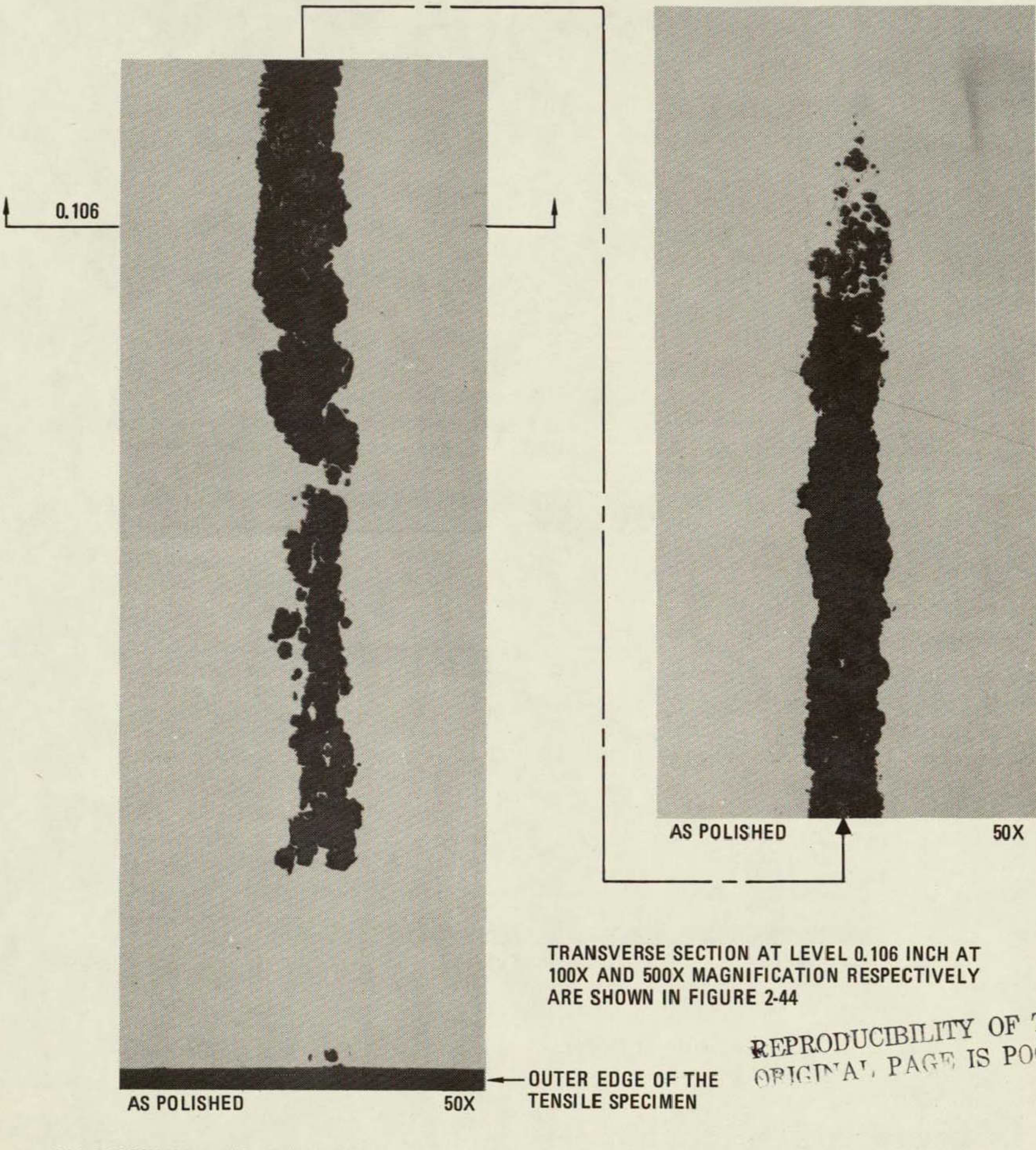

Figure 2-43. Appearance of a Plan View Section of Defect A About 0.003 inch Beneath the Surface

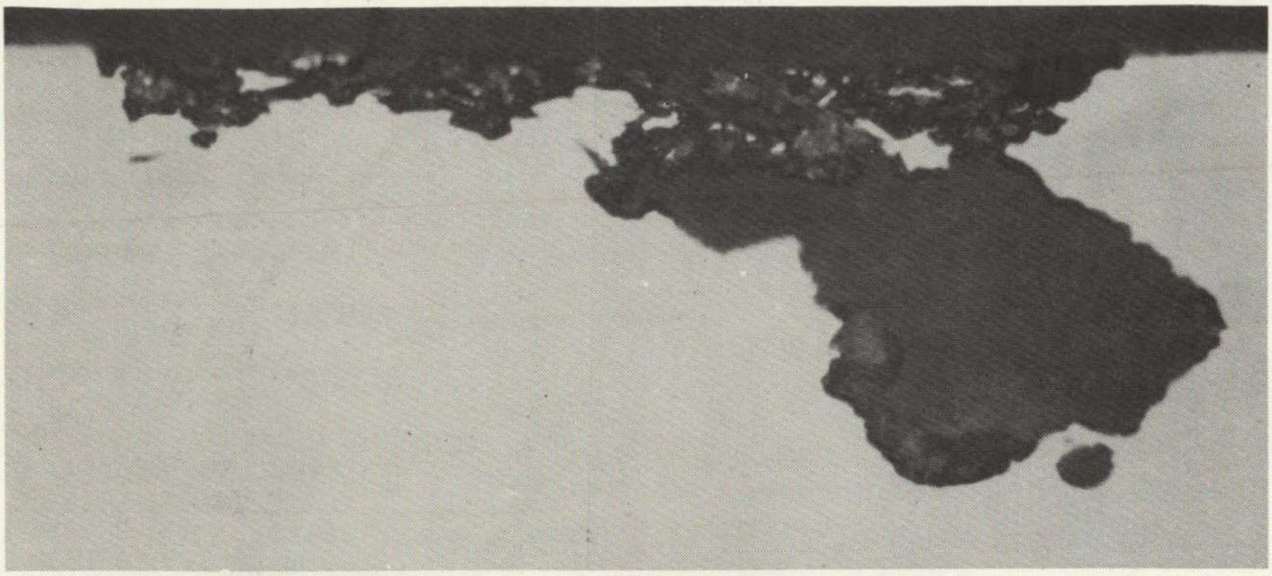

500X

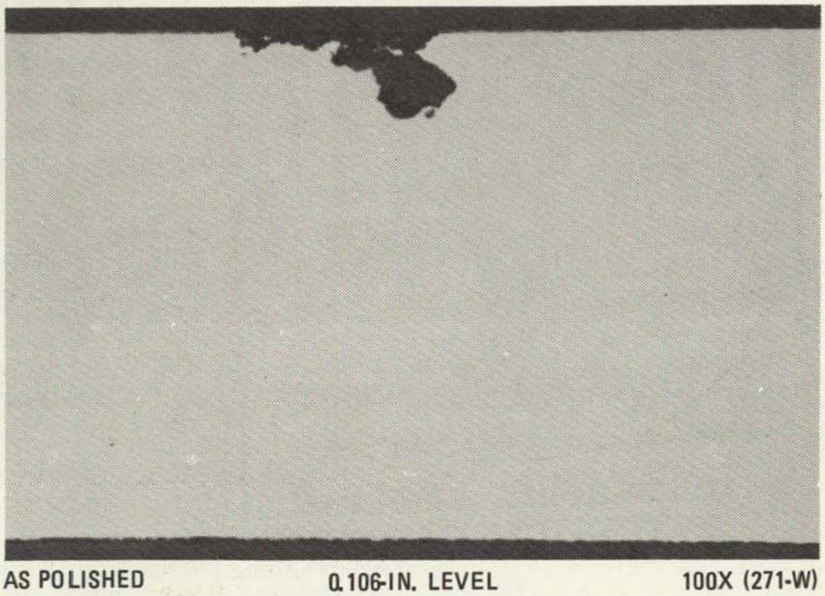

AS POLISHED 0.106-IN. LEVEL 100X (271-W) 65343-85

Figure 2-44. Appearance of Defect A at Transverse Section Level 0.106 (see Figures 2-42 and 2-43)

2.4.1 ORIGIN AND NATURE OF THE DEFECTS. The metallographic sections of all nine defect categories (Items) revealed a common factor; namely, that all defects had originated in the aft interface (faying surface) of the overlap joint due to crevice corrosion. The defect images (dark) were caused by:

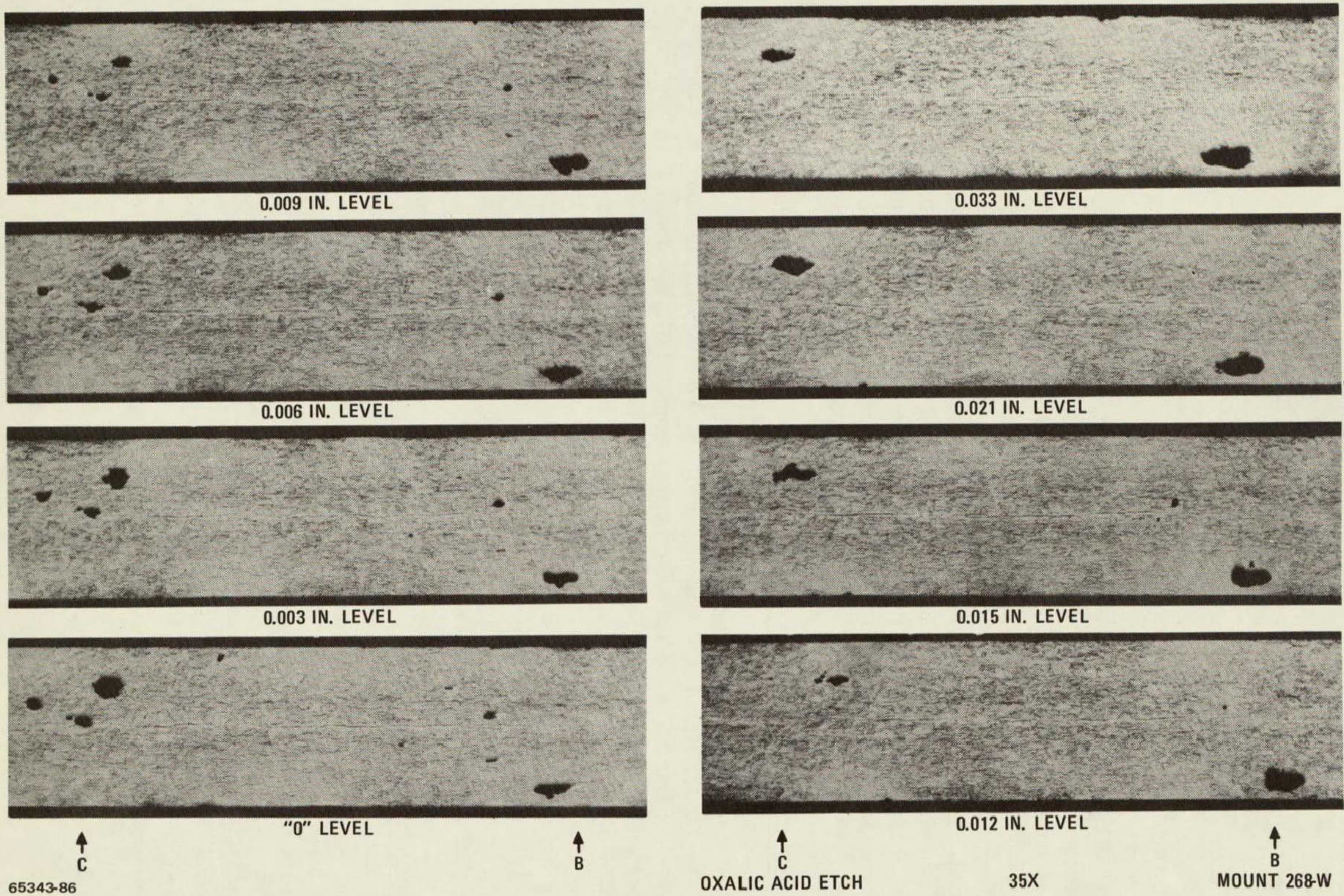

Figure 2-45. Appearance of Defects C and B at Nine Different Section Levels

a. "Pitting"-type attack.

b. Cracks, stress-corrosion.

c. A combination of (a) and (b).

2.4.2 "PITTING"-TYPE, ROUNDED IMAGE. Items 1 and 2 (Figures 2-6 and 2-9) are good examples of the "pitting"-type attack. The word pitting is put in quotations because the surface corrosion attack did not simply dissolve the metal and leave a void or cavity. Instead, just one phase of the multi-phased, cold-worked microstructure was attacked, transformed, and replaced with a lower density, nonmetallic material. Thus, the metallographic sections revealed the dark "pitting"-type images to be caused by a complex, laminated mixture of base metal (301 CRES) and low-density, nonmetallic material. As shown in Figure 2-41, the only differences detected between the defect area and the base metal were lower Fe, higher Si, and possibly higher K in the defect area.

2.4.3 "PITTING"-TYPE, LINEAR IMAGE. Item 5 (Figures 2-16 through 2-21) is a combination of a rounded and a linear "pitting"-type defect. The three section levels revealed that some of the pitting coincided with the weld-carbide precipitation zone (black band in the etched photomicrographs), not the internal, grain boundary carbides described earlier. The radiographic image associated with Section B-B is just barely visible. The total thickness of the defect at this location is 0.003 inch (0.0022 + 0.0008 = 0.0030) or about 4.6% of the total sheet thickness (0.065 inch). This is considered to be, therefore, about the smallest (filled) "pitting"-type defect that can be detected by radiography. The distinctive blurred image, and its position outside the white crescents, can be used to identify this image as a "pitting"-type defect and not a stress corrosion crack. Item 6 is a combination of linear "pitting" and stress corrosion cracking.

2.4.4 CRACKS, LINEAR IMAGES. All the other items (3, 4, 7, 8, and 9), whether they leaked or not, were caused by stress corrosion cracking (in combination with "pitting"-type corrosion in some cases, see Figure 2-12). All these cracks originated on the inside interface surfaces and propagated to the opposite surfaces as shown clearly in Figure 2-30. The stress corrosion cracks were primarily in the austenitic heat-affected zone of the spot or seamweld. Residual welding stresses are believed to be the primary source of the sustained tensile stress necessary to produce stress corrosion cracking. The tight, stress corrosion cracks that were oriented perpendicular to the hoop direction of the fuel tank were opened up by the 68 psig pressure test in October 1974. At the same time yielding (plastic flow) and possible crack propagation, occurred at the tip of some of the deeper cracks producing the typical V-shaped plastic zone, shown clearly in Figures 2-32 and 2-33.

SECTION 3

CHEMICAL ANALYSIS

As soon as leaks were detected during tanking tests of the Atlas 5013 tank, steps were taken to determine the nature, extent, and cause of the leaks.

3.1 INITIAL CHEMICAL ANALYSIS BY NASA MALFUNCTION INVESTIGATION STAFF, LABORATORIES DIVISION

Samples were taken at the open edge of seams adjacent to leaks for chemical analysis. MIS analyzed these samples by electron microprobe and X-ray diffraction techniques. The detailed results are reported in Reference 4.

These results can be summarized as showing the presence of stainless steel corrosion products (Fe, Ni, and Cr) and typical ETR environmental contaminants: sea salt, calcium carbonate, calcium sulfate, and sand.

3.2 CHEMICAL ANALYSIS OF TABS TAKEN FROM 5013 TANK

After preliminary analysis of X-rays and chemical test results, it was decided to cut tabs from the seams of the tank to obtain better samples for analysis. Figure 7-1 shows a typical tab cut from the tank, which clearly shows the stainless steel corrosion products. Samples were given to the NASA Malfunction Laboratory and to the General Dynamics Convair Chemical Laboratory.

3.2.1 <u>NASA MIS LABORATORY RESULTS</u>. The detailed discussion of the MIS Laboratory results is found in Reference 3. These results confirmed the earlier results that sea salt was the major contaminate.

3.2.2 <u>CONVAIR CHEMICAL LABORATORY RESULTS</u>. The results of the Convair chemical analysis of the material on the tabs are found in Reference 2. These results also confirm that the major foreign material present is sea salt. Since Reference 2 was published, a new instrument has become available called an ion chromatograph. With this instrument a profile of the anions in a given sample can be obtained. Cations can also be determined, but they have already been well characterized in References 2, 3, and 4. Chromatograms were prepared for the materials found in the seams, ETR seawater, ETR river water, ETR soil from near Complex 36A, and for standards. This data is shown in Figure 3-1 and Table 3-1. It can be seen from this data that the material in the seams in addition to the high chloride also contains minor constituents, (NO_3 and SO_4), which correspond roughly to the analysis of ETR seawater and sand when normalized to the chloride ion. This further confirms that the corrosive which caused the corrosion was the normal ETR environmental contaminant. No other corrosive was found.

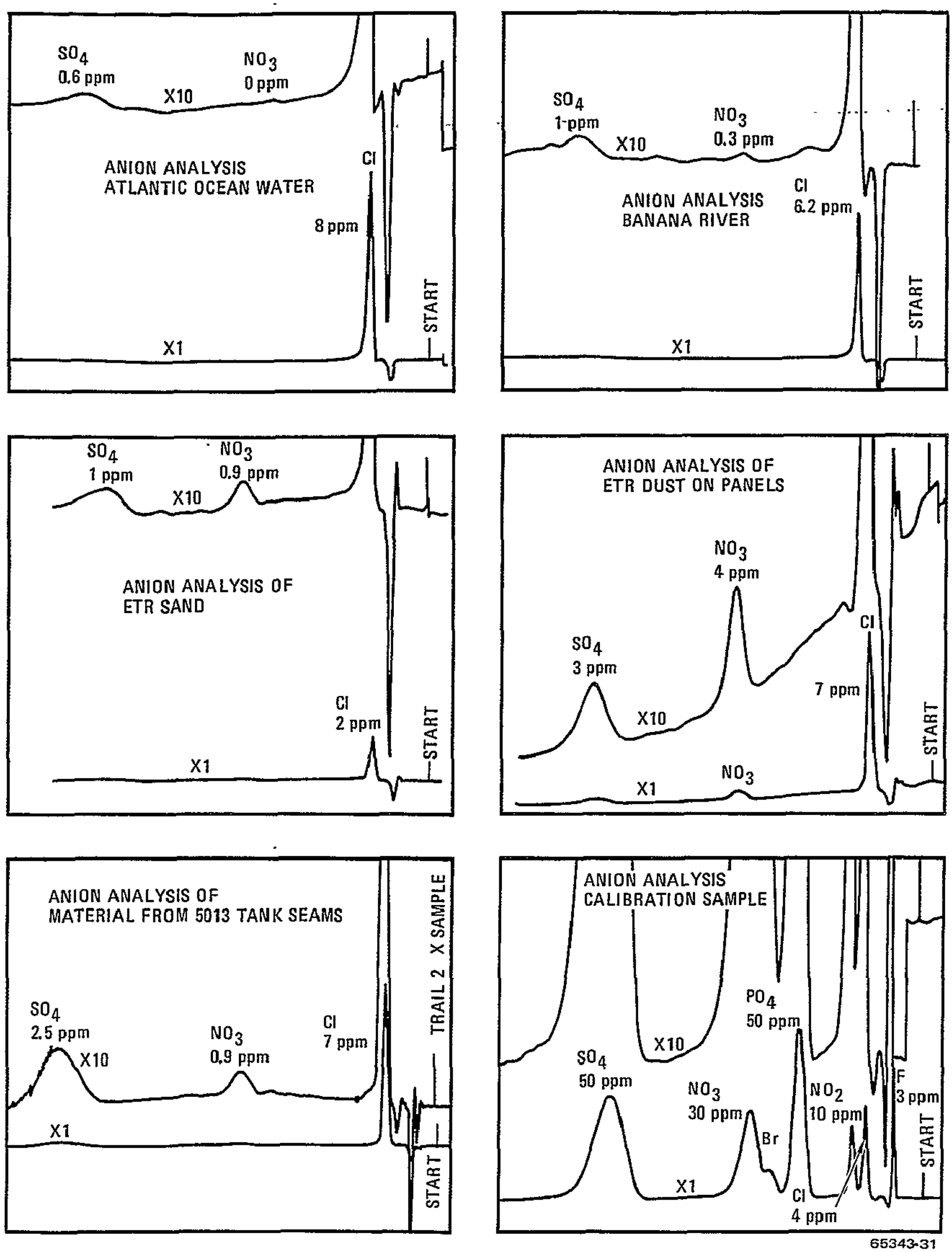

Figure 3-1. Ion Chromatograms of 5013 Tank Sample and Potential Sources

Table 3-1. Anion Analysis by Ion Chromatography

Sample	Comparison of Concentration of Major Anions		
	Chloride ‰	Sulfate* ‰	Nitrate* ‰
Standard Sea Water Analysis	19	2.6	—
Atlantic Ocean Water	19	1.9	—
Banana River Water	19	3.1	0.9
Sand	19	9.5	8.5
Dust on ETR Dogbones	19	8.1	10.9
Material Extracted from 5013 Seams	19	6.7	2.4

*Normalized to chloride at 19‰

3.3 SECTION CONCLUSIONS

1. Airborne sea salt from the ocean (and or river) was determined by chemical analysis to be the causitive agent of the observed corrosion.

2. Minor amounts of NO_3 and SO_4 are believed to play a minor role in the corrosion observed since chloride alone can produce similar corrosion of unprotected stainless steel.

SECTION 4

MECHANICAL PROPERTY TESTS

Uniaxial static tension tests and fatigue tests were performed on specimens from clean and corroded areas of the 5013 tank to determine the residual strength after its encounter with a corrosive environment. Similar tests were performed on specimens that had an additional 18 months exposure at Pt. Loma to determine the value of WD-40 to prevent further corrosion of clean and corroded areas.

4.1 LOCATION AND CONFIGURATION OF SPECIMENS

After the Atlas 5013 tank was returned to San Diego and stripped of non-tank items, the corroded areas were x-rayed. The analysis of these radiographs is contained in Reference 9. These results are summarized in Figure 4-1, which shows the location and degree of severity of the corrosion. From this data and a review of the x-rays, locations were chosen from which to cut out specimens for the mechanical property and corrosion tests. Corroded and clean specimens were taken from the areas shown in red in Figure 4-1. The details of the specimen configuration are shown in Figures 5-1 and 5-2. The assignment of specimens to various types of tests and test conditions as well as the type of corrosion represented by the specimen is shown in Figures 4-2 and 4-3. An x-ray positive print of typical defects is shown in Figure 4-4 and corresponds to the metallurgical section shown in Figure 2-36.

4.2 RESULTS OF STATIC TENSILE TESTS OF SPECIMENS FROM AS-RECEIVED TANK

The room temperature static tensile tests and the tensile fatigue tests of specimens cut from the 5013 tank as it was received from ETR are shown in Figures 4-5 and 4-6 and Tables 4-1 and 4-2. All of the samples designated corroded (D, F, Y, L, Z, 29) were from active leaking areas of the joints. From Figure 4-5 it can be seen that the average reduction in static strength comparing the "clean" specimens with the "corroded" specimens is about 10%. The strength of all of the specimens is above the design requirement of 184 ksi. The maximum total in-flight stress for joints represented by these specimens was not expected to exceed 78 ksi. Since these specimens represented the worst cases of corrosion, it appears that the tank joints had a wide margin of safety for static structural strength. The leakage per se is a separate consideration.

4.3 RESULTS OF FATIGUE TESTS OF SPECIMENS FROM AS-RECEIVED TANK

An examination of Figure 4-6, which shows the fatigue strength of the joint, reveals a similar, if not greater, safety margin. These first fatigue tests were performed at 0 to 100 ksi, which is higher than the 67 ksi required for this joint. This was done

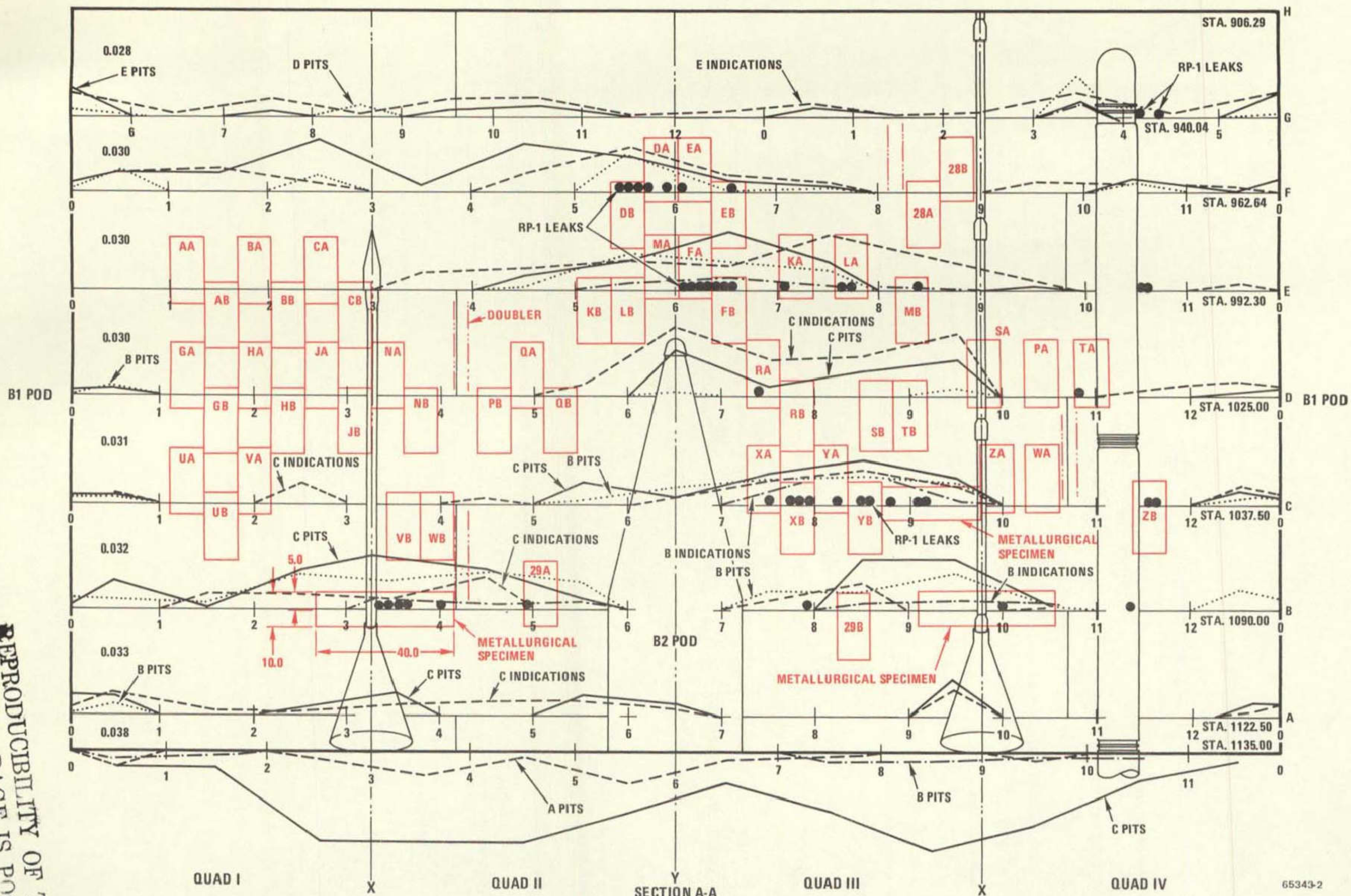

Figure 4-1. Circumferential Corrosion Distribution and Specimen Locations

SPECIMEN ID	JOINT ID	GAGE (MILS)	SPECIMEN TYPE	SPOT LOCATION STA	X-RAY NO.	CEN. SW NO.	TYPE OF CORROSION A	B	C	D	E	INITIAL CONDITION 0 = OILY	FINAL EVALUATION	RESULTS	SPECIMEN ID
B	A B	30 30	CLN	E E	1 2	42 9						-	STATIC	226 KSI	B
C	A B	30 30	CLN	E E	2 2	25 42			SLIGHT ●			-	STATIC	229 KSI	C
N	A B	30 31	CLN	D D	3 3	10 27						0	STATIC	227 KSI	N
G	A B	30 31	CLN	D D	1 1	9 25						-	FATIGUE	637～	G
H	A B	30 31	CLN	D D	1 2	42 9						0	FATIGUE	701～	H
J	A B	30 31	CLN	D D	2 2	25 42						0	FATIGUE	726～	J
D	A B	30 30	COR	F F	5 5	41 24	●			●		0	FATIGUE	759～	D
F	A B	30 30	COR	E E	6 6	8 24	●			●	●	0	FATIGUE	877～	F
Y	A B	30 30	COR	C C	7 8	46 14	●	●				0	FATIGUE	645～	Y
L	A B	30 30	COR	E E	7 5	34 25		●		●		0	STATIC	197 KSI	L
Z	A B	31 32	COR	C C	9 11	34 15	●				●	-	STATIC	215 KSI	Z
29	A B	32 33	COR				●				●	0	STATIC	209 KSI	29

65343-3

Figure 4-2. Assignment of As-Received Specimens from ETR

SPECIMEN ID	JOINT ID	GAGE (MILS)	SPECIMEN TYPE	SPOT LOCATION STA	X-RAY NO.	CEN. SW NO.	TYPE OF CORROSION A	B	C	D	E	EXPOSURE TIME	EXPOSURE CONDITION		FINAL EVALUATION	RESULTS	SPECIMEN ID
A	A B	30 30	CLN	E E	1 1	9 25						18 MO	UNLOADED	NO WD40	STATIC	– 23,500 196.32 KSI	A
V	A B	31 32	CLN	C C	1 3	39 18						18 MO	UNLOADED	NO WD40	FATIGUE	– 4546 ~	V
M	A B	30 30	COR	E E	5 8	42 13					●	18 MO	UNLOADED	NO WD40	STATIC	– 24,550 206.65 KSI	M
K	A B	30 30	COR	E E	7 5	9 9					●	18 MO	UNLOADED	NO WD40	FATIGUE	– 6883 ~	K
Q	A B	30 31	CLN	D D	4 4	31 48						18 MO	LOADED	NO WD40	STATIC	23,525 200.04 KSI	Q
W	A B	31 32	CLN	C C	10 3	9 35						18 MO	LOADED	NO WD40	FATIGUE	5418 ~	W
T	A B	30 31	COR	D D	10 8	42 42			●			18 MO	LOADED	NO WD40	STATIC	20,000** 168 KSI**	T
S	A B	30 31	COR	D D	9 8	28 24				●		18 MO	LOADED	NO WD40	FATIGUE	3491 ~	S
P	A B	30 31	CLN	D D	10 4	9 15					SLIGHT ●	18 MO	LOADED	WD40 EVERY 30 DAYS	FATIGUE	2464 ~	P
U	A B	31 32	CLN	C C	1 1	6 22						18 MO	LOADED	WD40 EVERY 30 DAYS	FATIGUE	2246 ~	U
E	A B	30 30	COR	F F	6 6	9 25					●	18 MO	LOADED	WD40* EVERY 30 DAYS	FATIGUE	2321 ~	E
X	A B	31 32	COR	C C	7 7	10 27			●			18 MO	LOADED	WD40* EVERY 30 DAYS	FATIGUE	1902 ~	X

*APPLICATION OF WD-40 CHANGED TO EVERY 90 DAYS AFTER NINE MONTHS OF EXPOSURE.
**PULL ROD BROKE AND DAMAGED SPECIMEN.

65343-4

Figure 4-3. Assignment of Pt. Loma Specimens

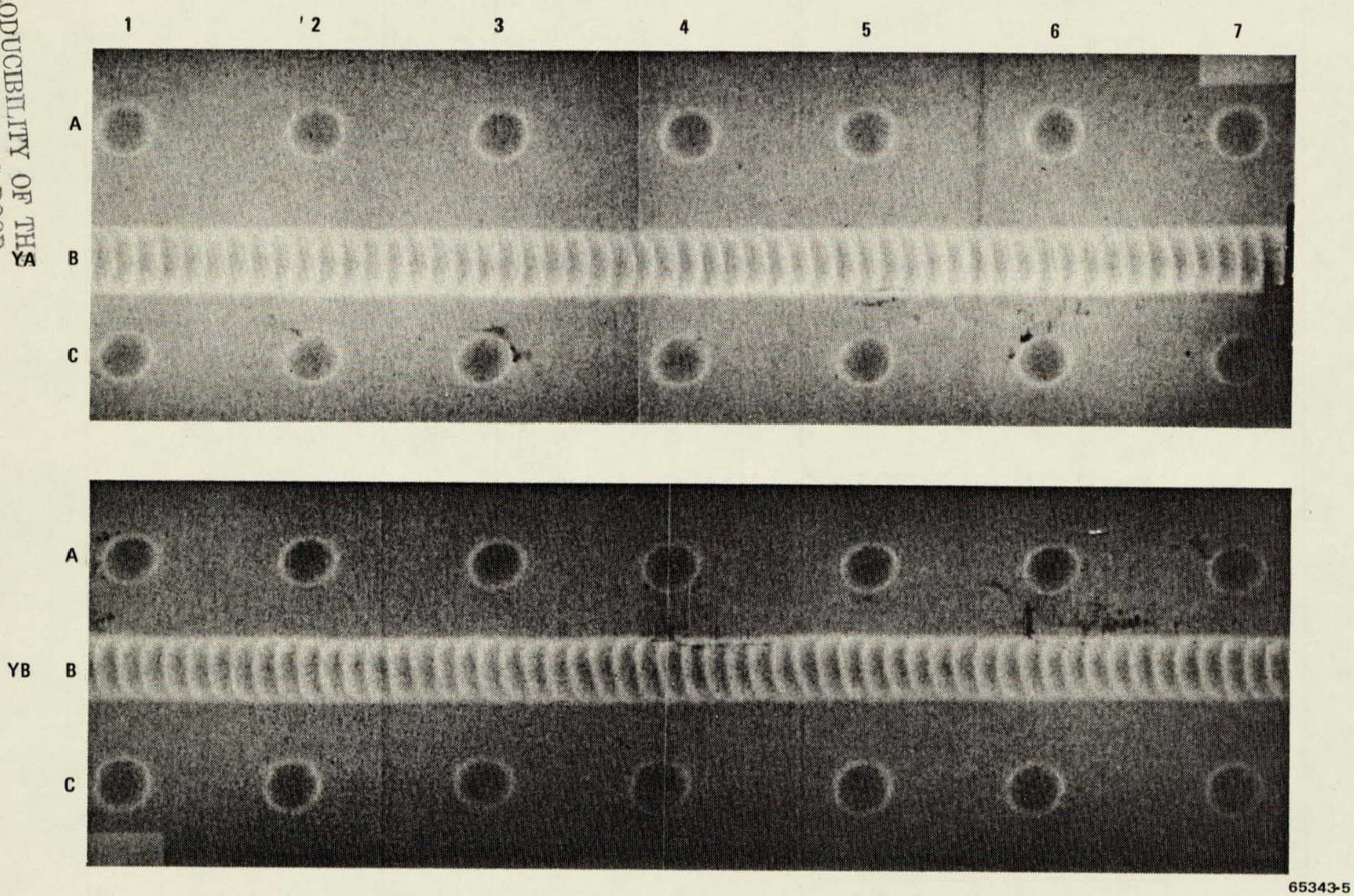

Figure 4-4. Radiograph of Typical Defects

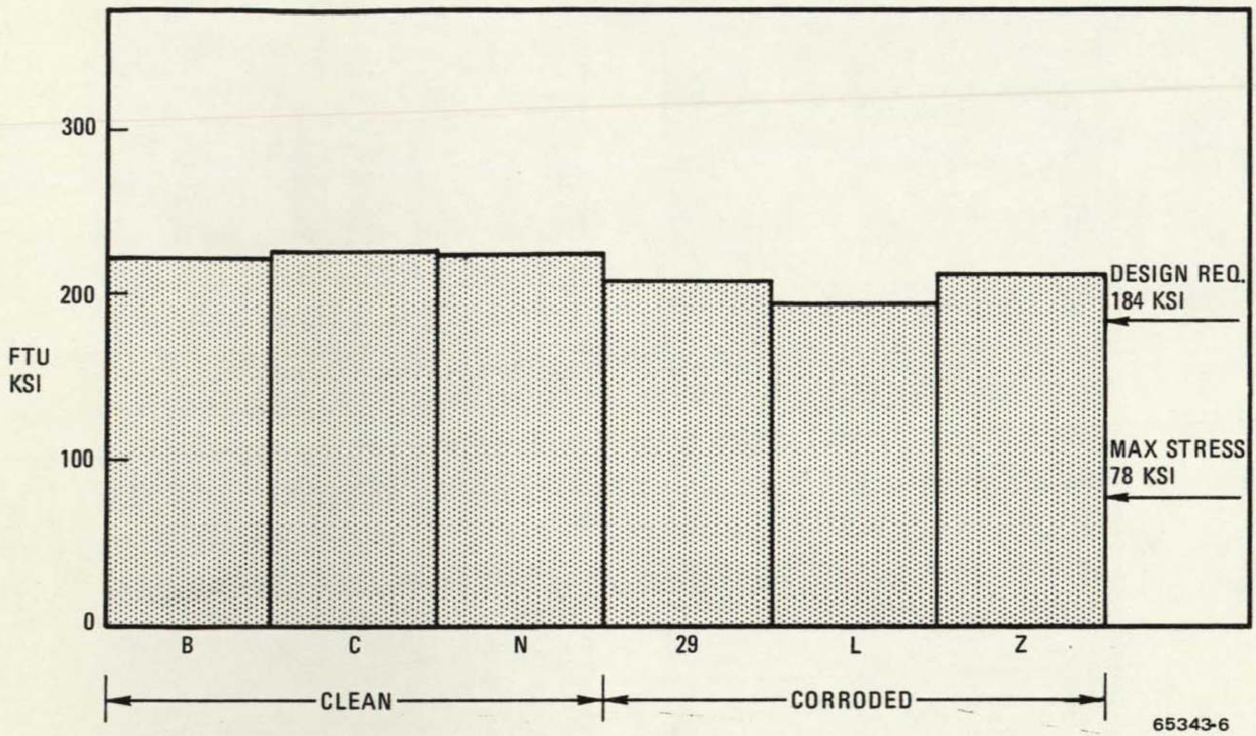

Figure 4-5. Static Tensile Tests (Room Temperature)

Table 4-1. Results of Static Tests on Corroded and Noncorroded Dogbone Test Specimens from 5013 Fuel Tank Joints as Cut from Tank

Specimen ID	Original Condition	Ultimate Tensile Strength (ksi)	Failure Location
B	Clean	226	Joint C Down
C	Clean	229	Joint B Up
N	Clean	227	Joint C Up
29	Corroded	209	Joint B Down
L	Corroded	197	Joint A Down
Z	Corroded	215	Joint A Down

Table 4-2. Results of Fatigue Tests on Corroded and Noncorroded Dogbone Test Specimens from 5013 Fuel Tank Joints as Cut from Tank

Specimen ID	Original Condition	Cycles Completed Before Failure*	Failure Location
G	Clean	637	Splice Joint
H	Clean	701	Spotweld Row B Down
J	Clean	726	Spotweld Row B Down
D	Corroded	759	Splice Joint Up
F	Corroded	877	Splice Joint Down
Y	Corroded	645	Seam Weld Joint B Down

*Cycled 0 - 100 ksi, 6 cycles per minute

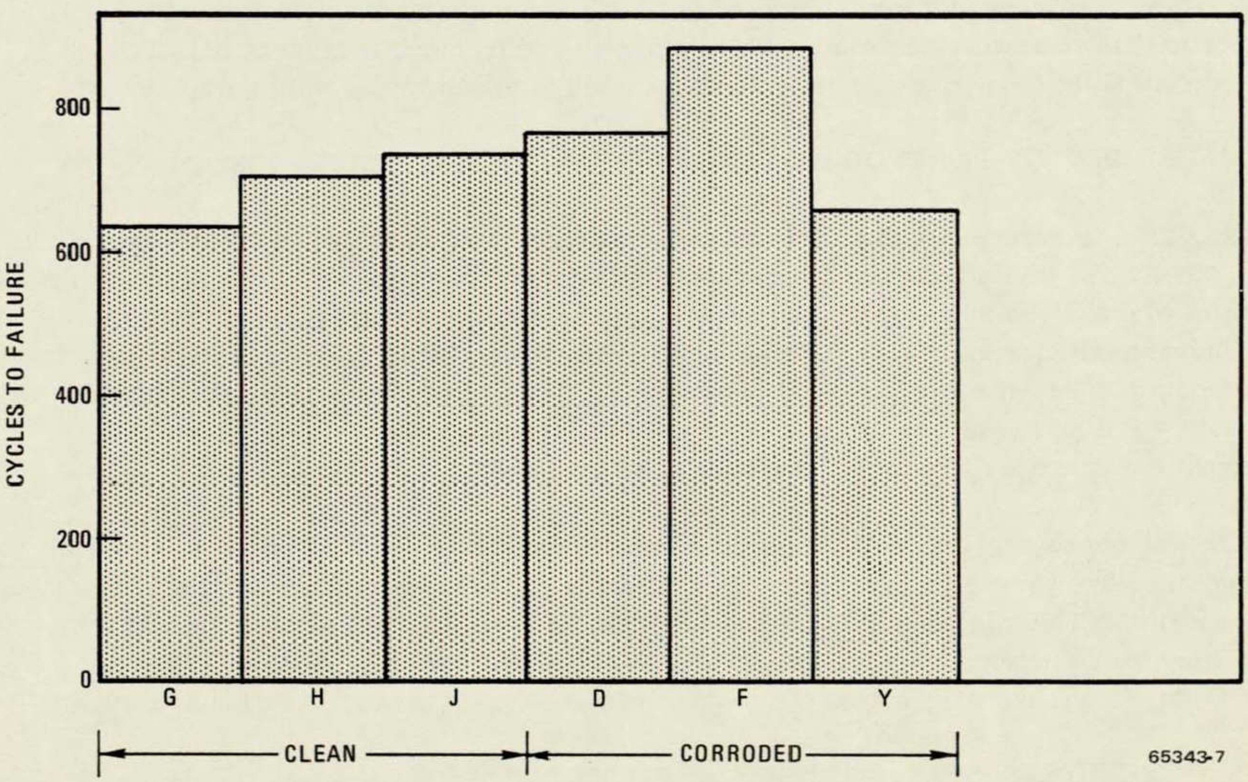

Figure 4-6. Tensile Fatigue Tests (0 to 100 ksi) at Room Temperature

because previous testing experience indicated they would pass at even a higher stress, and it allowed comparison data much faster. The difficult problem is to explain why the average of the corroded specimens is approximately 10% higher than the noncorroded specimens. One idea is that the corrosion attacks at points of high stress concentration and thus the load is distributed better. The idea that it is caused by experimental scatter is challenged by subsequent data of even more extensively corroded specimens. It also appears that there is significantly more scatter in the fatigue data for the corroded samples than there is for the noncorroded samples. In any case it is pretty hard to sell corrosion as a way to increase fatigue resistance.

4.4 GROWTH OF CIRCUMFERENTIAL CRACK

X-rays were taken every 100 cycles of the fatigue test on specimen "Y" to follow the growth of a typical circumferential defect. This defect is a crack that occurs in heat affected zone at the edge of the seam weld. Metallurgical cross sections of this type of defect are shown in Section 2. Figure 4-7 shows the progression from 100, 500, and 646 cycles for specimen YA. The specimen failed at the YB joint at 646 cycles. The progression of YB is shown in Figure 4-8 at 100 and 500 cycles.

This room temperature data shows that crack-like defects cannot be ignored as sites for fatigue failure, but for the Atlas/Centaur missions where only a few cycles will occur it is somewhat academic. Crack growth and fracture toughness calculations indicate little loss in toughness when compared to noncorroded joint data.

4.5 REVIEW OF POINT OF FAILURE OF STATIC AND FATIGUE SPECIMENS

As shown in Figure 5-1 the static and fatigue specimens were constructed from material and joints from the 5013 tank. Two joints were connected by a third center joint to make one specimen. The center joint was a new clean joint. This joint was inadvertently designed with six instead of seven spots. This is only slightly less strong than seven spots by actual test. This did result in only two specimens ultimately failing in the 5013 joints. This is a conservative factor because with seven spots the average data might have been slightly higher.

Another factor that caused some specimens to break outside of all of the joint areas was the edge corrosion that occurred. This was in the form of deep but small diameter edge pits. This also resulted in conservative data for the test joints. This type of pitting would not occur on the tanks because these end gain edges do not exist in the design. The characterization of this type of pitting is covered in Section 2.3.7.

4.6 RESULTS OF STATIC TENSILE TESTS AFTER PT. LOMA EXPOSURE

In addition to the 12 specimens dedicated to mechanical property tests of the as-received tank, 12 additional specimens were further exposed to the corrosive

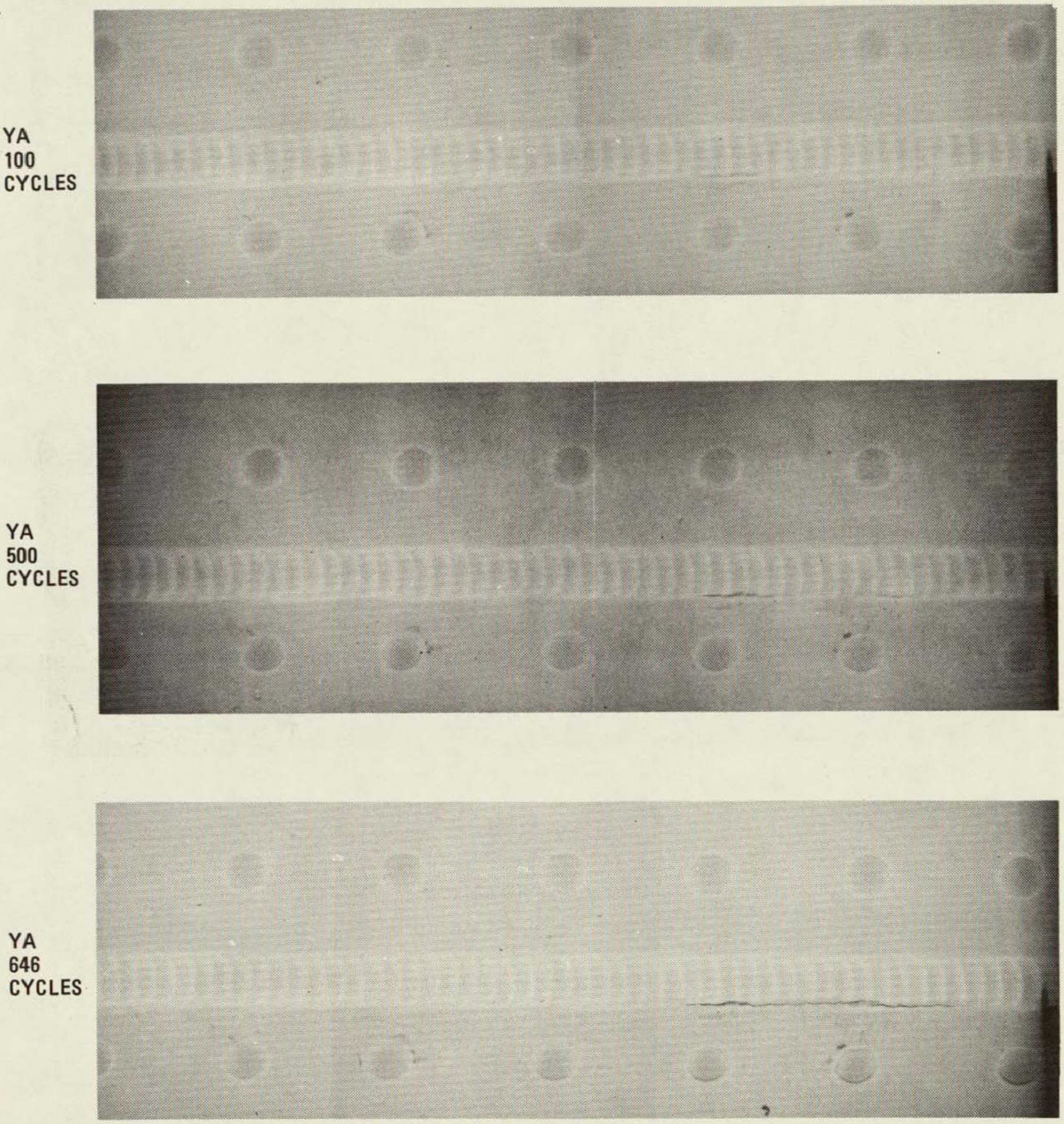

65343-38

Figure 4-7. Crack Growth as a Function of Fatigue Cycling (Joint YA, 0 - 67 ksi, Room Temperature)

YB
100
CYCLES

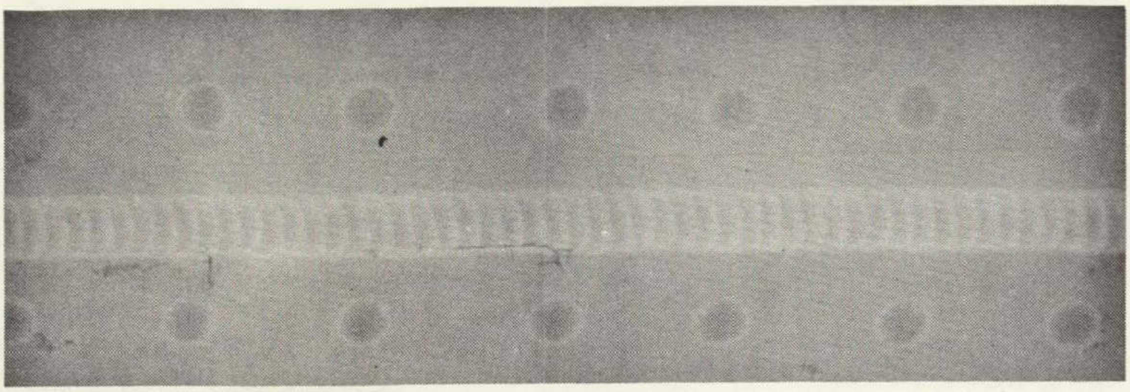

YB
500
CYCLES

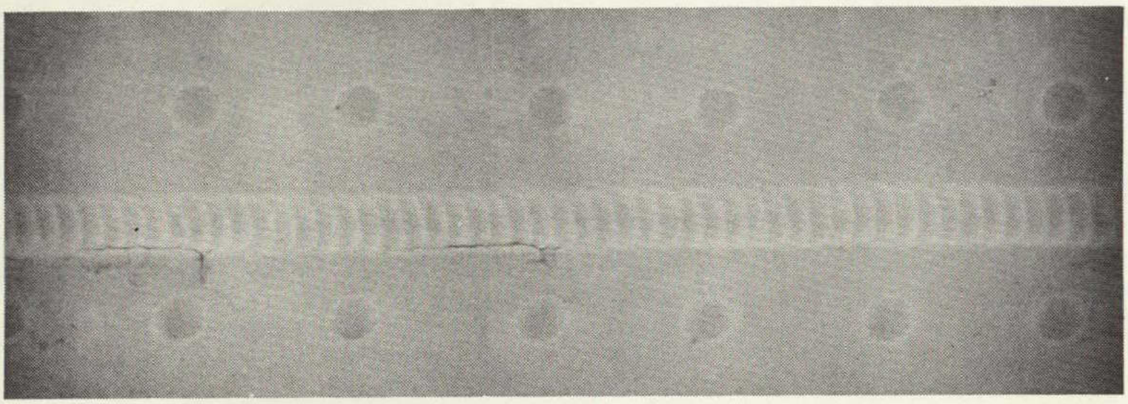

YB
646
CYCLES

SPECIMEN FAILED

65343-39

Figure 4-8. Crack Growth as a Function of Fatigue Cycling (Joint YB, 0 - 67 ksi, Room Temperature)

Table 4-4. Results of Fatigue Tests on Corroded and Noncorroded Dogbone Test Specimens from 5013 Fuel Tank Joints after 18 Months of Exposure at Pt. Loma

Specimen ID	WD-40	(1) Original Condition	Cycles Completed Before Failure*	Failure Location
V	No	Clean	4546	Up side of Center Joint
K	No	Corroded	6883	Up side of Center Joint
W	No	Clean	5418	Down side of Joint "A"
S	No	Corroded	3491	Parent Metal
P	Yes	Clean	2464	Down side of Center Joint
U	Yes	Clean	2246	Down side of Center Joint
E	Yes	Corroded	2321	Down side of Center Joint
X	Yes	Corroded	1902	Down side of Center Joint

(1) Original Condition of Joints A and B. At test the center joints in specimens V, K, W, and S were corroded, while the center joints in specimens P, U, E, and X were clean.

* Cycled 0-67 ksi, 6 cycles per minute.

limited data it appears that even though the corroded specimens required a higher number of cycles to fail, the variation in the data and other overriding factors, such as tensile strength, do not support the use of corrosion to increase fatigue life.

4.8 ANALYSIS OF CRACK GROWTH

During the cycle tests of the specimens fabricated from material excised from the 5013 tank, corrosion cracks propagated. A record of the crack lengths was maintained at various number of applied loads for each of the cracks in specimens YA and YB.

Inasmuch as this data was available, it seemed prudent to compare the crack growth rates with those of the base material.

The standard method of presenting such data is to provide a plot of the variation of crack growth per cycle (da/dn) with the crack intensity factor range (ΔK).

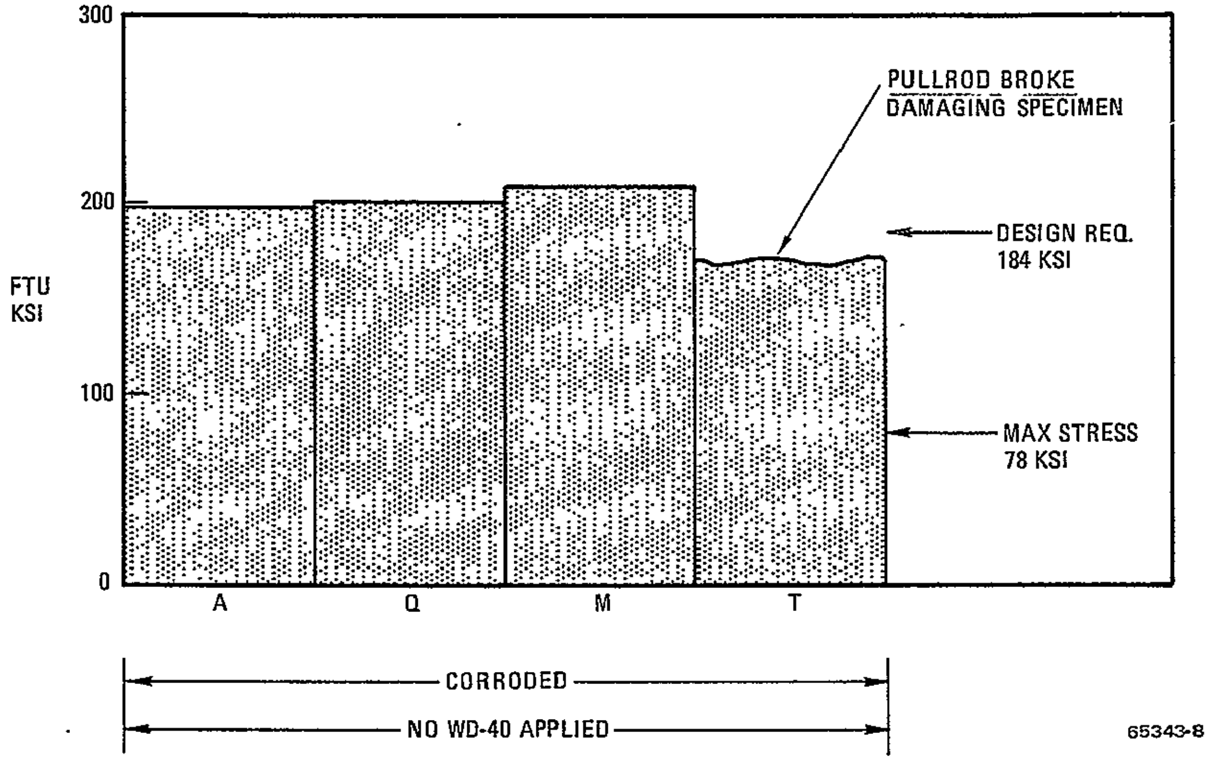

Figure 4-9. Static Tensile Tests After Exposure at Pt. Loma for 18 Months (Room Temperature)

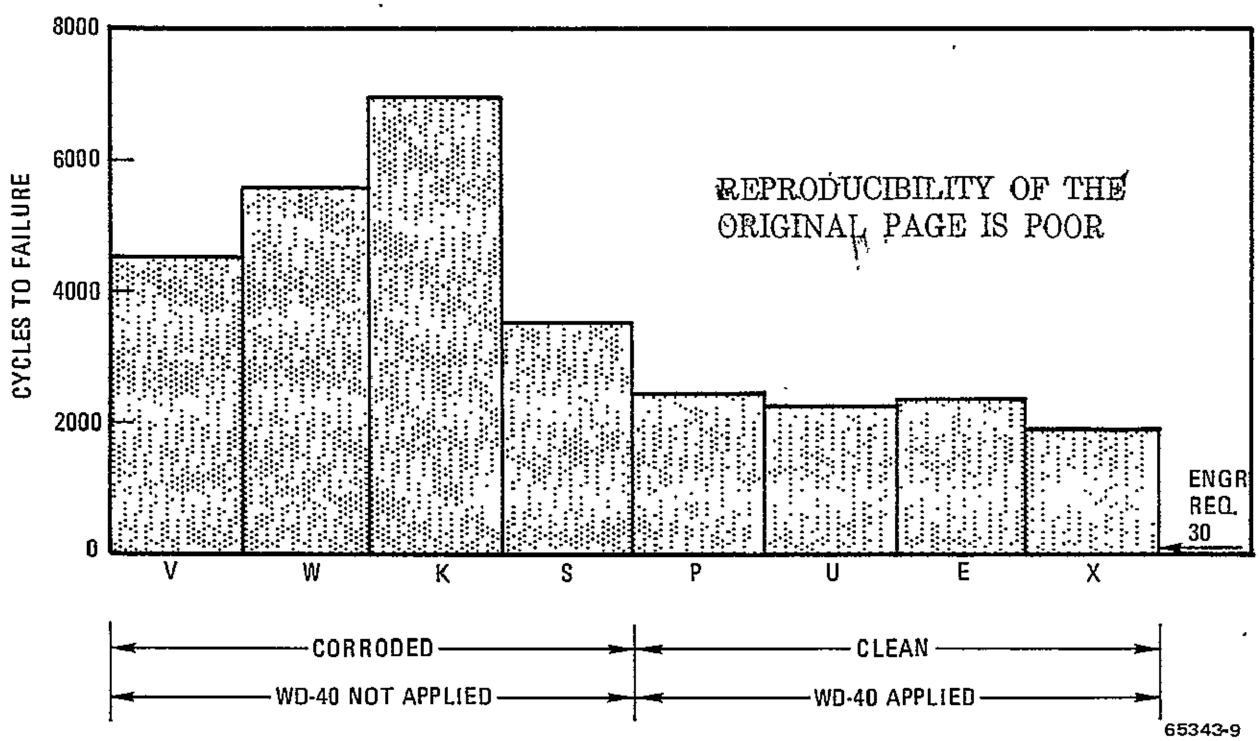

Figure 4-10. Tensile Fatigue Tests After Exposure for 18 Months at Pt. Loma (0 to 67 ksi, Room Temperature)

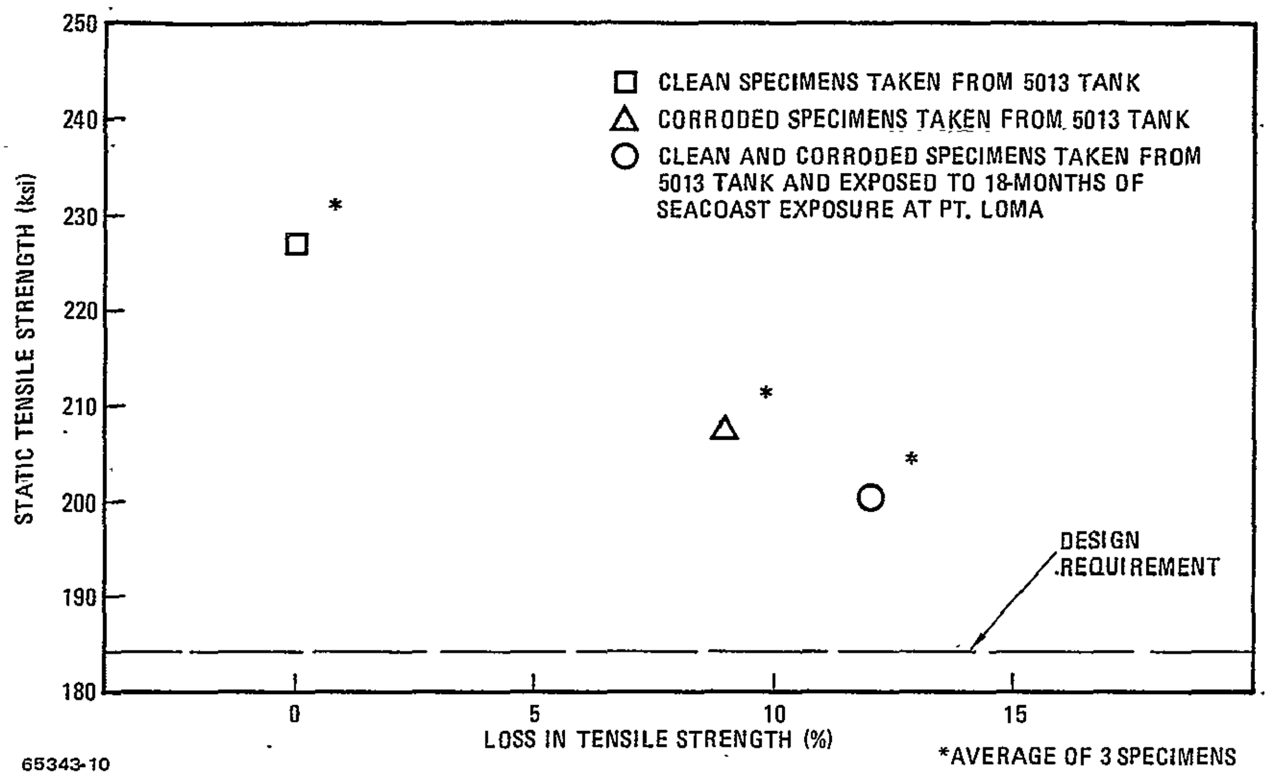

Figure 4-11. Comparison of Static Tensile Strength of Specimens

The crack intensity factor (sometimes called fracture toughness) was calculated using the general equation for a through-the-thickness crack:

$$K = \sigma_G \sqrt{\pi a}$$

where

K = crack intensity factor
a = one-half of the crack length
σ_G = the gross stress at the cracked section

Unfortunately, the exact stress is very difficult to determine in the region of the cracks. Consequently, the limits of applied crack intensity factor were calculated using the single sheet gross stress of 67 ksi maximum and a lower limit stress of 34 ksi.

The crack growth rate (da/dN) is plotted as a function of crack intensity range (ΔK) for the cracks in the two specimens in Figure 4-12. Superimposed on the same plot is a curve for the crack growth rate of 301 XFH stainless steel parent metal.

Table 4-5. Variation in Fatigue Data

Condition	Specimen No.	Cycles	$\overline{X}$	σ	Variation %	2σ	%	3σ	%
Clean	G	637							
Clean	H	701	688	45.9	(±6.7)	91.8	(±13.3%)	138	(±20%)
Clean	J	726							
Corroded	D	759							
Corroded	F	877	760	116	(±15.3)	232	(±30.5%)	348	(±45.7%)
Corroded	Y	645							
Corroded	V	4546							
Corroded	K	6883	5084	1435	(±28.3)	2869	(±56.4%)	4304	(±84.6%)
Corroded	W	5418							
Corroded	S	3491							
Clean	P	2464							
Clean	U	2246	2233	238.6	(±10.)	477.3	(±21.3%)	715.9	±32%
Clean	E	2321							
Clean	X	1902							

Refer to Figures 4-6 and 4-10.

Although the material in the vicinity of the weldments (heat-affected zone) is probably somewhat different than the 301 XEH parent metal, there seems to be good agreement between the two materials as far as crack growth rate is concerned.

4.9 DISCUSSION

The uniaxial mechanical property tests of corroded joints all point toward a conservative situation and indicate that the Atlas tank design has a high tolerance for corrosion defects. The only unknown factor is the effect of biaxial loading on the corrosion defects. Certain defects, as pointed out in the metallurgical analysis, Section 2, appearing as cracks oriented in the fore and aft direction, show evidence of yielding. This yielding, due to hoop loads, was not duplicated by the uniaxial specimens selected by this program. So far as we know, no miniature tank tests have been performed on corroded joints to demonstrate the biaxial effect. The threat of these types of defects may be assessed by metallurgical and stress analysis.

Horizontal defects oriented parallel to the hoop direction were exercised by the uniaxial tests performed on this program and show a wide margin of safety.

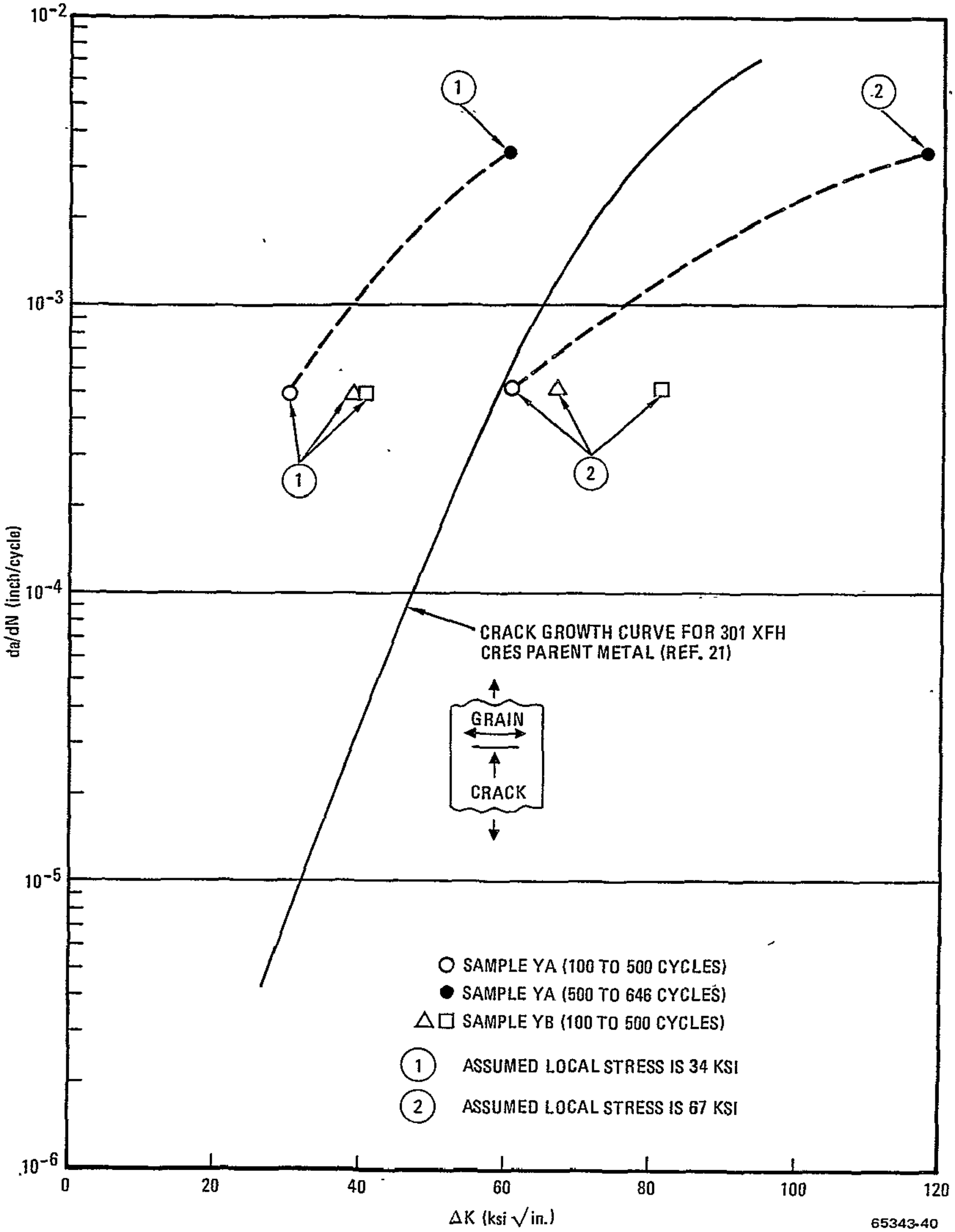

Figure 4-12. Variation of Crack Growth with Stress Intensity Range for 301 SS Joints (Tank 5013)

4.10 SECTION CONCLUSIONS

1. The room temperature static tensile properties of circumferential joints made from the corroded part of the 5013 tank were reduced 9% when compared to similar uncorroded specimens and were still well above engineering requirements.

2. The room temperature tensile fatigue data at 0 - 100 ksi for corroded specimens from the 5013 tank were, oddly enough, higher than the clean control specimens. All values were much higher than engineering requirements.

3. Other corroded and noncorroded specimens made from the 5013 tank and exposed to an additional 18 months of seacoast environment were tested for static and fatigue strength.

   a. The static tensile strength after 413 days at ETR and 18 months of exposure at Pt. Loma decreased 12% as compared to clean specimens.

   b. The fatigue strength of the corroded specimens increased an average of 127% over the uncorroded specimens. This increase was offset by a high degree of variability.

SECTION 5

5013 TANK LONG TERM ENVIRONMENTAL EXPOSURE TESTS AT PT. LOMA

In October 1974 the Atlas 5013 (AC-33) tank was found to be leaking RP-1 fuel. This was due to stress corrosion cracks in the faying surface of the cylindrical skin overlap joint. As a result of this problem, it was decided to conduct, among other things, a long-term test program that exposed various parts of the tank to a natural marine environment. During this exposure some of the test specimens were to be protected using standard protection procedures. This section documents the exposure of these specimens at the Convair Pt. Loma Test Site in San Diego, CA for 18 months.

5.1 TEST PROCEDURE

The test specimens consisted of twelve 36 by 4 inch standard "dogbones" made from 5013 tank weld joints. The details of the specimens are given in Convair drawing SD671-2-138, Test Specimen - Corroded Tank. The drawing defines the location on the 5013 tank from which each test joint was taken. Each test specimen was made up of two 4-inch test joints and a new splice joint in the center. This was used to attach the two test joints together to make the dogbone. Appropriate ends were applied to the test joints so that they could be dead-weight loaded and tested. The joints are depicted in Figure 5-1.

A summary of the specimen variables is given in Table 5-1. The variables were initial condition (clean or corroded), stress condition (unloaded or standby pressurization), corrosion protection (none or WD-40), and final evaluation (static to failure or fatigue to failure).

The 12 specimens were exposed on the tip of Pt. Loma at San Diego, CA. The test site location was about 40 feet above and 40 feet inshore from the high-tide line. Figure 5-2 shows the tester and the test specimens during exposure. Every month the specimens were removed from the tester and reexposed at a different location on the tester so that all specimens received equivalent exposure with respect to direction. While the specimens were unloaded, WD-40 was applied to P, U, E, and X for the first nine months according to the techniques described in (GD/C Specification) 0-79026. For the next nine months, P and U had WD-40 applied to the joints monthly while E and X were treated only every three months.

An X-ray examination was made of each specimen initially and monthly for the first nine months. During the next nine months the X-rays were taken every three months.

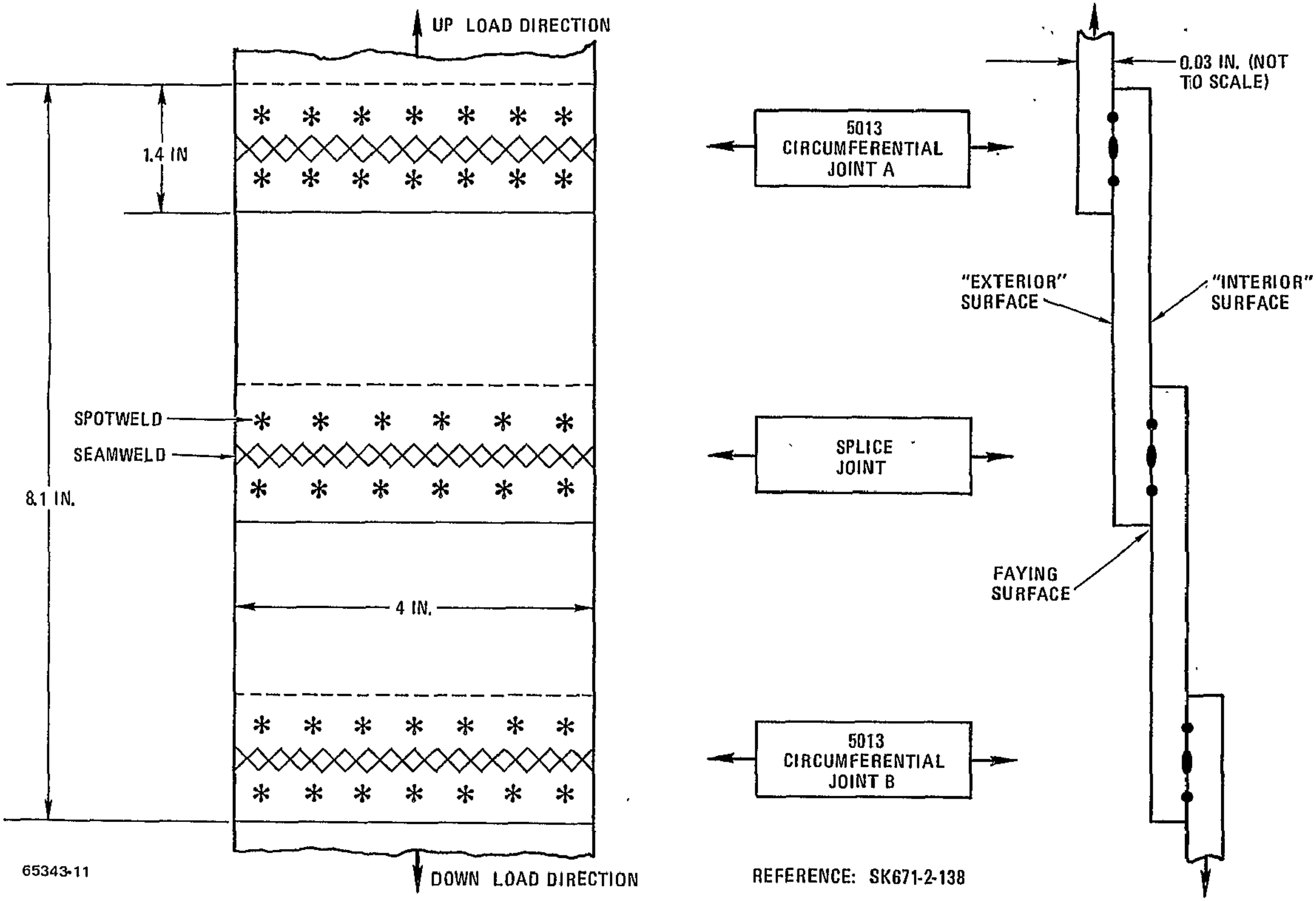

Figure 5-1. Test Specimen Joint Details

Table 5-1. Pt. Loma Specimen Variables

Specimen ID	Initial Condition		Stress Condition		Corrosion Protection		Final Evaluation	
	Clean	Corroded	None	16.1 ksi (1)	None	WD-40 (2)	Static	Fatigue
A	•		•		•		•	
V	•		•		•			•
M		•	•		•		•	
K		•	•		•			•
Q	•			•	•		•	
W	•			•	•			•
T		•		•	•		•	
S		•		•	•			•
P	•			•		•		•
U	•			•		•		•
E		•		•		•(3)		•
X		•		•		•(3)		•

NOTES:
(1) This represents the standby pressurization stress.
(2) WD-40 applied every 30 days per E.S. 0-79026.
(3) WD-40 applied every 30 days for the first 9 months and every 90 days for the next 9 months (E.S. 0-79026).

After 18 months of exposure the specimens were tested to failure either by static or fatigue loading as specified in Table 5-1.

5.2 TEST RESULTS

The effect of the marine environment on each test specimen is given in Figures 5-3, 5-4, and 5-5. These figures document all of the x-ray analyses that were performed. Visually, the areas protected with WD-40 remained free of red rust corrosion while all of the other areas showed corrosive attack within one month.

Figure 5-6 describes the X-ray data presented in Figures 5-3 and 5-4. Each test specimen (dogbone) is represented by a plot of X-ray results as a function of exposure time. In each box the specimen ID is given along with its initial condition, stress condition, and protection variable. The X-axis represents exposure time in months.

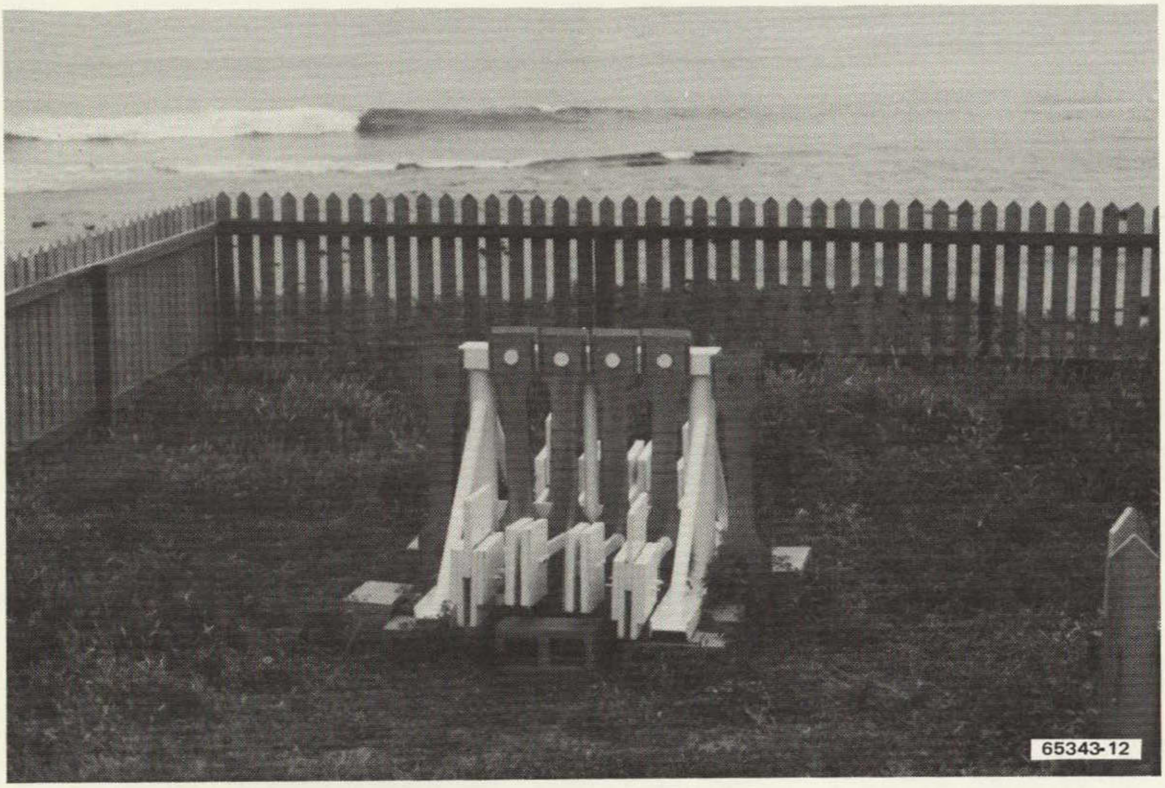

Figure 5-2. Pt. Loma Test Site

The Y-axis is a double scale of the number, N, of X-ray indications on the left side and length, L, of X-ray indications on the right. N is the cumulative increase in the number of X-ray indications. An X-ray indication is a defect in the specimen joint that appears to indicate a corrosion crack. This is in contrast to a corrosion pit, which doesn't have any length. L is the cumulative increase in the total length of the X-ray corrosion indications. The specimen's initial X-ray examination before the Pt. Loma exposure is represented by the two vertical lines in the center of each specimen's results. The lengths of the vertical lines indicate the N and L initial values. They show the corrosion that took place during the joint's life prior to the Pt. Loma exposure. The N and L values plotted are the cumulative increases over these initial values.

Figure 5-3 gives the results for the two tank joints of each dogbone while Figure 5-4 presents the same data for the splice joint. Because there were two tank joints and one splice joint on each specimen, the splice joint results were doubled and plotted on Figure 5-4. Therefore, Figures 5-3 and 5-4 are comparable.

Figure 5-5 is a plot of the total number of X-ray corrosion pits and indications for each specimen as a function of exposure time. Two curves are given for each specimen. One is for the tank joints and the other for the splice joint. Initial conditions are also shown.

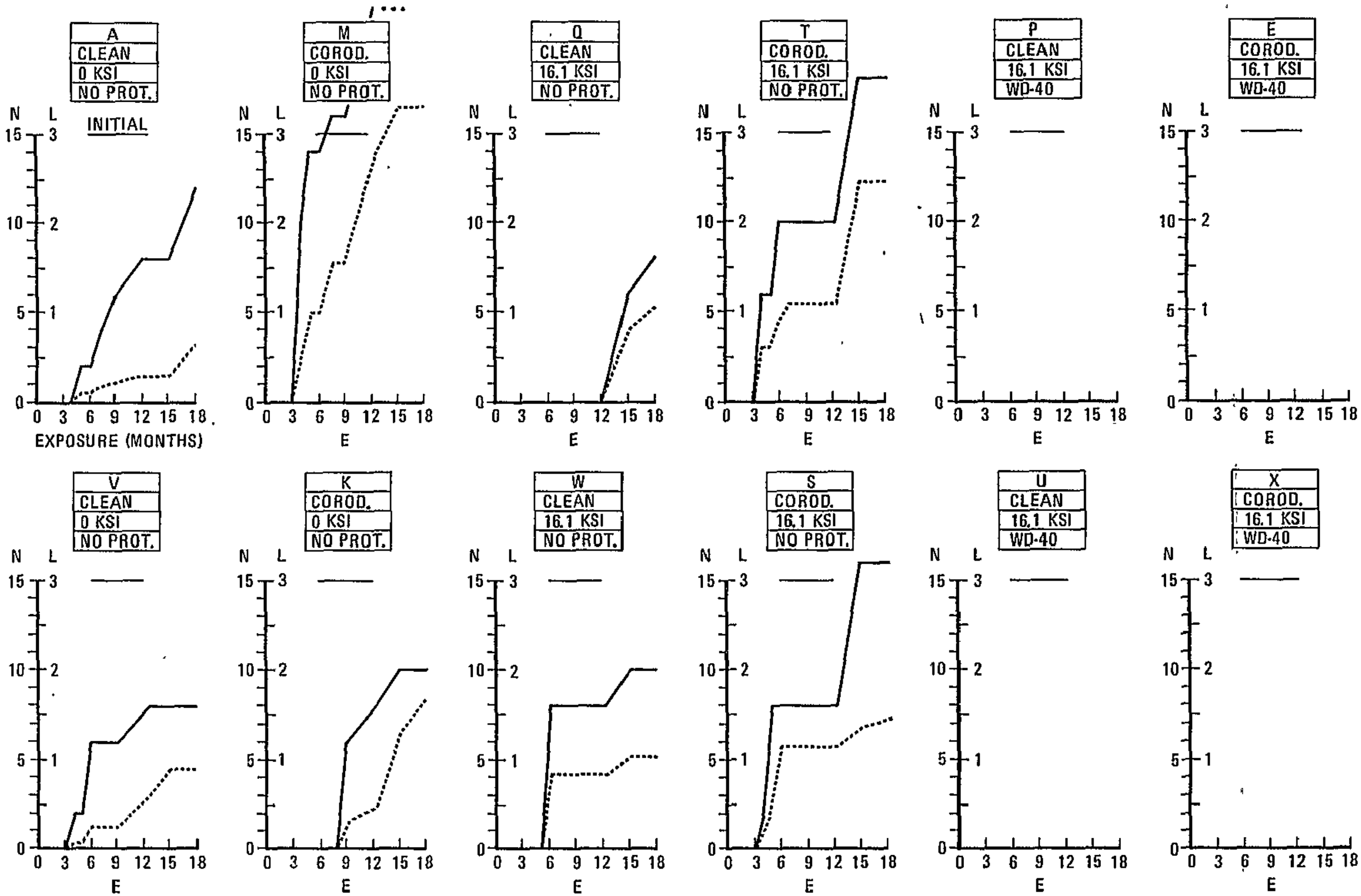

SEACOAST ENVIRONMENTAL EXPOSURE (E, MONTHS) EFFECT ON THE NUMBER (N———) AND LENGTH (L---------), (INCHES), OF X-RAY CORROSION INDICATIONS, SK671-2-138 – SPLICE JOINT (2X)

65343-14

Figure 5-4. Test Results for the Splice Joint of Each Specimen

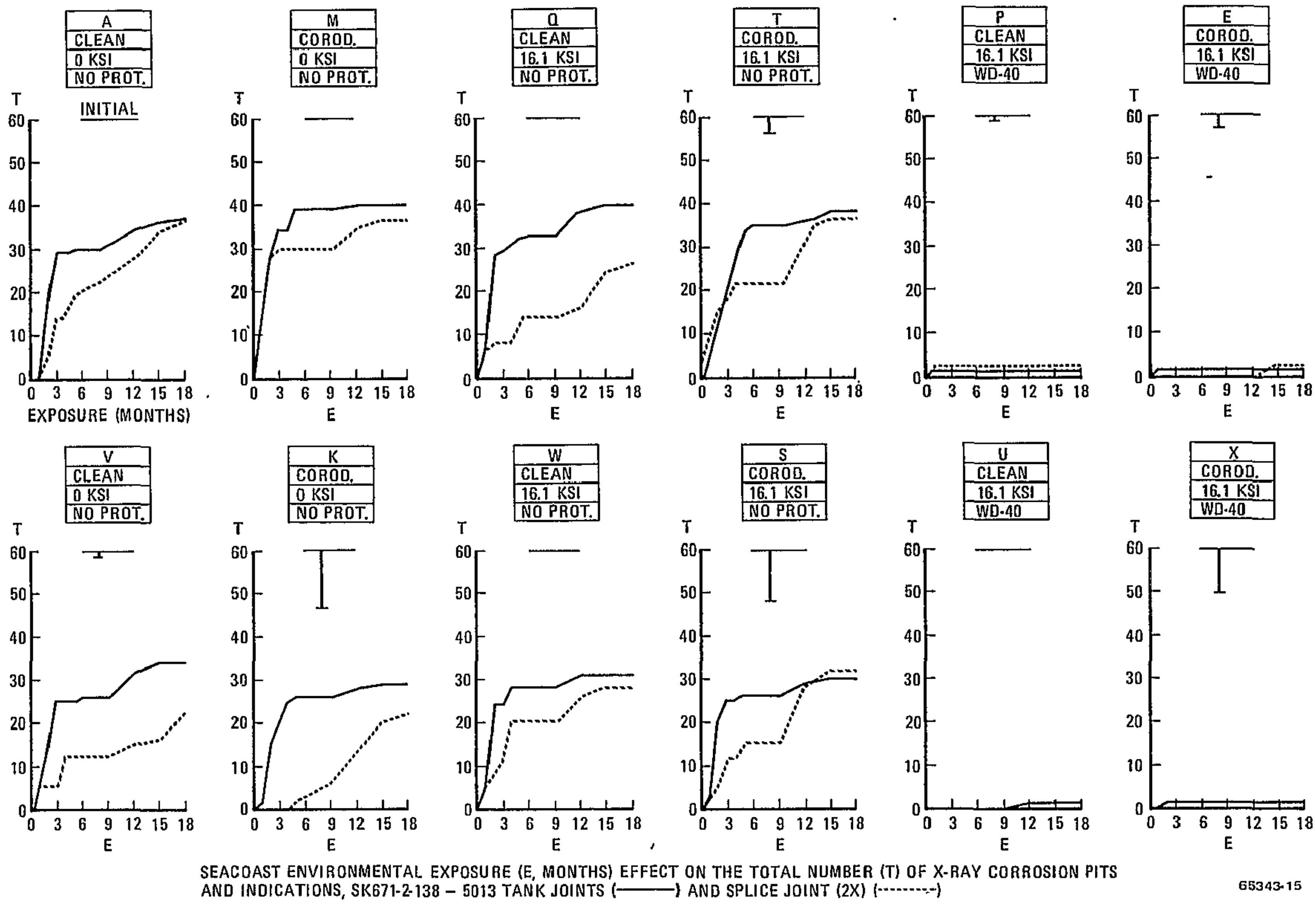

Figure 5-5. Test Results for Each Specimen as a Function of Exposure Time

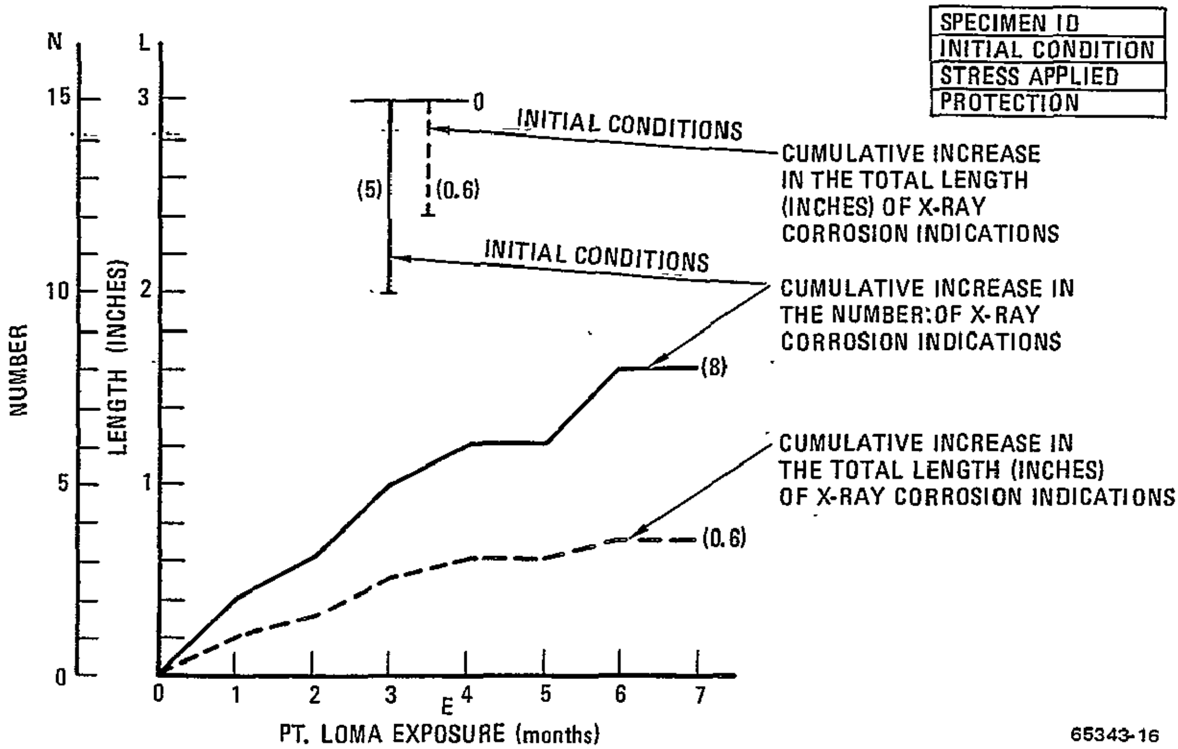

Figure 5-6. X-ray Result Figures

After the 18-month exposure test, the specimens were tested to failure either by static or fatigue loading. These results are presented in Section 4 of this report.

5.3 DISCUSSION OF TEST RESULTS

Examination of Figure 5-3 shows that, with a few exceptions not many additional corrosion indications were noted on the 5013 tank joints after a one month exposure. After two or three months, many corrosion indications were noted on all of the eight unprotected dogbones. The four specimens protected with WD-40 had essentially no attack. One indication was noted on two of the specimens. None was noted on the other two. It is interesting that one of the unaffected specimens had had significant previous corrosion. This trend continued throughout the entire 18-month exposure. No further changes were noted on the WD-40 protected specimens, while corrosion on all eight of the unprotected dogbones increased. The variables of initial condition or stress condition appeared to have no effect on the magnitude of corrosive attack.

The results of the splice joint (Figure 5-4) followed a somewhat similar pattern. It should be recalled that the splice joints were made just prior to exposure at Pt. Loma. They were made under optimum factory conditions and were initially clean and uncontaminated. The first indications of corrosion were not noted until after four or five months. Two unprotected specimens were unaffected even longer.

The four WD-40 protected specimens had no indications for their entire exposure period. It should be noted that the change of the WD-40 application period from 30 to 90 days on specimens E and X for the final nine months had no effect on the number of corrosion indications.

Figure 5-5 shows the total corrosion activity (corrosion pits and corrosion indications) during the exposure period. It can be seen that corrosion pits were observed in most cases during the first month. As exposure time increases, the total number of corrosion pits and indications becomes relatively constant. It was noted that the corrosion pits turn into indications. This levels off the totals. It is also apparent that the totals for the splice joint somewhat lag the tank joints. This is especially true during the initial and middle stages of exposure. The WD-40 specimens were essentially unaffected by the exposure. It is interesting to note that specimen E shows one or two pits after the WD-40 protection interval was changed. However, specimen U also showed a pit during this interval. Its protection was not changed. It seems that no real changes took place because of the modification of the WD-40 application.

5.4 SECTION CONCLUSIONS

1. A protective oil applied according to established procedures effectively inhibits corrosion of Atlas tank joints exposed to a marine environment. Application must be periodic and according to E.S. 0-79026.

2. Initial condition and exposure to standby pressurization stress have no effect on the corrosion.

3. Some evidence exists for concluding that the application interval may be increased from 30 to 90 days without any increase in corrosion. It is felt that more work is necessary to draw a final conclusion on this point.

4. The corrosion experienced on unprotected specimens exposed for 18 months to a natural marine environment did not reduce static or fatigue joint properties below specification requirements. (See Section 4.)

SECTION 6

5013 TANK LONG TERM ENVIRONMENTAL EXPOSURE TESTS AT EASTERN TEST RANGE (ETR)

At the same time the Pt. Loma specimens were being tested, a series of dogbone specimens was also being exposed at ETR. Most of these specimens were newly manufactured and did not represent corroded tank section joints as tested at Pt. Loma. The objectives of the ETR tests included investigation of the effect of undissolved grain boundary carbides, the application frequency of the corrosion control compound (WD-40), and the effectiveness of the compound's ability to inhibit further corrosion in previously corroded joints. This section documents the testing of the ETR dogbone specimens.

6.1 TEST PROCEDURE

The test specimens consisted of thirty-two 36- by 4-inch standard "dogbones" made from CRES 301 EH material (0-71004) with the exception that two of the specimens were made from 5013 weld joints (see Section 5). The details of the specimens are given in Convair Drawing SK671-2-120, Test Specimens — Tank Corrosion Test (Reference 12). Each specimen was made up of four 4-inch-wide standard "spot-seam-spot" overlap weld joints. The specimens were fabricated to the usual flight vehicle standards of workmanship and inspection. Figure 6-1 shows the typical specimen joints and the materials used.

The variables are shown in Table 6-1. They consisted of the amount of undissolved grain boundary carbides, the WD-40 application interval, and the stress condition (unloaded or dead weight loaded so that a constant tensile stress of 12.5 ksi was applied across the weld joint.)

The specimens were exposed in vertical chains of two specimens per chain on the fourth level of the ETR Complex 36A service tower (see Figures 6-2 and 6-3). This level is adjacent to the Atlas fuel tank. The specimens were treated periodically with WD-40 as specified in Table 6-1. They were subjected to periodic radiographic examination. The examinations were monthly for the first year and quarterly thereafter. The detailed procedure for WD-40 application and other ETR activities is documented in Convair Procedure 55-30045-BK1 "Tank Specimens Corrosion Test" — CTP-MECH-0002, dated 02 March 1976 (Reference 20).

6.2 TEST RESULTS

The effect of the marine environment on the test specimens is given in Figures 6-4, 6-5, and 6-6. All of the periodic x-ray analyses are presented by these figures. A

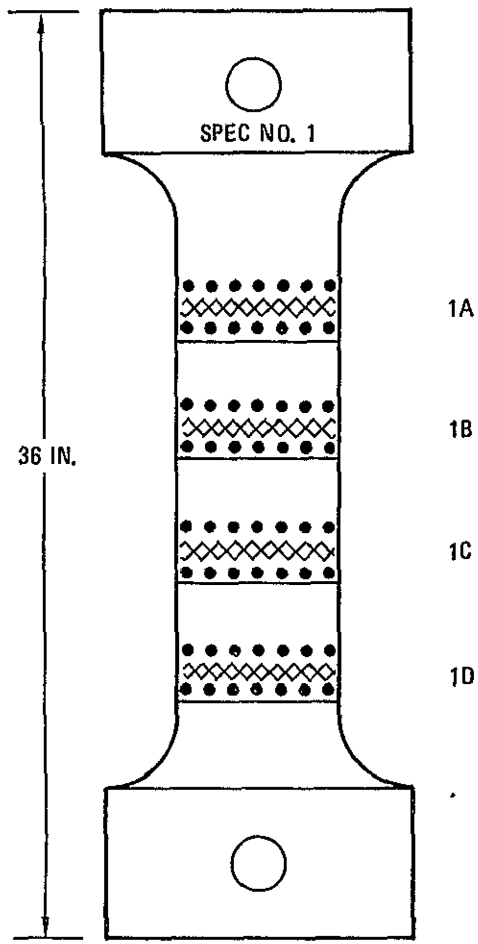

SPECIMEN NO.	GRAIN BOUNDARY CARBIDES (%)	CRES 301 EH, 0-71004 HEAT	COIL
1, 2, 3	20	298213	65329-B4
4, 5, 6	20	298213	65329-B4
7, 8, 9	20	298213	65329-B4
10, 11, 12	5	141616	94942-B
13, 14, 15	5	141616	94942-B
16, 17, 18	5	141616	94942-B
19, 20, 21	40	206831	72106-B1
22, 23, 24	40	206831	72106-B1
25, 26, 27	40	206831	72106-B1
*28	N/A	–	–
*29	N/A	–	–
30, 31, 32	20	298213	65329-B4

* THESE SPECIMENS WERE FABRICATED FROM CORRODED JOINT AREAS OF THE 5013 ATLAS TANK, WITH TWO TEST WELD JOINTS PER SPECIMEN.

65343-32

Figure 6-1. ETR Dogbone Test Specimens

Table 6-1. ETR Test Variables

Specimen No.	Grain Boundary Carbides (%)	WD-40 Application Interval	Stress Condition is 12.5 ksi Except:
1,2,3	20	None	No. 3
4,5,6	20	30 Days	6
7,8,9	20	90 Days	9
10,11,12	5	None	12
13,14,15	5	30 Days	15
16,17,18	5	90 Days	18
19,20.21	40	None	21
22,23,24	40	30 Days	24
25,26,27	40	90 Days	27
*28	N/A	None	—
*29	N/A	30 Days	—
30,31,32	20	Initial application only	32

*These specimens were fabricated from corroded joint areas of the 5013 Atlas tank, with two test weld joints per specimen.

visual examination of the specimens at the conclusion of their exposure showed some dust and red rust corrosion on the unprotected specimens. All of the WD-40 protected specimens showed no signs of corrosion.

Figure 6-4 shows the effect of the exposure on specimens that were unprotected by WD-40. With the exception of specimens 30, 31, and 32, which had WD-40 applied only when they were initially exposed, the specimens had no protection during their entire exposure.

In a manner similar to the Pt. Loma results, each test specimen is represented by a plot of X-ray results as a function of exposure time. The box near each plot contains the specimen ID, the amount of undissolved grain boundary carbides, and the stress it was subjected to during exposure. The X-axis represents the exposure time in months. The Y-axis is a double scale of N and T on one side and L on the other. N is the number of X-ray corrosion indications. A corrosion indication is a defect in

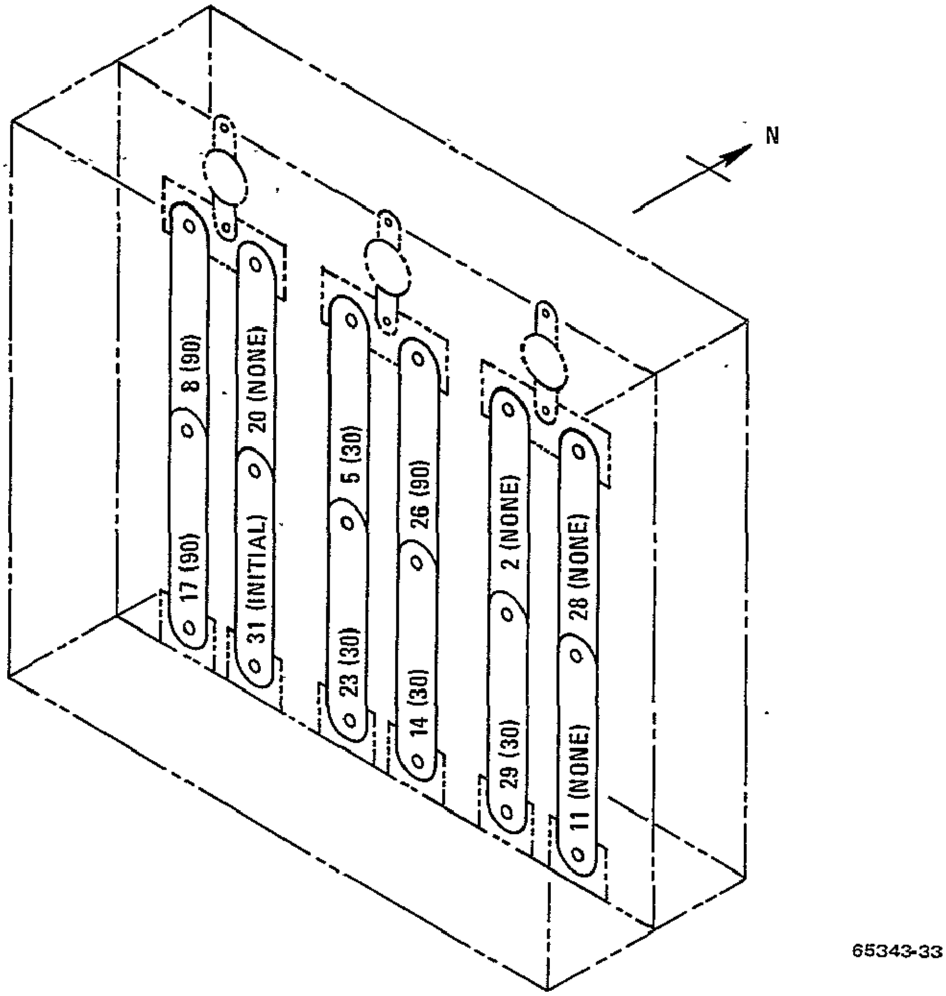

Figure 6-2. Test Fixture 1, Test Specimens Arrangement, Complex 36A Service Tower Fourth Level

the specimen joint that appears to indicate a corrosion crack. T represents the total number of X-ray corrosion pits and indications. A corrosion pit doesn't have any length. L is the total length of the corrosion indications. This terminology is consistent with that used for the Pt. Loma specimens (Section 5).

Figure 6-5 gives the results of the specimens that received WD-40 protection every 30 days.

Figure 6-6 presents the results of the specimens that received WD-40 protection every 90 days.

6.3 DISCUSSION OF TEST RESULTS

An analysis of Figure 6-4 shows that much less corrosion occurred than noted on the Pt. Loma specimens. However, the environment probably was less aggressive. The

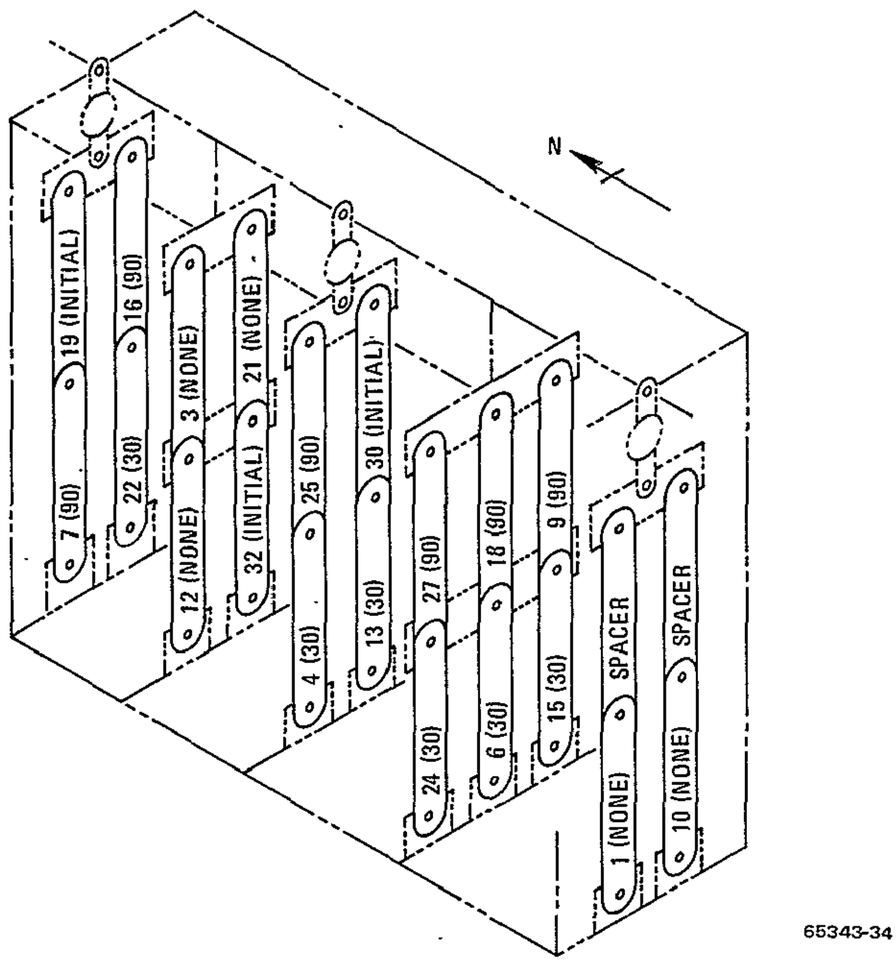

Figure 6-3. Test Fixture 2, Test Specimens Arrangement, Complex 36A Service Tower Fourth Level

ETR specimens were farther from the ocean and were somewhat protected by the service tower. This more benign environment probably also contributed to the inconsistency of results. Only about one-half of the unprotected specimens, which would have been expected to corrode, did so. The results also show that the tensile stress and percent of undissolved grain boundary carbides had little influence, if any. Studies in this program have revealed that the grain boundary carbide effect does not influence the surface. Therefore, for these exposures, it now seems logical for the percent carbides to have no influence on the results. (See Section 2, Metallurgical Analysis.) Specimen 28, which was prepared from a 5013 joint section, was also essentially unaffected by the exposure. However, it should be noted that some evidence of WD-40 was observed on this specimen during post-exposure examination. Its history, with respect to WD-40 protection, therefore, is questionable. According to the procedures it should have not seen any WD-40. Examination of the other specimens revealed no inconsistencies.

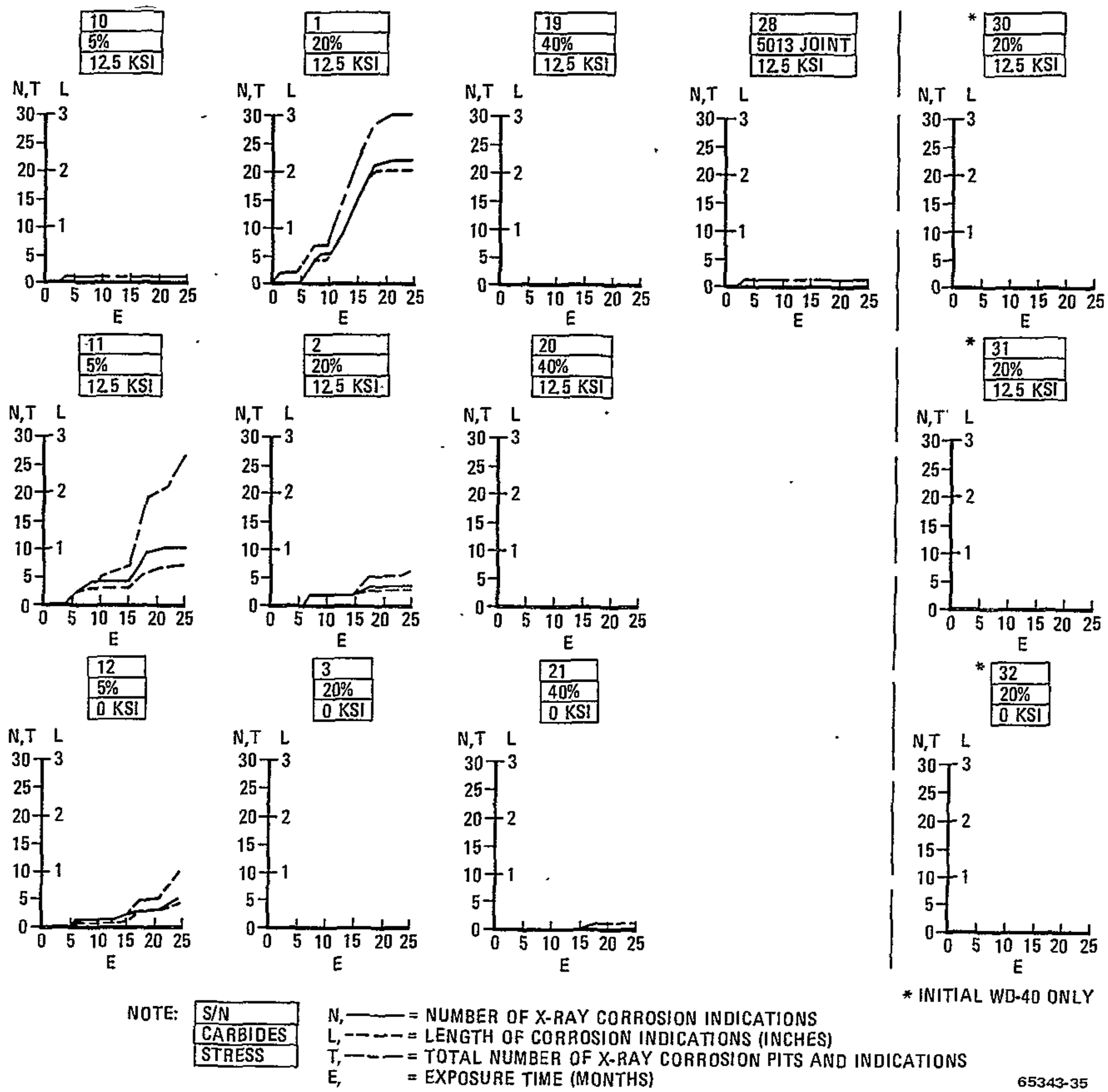

Figure 6-4. ETR Environmental Exposure Effect on Test Specimens Having No or Only Initial WD-40 Protection

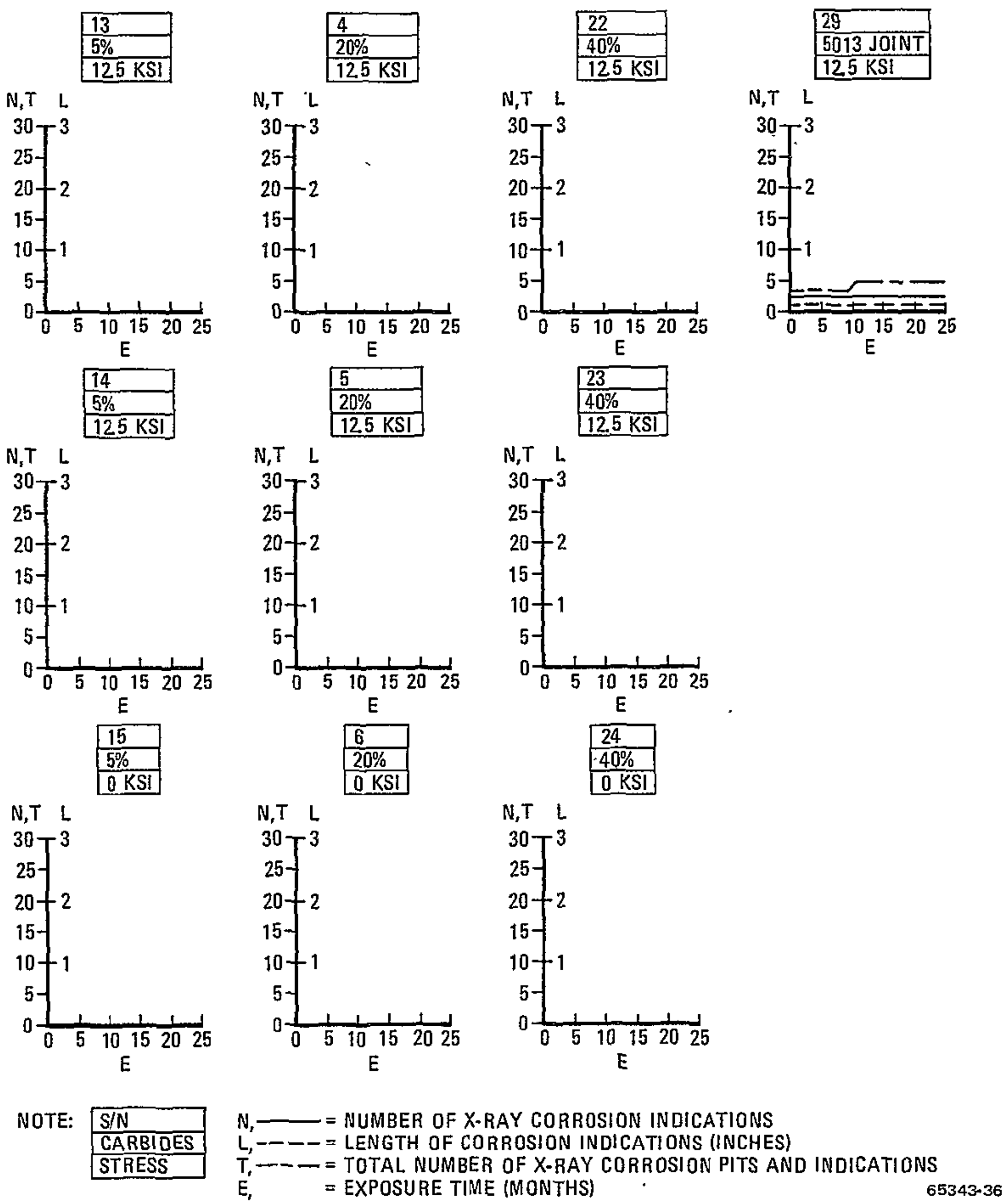

Figure 6-5. ETR Environmental Exposure Effect on Test Specimens Having WD-40 Protection Every 30 Days

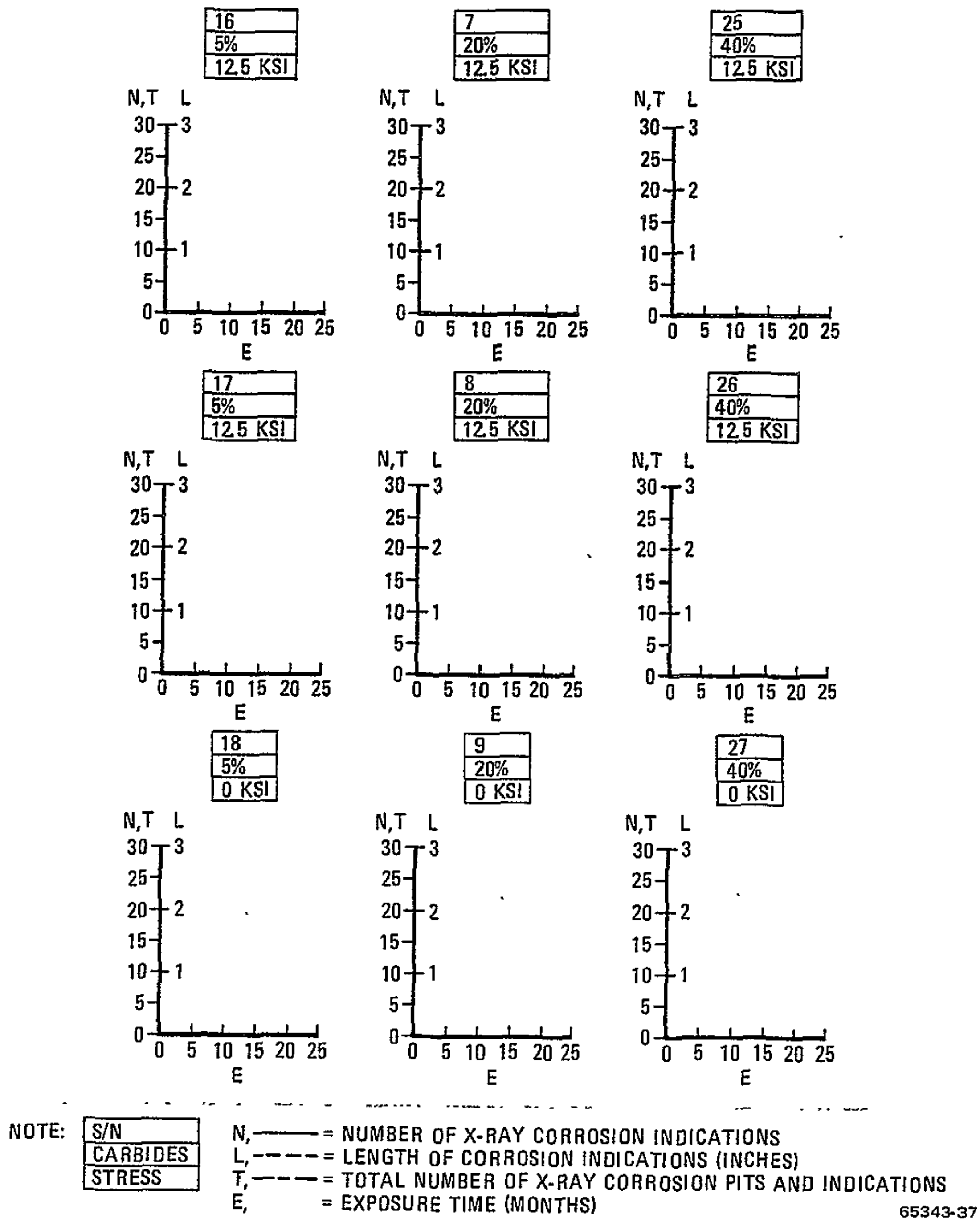

Figure 6-6. ETR Environmental Exposure Effect on Test Specimens Having WD-40 Protection Every 90 Days

The three specimens (30, 31, 32) that had only an initial application of WD-40 were completely free of defects. One could argue, however, that specimens 3, 10, 19, 20, and 21 were also essentially defect free. These specimens had no WD-40 protection. It appears that, as usual, corrosion is a statistical process and in the relatively non-corrosive environment of the service tower clear-cut results were not obtained.

Figures 6-5 and 6-6 document the results of 19 dogbone specimens that were protected either every 30 or 90 days with WD-40. Specimen 29, which was made from 5013 joints, had initial corrosion. WD-40 was effective in stopping any further significant increase in corrosion. All of the other protected specimens showed no signs of corrosion whatsoever. It is what one would expect, however, based on the Pt. Loma specimen results (Section 5). It should also be kept in mind that these WD-40 applications were made in a very controlled manner according to explicit engineering instructions. It should also be noted that the service tower environment the specimens were exposed to may be somewhat different from that experienced by a tank section. Cryogenic tanking, residue being washed onto the surface, or other unknown factors were not completely duplicated for the test specimens. Their material makeup and general exposure location were the main similarities to the 5013 tank.

6.4 SECTION CONCLUSIONS

1. Undissolved grain boundary carbides do not appear to cause significant corrosion.

2. The ETR Complex 36A service tower environment is less aggressive to dogbone test specimens than Pt. Loma.

3. The results of this ETR test showed that proper application of WD-40 either initially, every 30 days, or every 90 days provides complete protection of typical spotwelded CRES joints when exposed to a service tower environment. However, based on the results obtained on specimens with no protection, it is concluded that the test environment may have been less aggressive than could be typically expected on a tank section. Periodic application of the corrosion control compound would be prudent.

4. The corrosion control compound is effective in inhibiting further corrosion in previously corroded joints.

SECTION 7

PERSISTENCE OF CORROSION INHIBITOR WD-40

Considerable interest has been shown in persistence data for WD-40 in order to determine reasonable times for renewal.

Several direct and indirect methods were tried to determine realistic values. The following tests were performed:

7.1 TEST OBJECTIVES

a. Sampling of the 5013 tank at corroded and noncorroded areas.

b. Direct weighing of a sample of WD-40 exposed to air as a function of time and the direct weighing of a subsize joint specimen filled with WD-40.

c. Sampling of a new, full-sized (10-foot diameter) joint as a function of time.

d. Monitoring the corrosion activity of 4-inch joints in a corrosive environment, as a function of time and WD-40 treatment. The results of these last tests are reported in Sections 5 and 6. The other tests are reported here.

7.2 SAMPLING OF THE 5013 TANK

Fourteen samples such as shown in Figures 7-1 and 7-2 were submitted to infrared absorption analysis to determine the hydrocarbon content, which is related to the WD-40 content. The initial samples B and F were taken while the tank was still at ETR. The remainder were taken at Plant 19 at San Diego. Where the samples were taken from the tank is shown in Figure 7-3.

The identification, condition of the surface of specimens, and results of the WD-40 analysis are shown in Table 7-1. Sample B represents one of the most corroded areas and is shown in Figure 7-1. Sample F, shown in Figure 7-2, is typical of a noncorroded area. Further details are found in Reference 2.

A review of the data in Table 7-1 shows good correlation between rusty samples and low WD-40 and clean samples and high WD-40. Samples 3 and 5 are notable exceptions. Sample 3 was clean and had low WD-40. This could be explained by the possibility that no corrosive reached this area. Sample 5, on the other hand, measured high on WD-40 and had slight corrosion. Some rust may have been transported from an adjacent area because water marks are definite on the specimen.

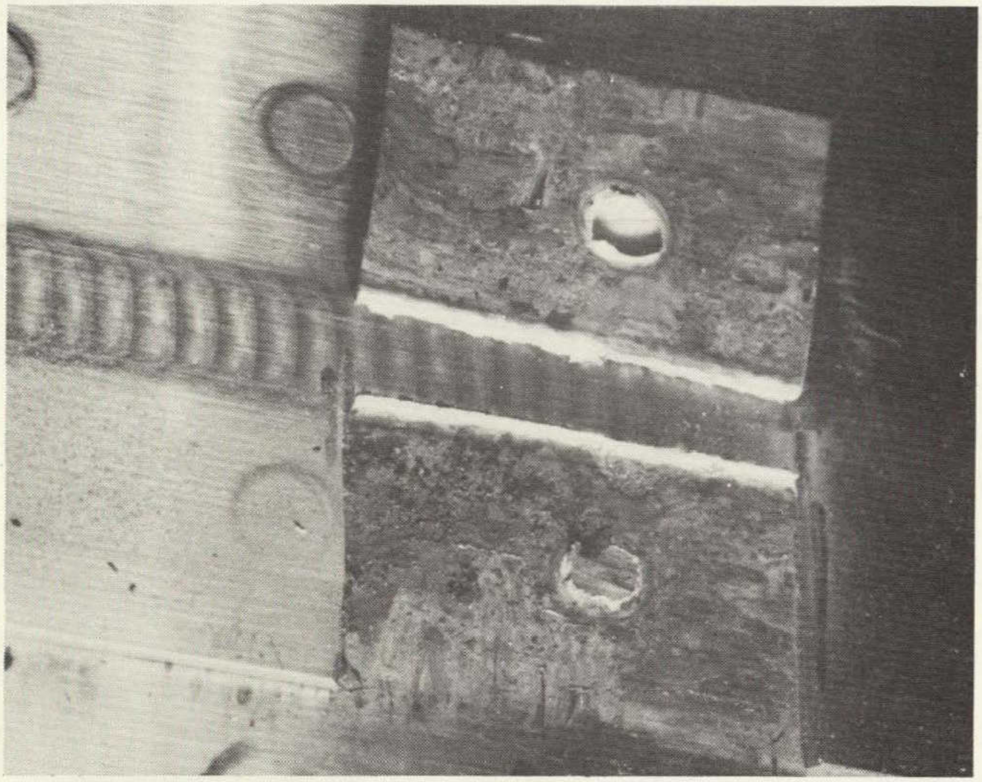

65343-18

Figure 7-1. Sample B Cut from 5013 Tank

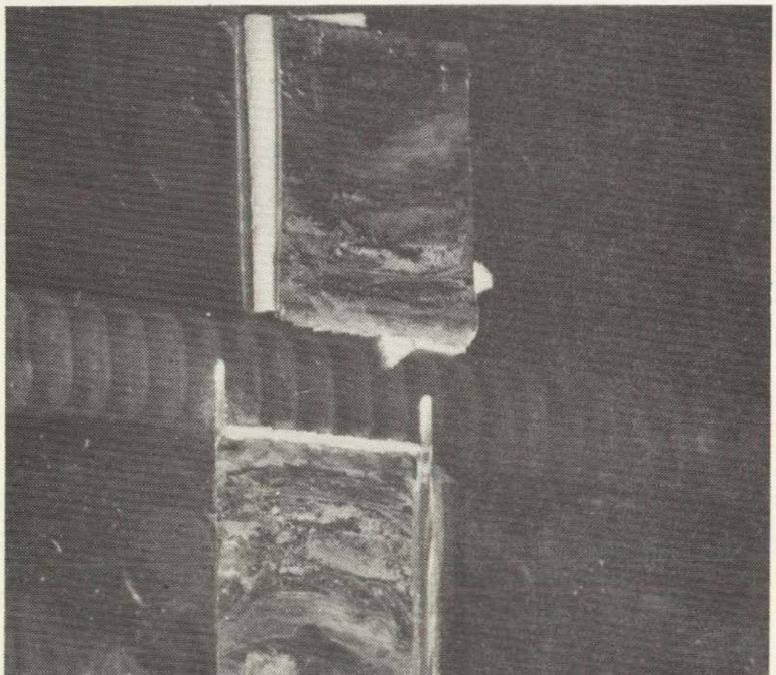

65343-19

Figure 7-2. Sample F Cut from 5013 Tank

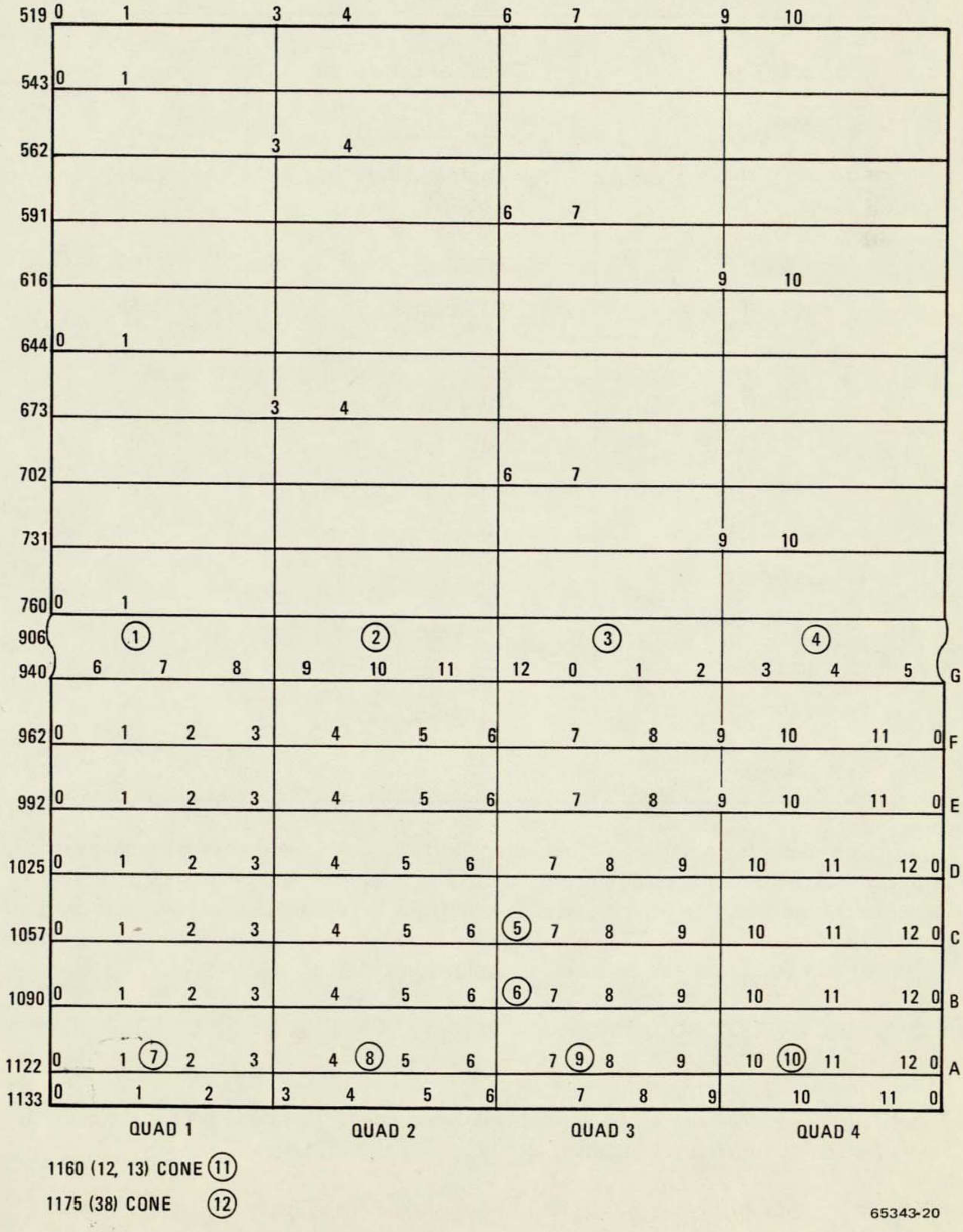

Figure 7-3. Location of Samples Taken for WD-40 Analysis

Table 7-1. Results of WD-40 Analysis of 5013 Tank Specimens

Sample No.	Surface Condition	WD-40 $\mu g/cm^2$
1 - 906Q1	sl. stain, oily	55
2 - 906Q2	stained, dry	134
3 - 906Q3	clean, dry	16
4 - 906Q4	stained, sl. oil	105
5 - 1057 (6-7)	sl. rust, dry	152
6 - 1090 (6-7)	sl. rust, sl. oil	48
7 - 1122 (1-2)	stained, sl. oil	75
8 - 1122 (4-5)	sl. stain, oily	105
9 - 1122 (8)	sl. stain, sl. oil	199
10 - 1122 (11)	clean, oily	69
11 - 1160 (12-13)	rusty, dry	5
12 - 1175 (7-8)	no rust, sl. oil	42
B - 1057 (8)	rust, dry	0.3
F - 1057 (7)	sl. rust, dry	0.8

sl. = slight

On balance these tests show: 1) that where WD-40 was found, corrosion was minimal; 2) that the WD-40 was applied erratically to the joints but had been applied at least once during the tank life in some areas; and 3) the aft conical area also suffered from inconsistent application of WD-40 to the joints, (Specimens 11 and 12); and 4) WD-40 in amounts of $50\mu g/cm^2$ in the seam prevented corrosion.

7.3 DIRECT WEIGHING OF WD-40 DURING EXPOSURE TO AIR AND IN A SUBSIZE JOINT SPECIMEN

A drop of WD-40 was placed on a clean, weighed cover glass and its weight recorded as a function of time on a ventilated automatic balance (Figure 7-4).

In a similar manner, a 3-inch section of a typical joint (Figure 7-5) was weighed, treated with WD-40, and reweighed. The loss in weight was followed as a function of time. The results of these two tests are shown by Figure 7-6.

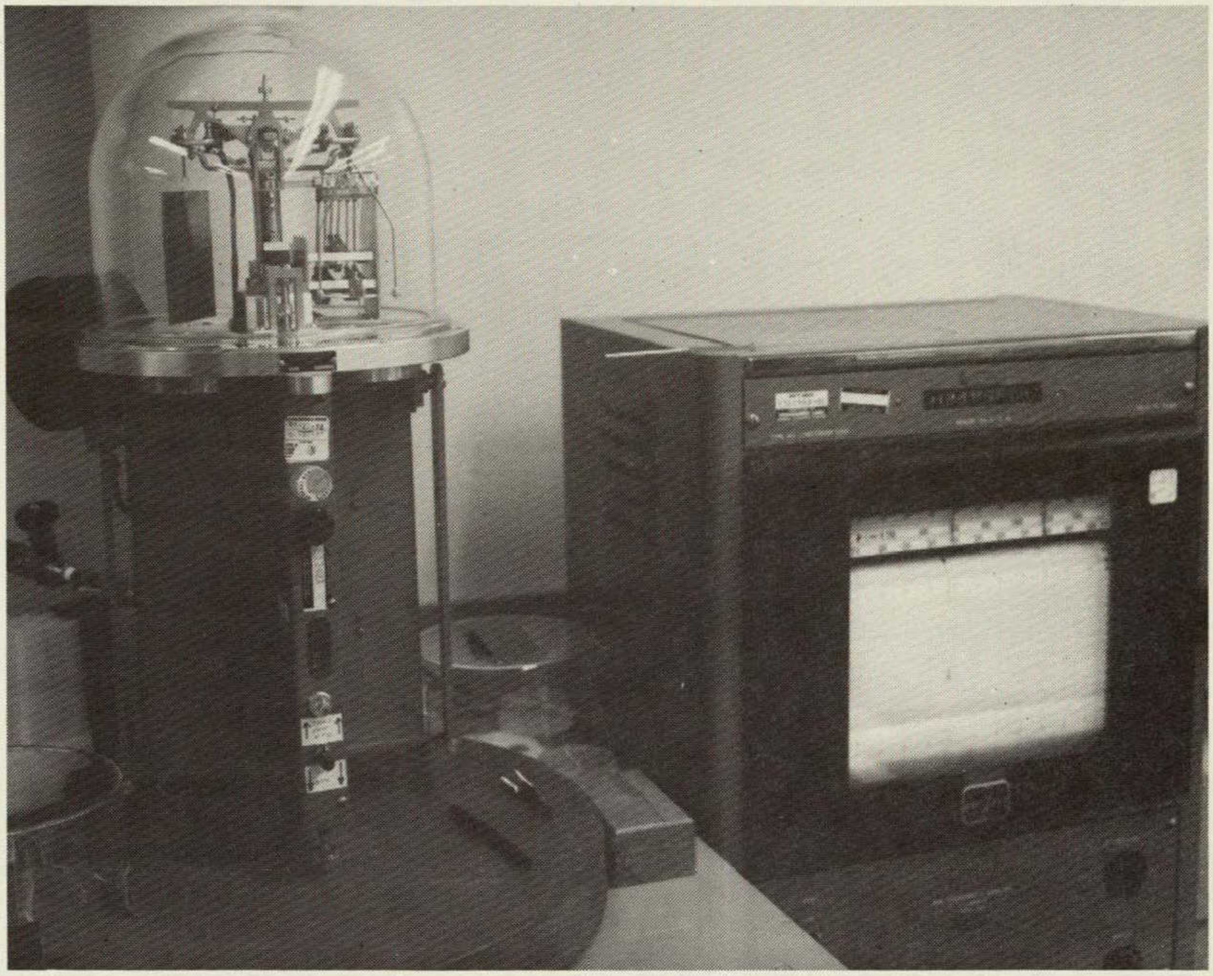
65343-21

Figure 7-4. Automatic Weighing Balance

A drop of WD-40, open to the air, loses 70% of its weight in the first hour; after this it loses only 2% in the next 30 days. This is to be expected because this is close to the vendors formulation for solvent and oil.

On the other hand, where the fluid is restricted from the air as in the joint, Figure 7-6 shows that the initial evaporation is much slower. It finally reaches equilibrium at about 30 days with 35% retained. After that, the loss is very low even out to one year. It is probable that with time the oil thickens due to air oxidation and by dust accumulation.

These direct tests, independent of variation in gap thickness or application technique, clearly show that WD-40 does not lose its effectiveness because of evaporation. Accumulation of soil or other factors may reduce its effectiveness. These factors are investigated by corrosion tests reported in Sections 5 and 6.

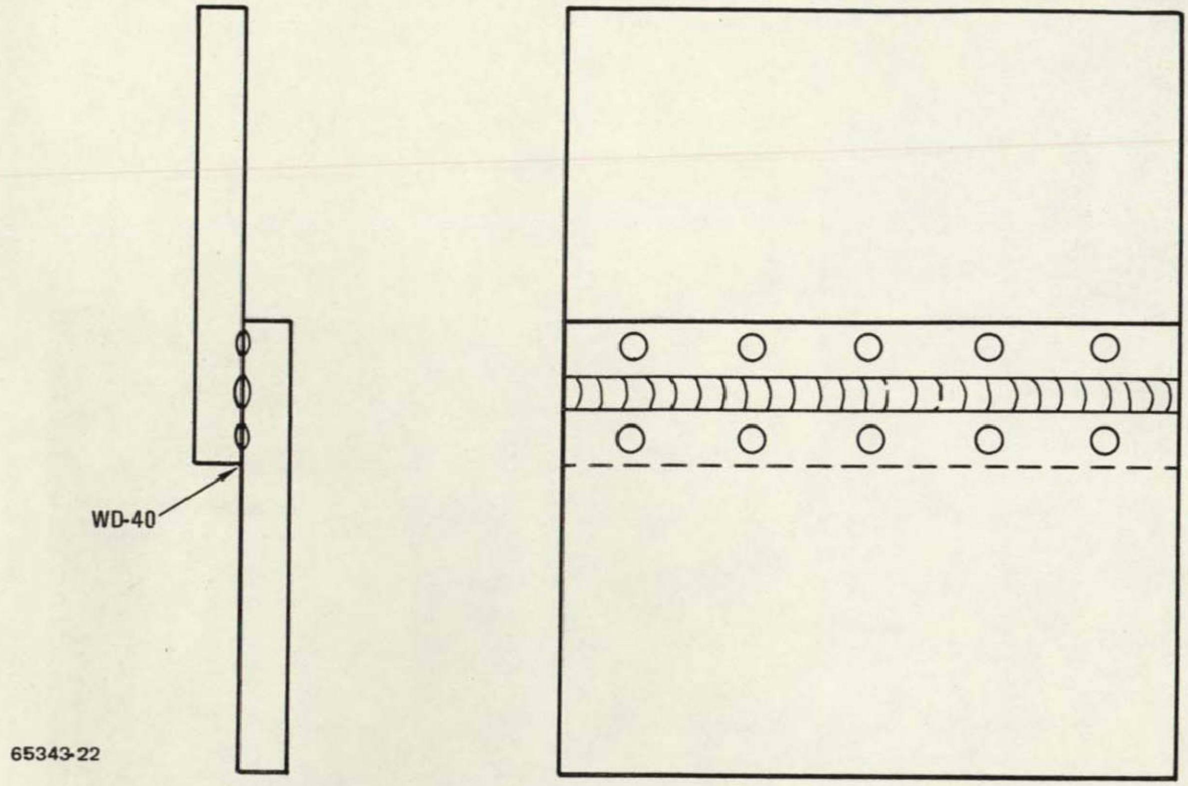

Figure 7-5. Subsize Specimen of Typical Joint

7.4 SAMPLING OF A NEW FULL-SIZED TANK JOINT AS A FUNCTION OF TIME

There was some concern that WD-40 could not be effectively applied to a full joint because there were no sides for the displaced air to escape as in the 4-inch dogbone specimens. There was also concern that repeated condensation of water on the tank would wash away the oil; consequently, a full-sized hoop containing two seams was secured from the 5013 tank (Figure 7-7) for test.

The upper interior seam was chosen for test because it had not been previously treated with WD-40, while the outside seams were questionable.

After general cleaning, the seam was treated with WD-40 according to the currently required procedure: GD/C E.S. 0-79026J (8-26-77). The seam was then divided into quadrants, and each quadrant was divided into two segments — one of which received weekly water spray. The procedure for applying moisture weekly is shown in Figure 7-8. One sample was taken from each quadrant for each condition for each time period.

The 1 by 1/2 cm samples for WD-40 analysis were removed by careful grinding as shown in Figure 7-9. The samples were taken about 10 cm apart so that the sample to be taken at the next time period would not be affected by a nearby open edge.

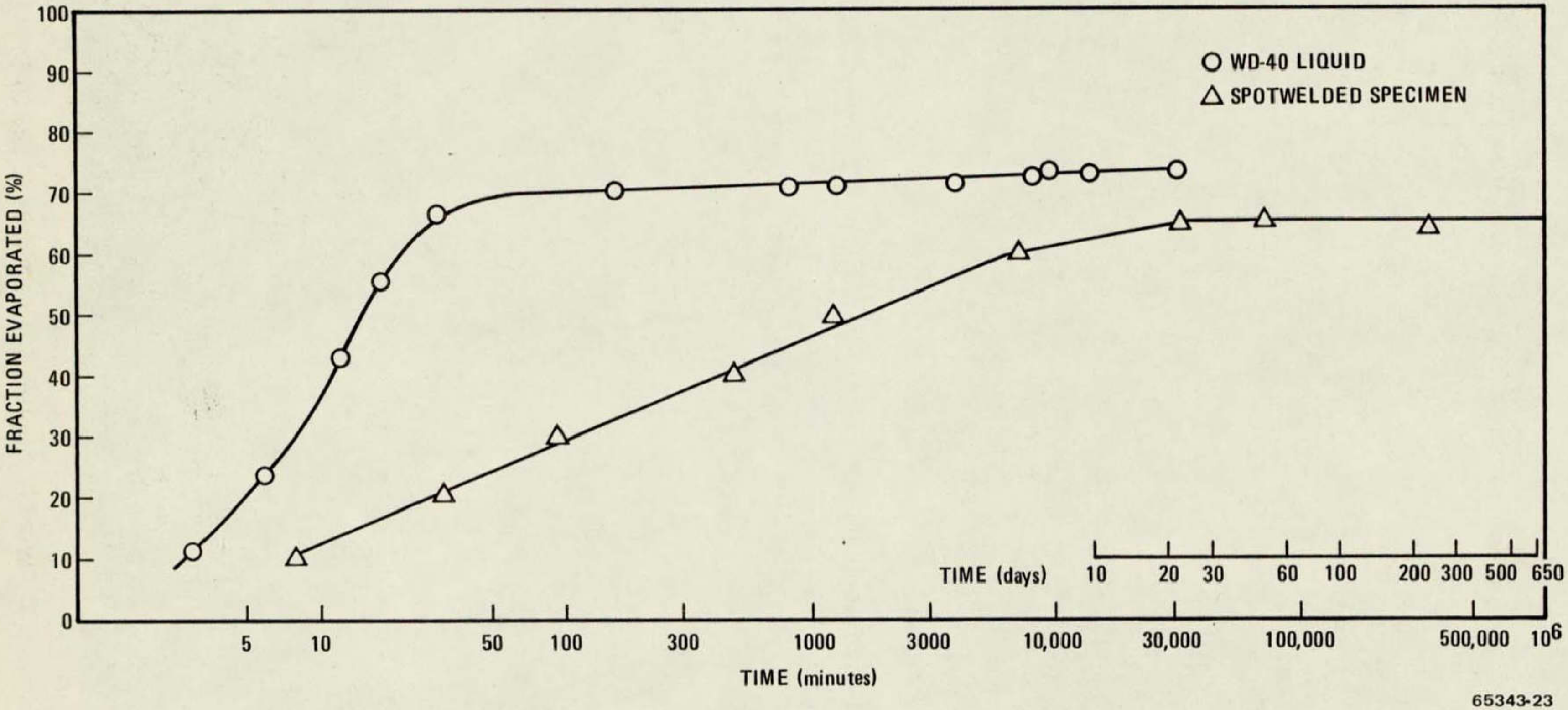

Figure 7-6. WD-40 Weight Loss as a Function of Time

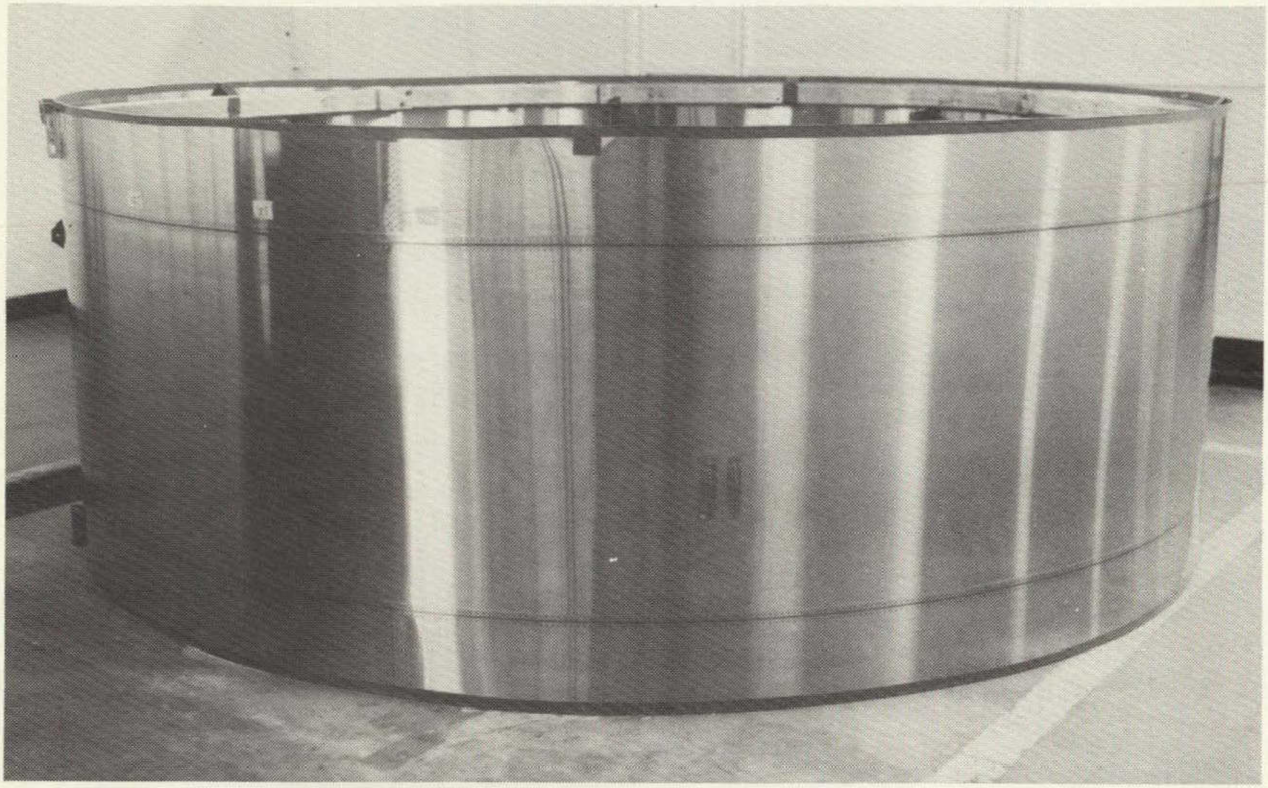

65343-24

Figure 7-7. Full-Size Hoop Section of 5013 Tank Used for WD-40 Persistence Test

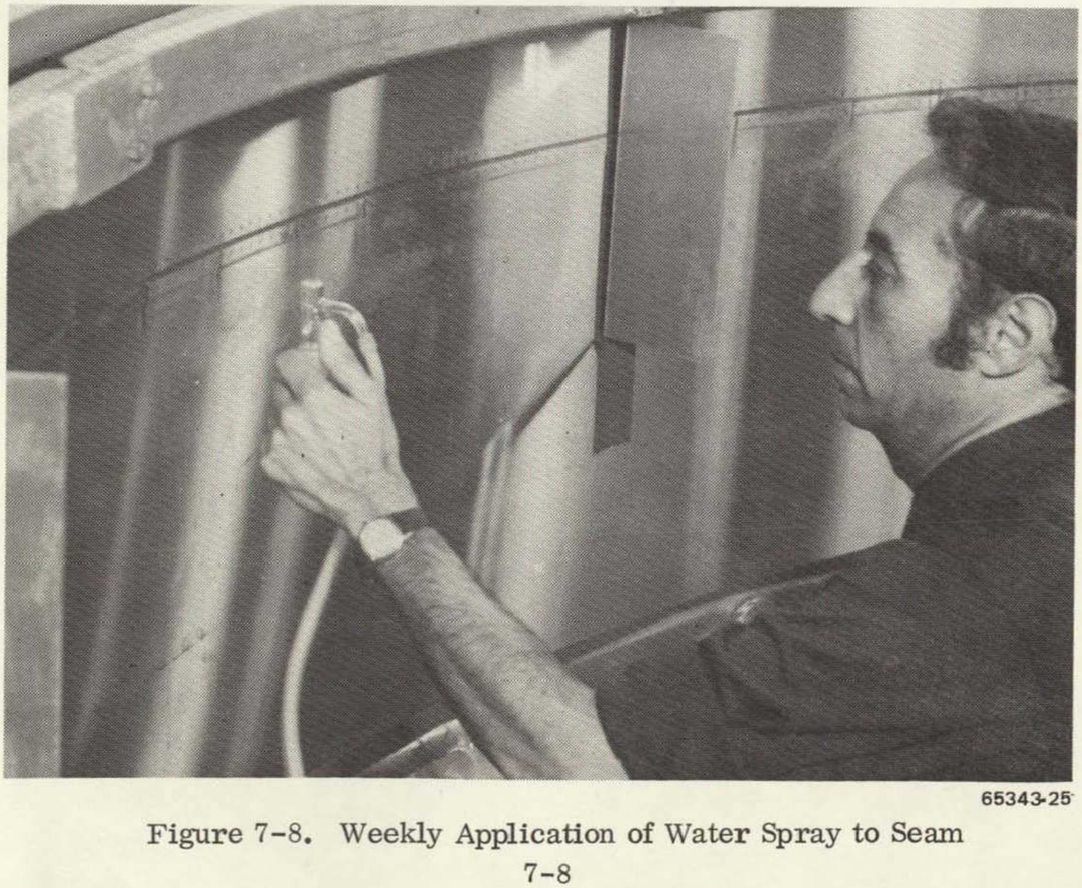

65343-25

Figure 7-8. Weekly Application of Water Spray to Seam

65343-26

Figure 7-9. Sampling Seam for WD-40 Determination

Sampling was done initially and at 1, 7, 14, 30, 60, 90, and 160 days. The residual WD-40 as a function of time, sample location, and water spray is shown in Figures 7-10 and 7-11. A study of this data shows random values for both the water-sprayed areas and nonsprayed areas. The expected gradual decrease in residual WD-40 is not apparent.

At this point, a test was performed to determine the precision of the residual WD-40 test. A thin sheet of stainless steel was uniformly coated with WD-40 to a thickness similar to the average seam results. The precision data in Figure 7-12 clearly shows that the variations in Figures 7-10 and 7-11 cannot be explained by variations in the WD-40 determination.

In a further effort to explain the data, measurements were made of the thickness and depth of the void volume of the seam as a function of the length of the seam. The void size data is plotted in Figure 7-13 in such a way that it can be compared with the residual WD-40 data as a function of position along the seam. From these comparisons the following conclusions can be drawn.

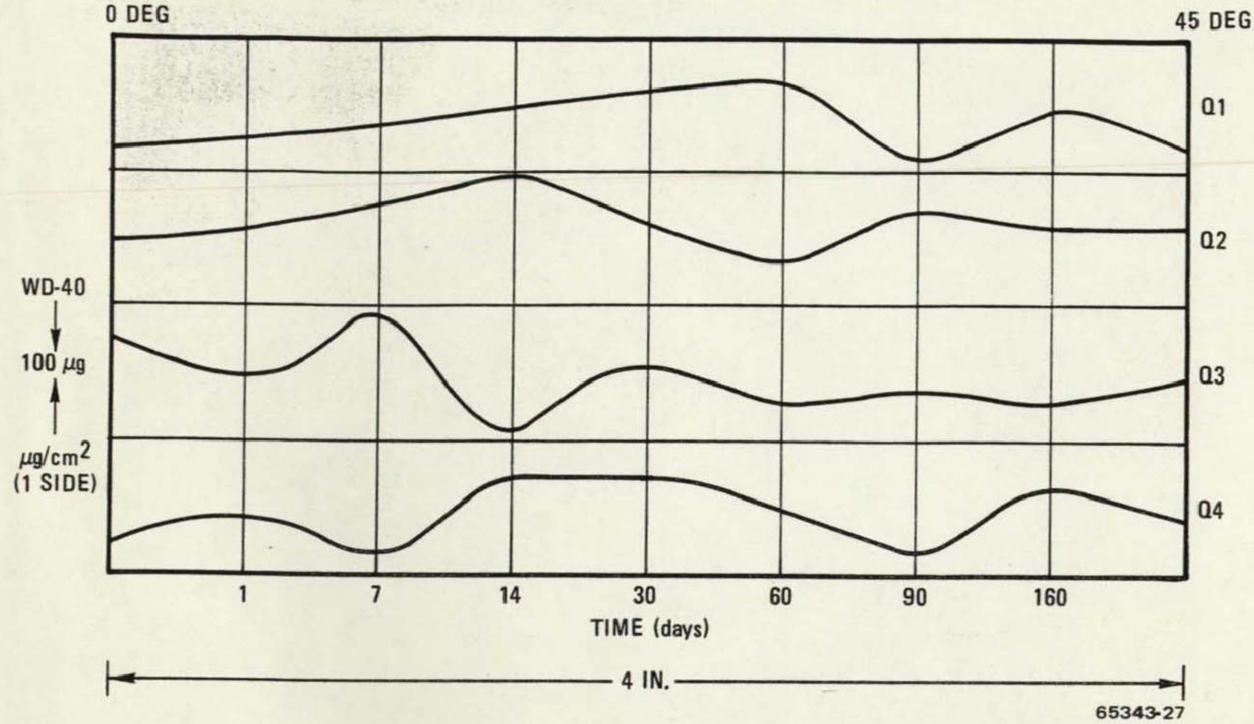

Figure 7-10. Persistence of WD-40 as a Function of Time and Sample Location (No Water)

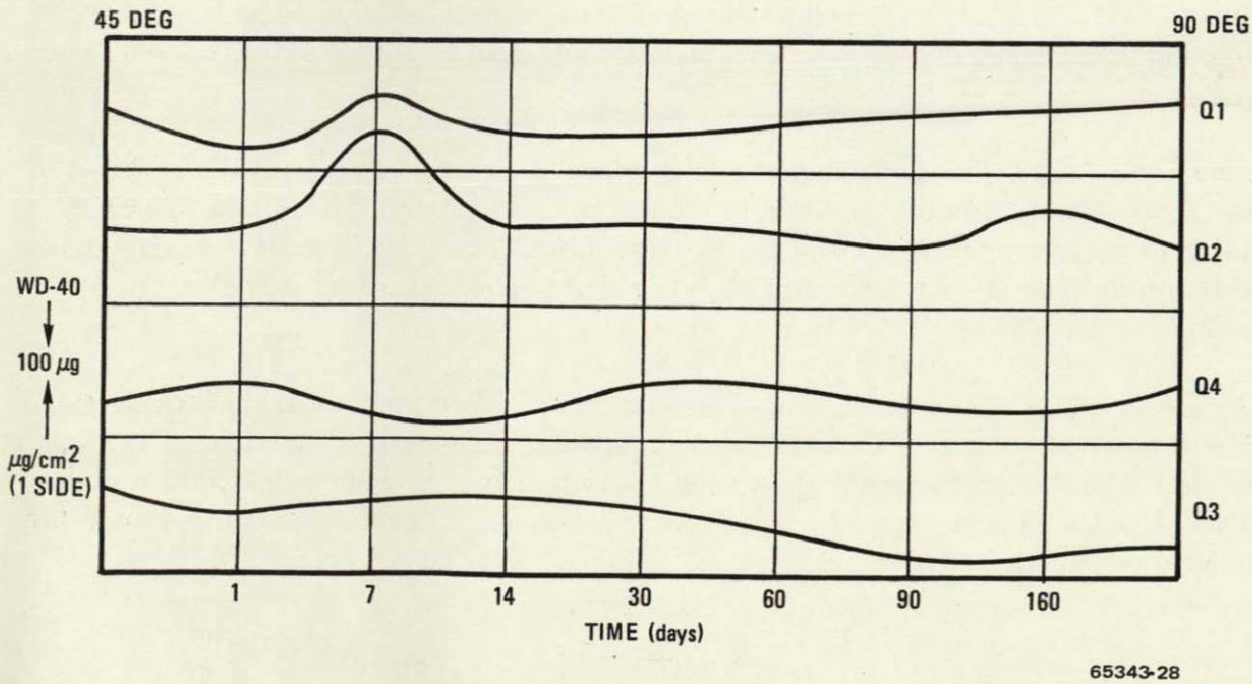

Figure 7-11. Persistence of WD-40 as a Function of Time and Sample Location (Water Spray)

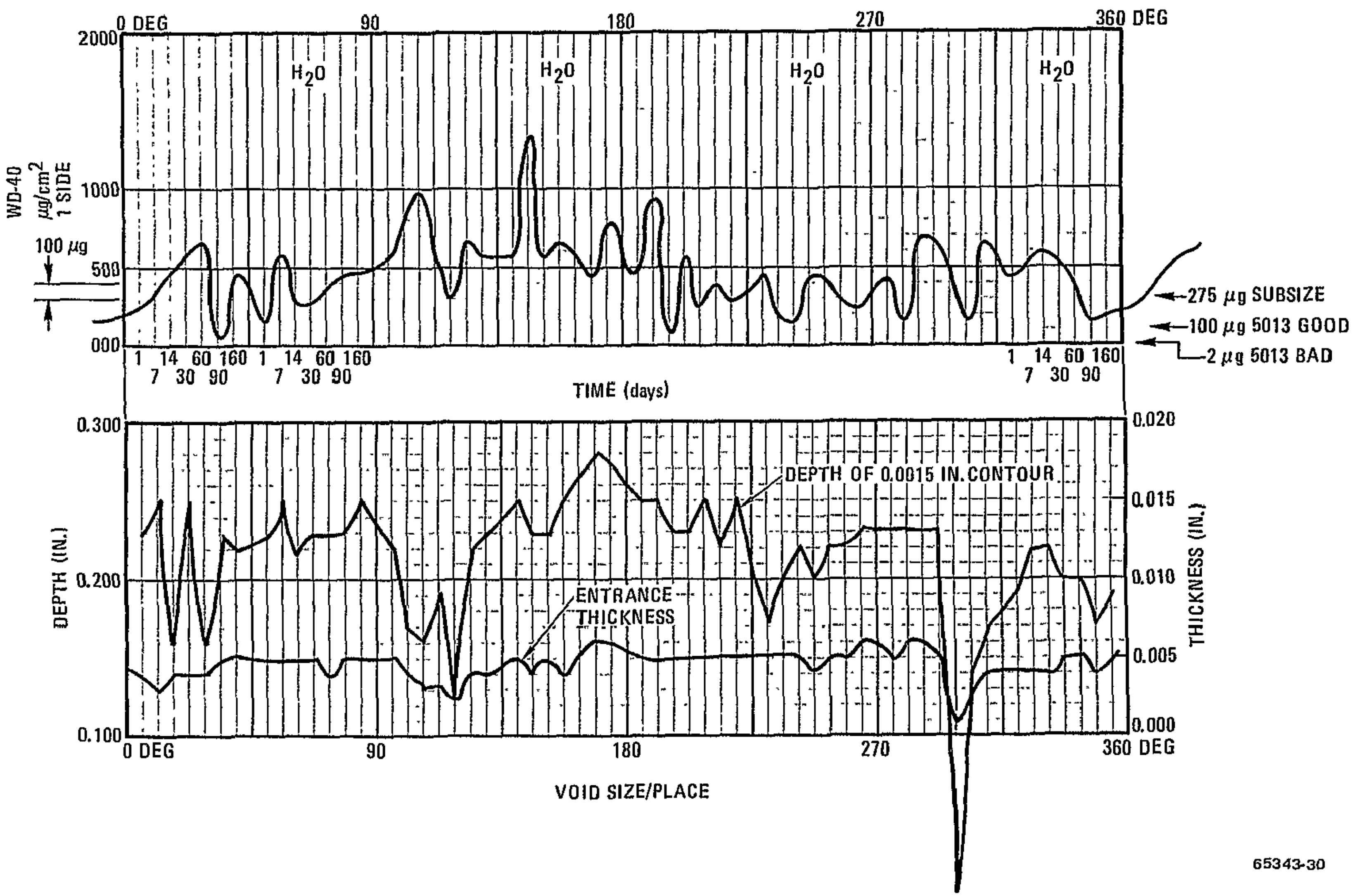

Figure 7-13. Comparison of Void Size and Residual WD-40 as a Function of Seam Length and Time

SECTION 8

DISCUSSION

A summary of all of the test results from all of the sections of this report indicates that the major objectives of the test program were satisfied.

8.1 METALLURGICAL ANALYSIS

The results of the metallurgical analysis clearly show that the leakage observed was caused by corrosion: specifically, stress corrosion that is shown to occur in a typical manner in the aft portion of the overlap joint exposed to the outside environment, around spotwelds, and near the resistance seamweld. These types are characterized by metallurgical sections and related to X-ray images for future use in interpreting radiographs.

Several peripheral discoveries were made as a result of the metallurgical analyses.

a. The existence of a surface layer of low carbide material on each side of the 301 stainless steel sheet. This may explain why nominal high carbide material seems to have about the same surface corrosion resistance as low carbide material.

b. The existence of a laminar, metal-nonmetal structure in some of the pitting corrosion observed.

c. Existence of exceptionally deep and narrow edge pitting on specimens exposed to the Pt. Loma seacoast environment. This last discovery is of no consequence as far as the Atlas/Centaur tanks are concerned because they have no exposed end grain, but it does explain why several specimens failed in the base metal rather than in the corroded joint.

8.2 CHEMICAL ANALYSIS

The chemical analysis of the corrosion products found between the faying surfaces of the joint showed the major contaminant to be sea salt and sand from the ETR area. This is consistent with the fact that unprotected type 301 EH Stainless Steel can be corroded by sea salt, especially in the presence of crevices.

The fact that unprotected specimens, exposed in the Complex 36A tower for the subsequent two years, did not corrode as badly as the 5013 tank suggests that more, or a stronger corrosive was present during the time 5013 was on the stand. Extensive chemical analysis has not found such a corrosive. Variation in yearly weather may be the answer. Another variable that might explain the mild corrosion on the ETR

dogbone specimens is the liquid-oxygen tanking that occurred near the beginning of the 5013 tank exposure (1973). If the tank had accumulated dust and sea salt, water from the frost, from the liquid-oxygen tanking, could transport the salt down across and into the seams. The test specimens did not experience this treatment. There was some evidence of condensate from normal dew running down the panels but not to the extent experienced by the tank.

8.3 MECHANICAL PROPERTIES

Both the static and fatigue strength of joints made from the 5013 tank were above engineering requirements. This indicates that the design can withstand considerable corrosion damage without jeopardizing its structural strength. The fuel leaks that resulted from the corrosion poses a problem not treated here.

Static and fatigue tests were performed on similar specimens made from the 5013 tank and further exposed to 18 months at Pt. Loma. These results also exceeded engineering requirements. There was a 12% total loss in static strength and an increase in fatigue strength. The variable nature of the fatigue data on corroded specimens when compared with the noncorroded data precludes the use of corrosion to increase fatigue strength.

8.4 PT. LOMA TESTS

The Pt. Loma tests clearly show the value of WD-40 in preventing corrosion in new specimens and arresting previous corrosion. The tests also showed that after a year of monthly application of WD-40, no new corrosion appeared upon going to a 90 day application schedule.

8.5 ETR TESTS

The exposure of dogbone specimens, made from new material, at ETR for two years did not show nearly the corrosion that was experienced by the 5013 tank. The corrosion that did occur was only on unprotected specimens. This supported the Pt. Loma results that WD-40 is effective in preventing corrosion of stainless steel joints. This data would indicate that even initial application of the WD-40 is adequate for two-year protection. The fact that some of the controls without WD-40 did not corrode detracts from the validity of this result.

The corrosion of the specimens representing various amounts of undissolved carbides was random in nature and could not be correlated. This fits with the fact that there is a surface layer of zero undissolved carbide on all specimens regardless of the internal carbide level.

8.6 WD-40 PERSISTENCE TESTS

Direct weighing of a typical WD-40 treated joint specimen as a function of time gave the best results for the persistence of the fluid in the joint. After the loss of the solvent, the remaining 35% of the WD-40 remains in the joint. Direct chemical analysis of the joints on 5013 indicated very low WD-40 levels where corrosion occurred. Higher levels were recorded where there was no corrosion.

The full scale joint test showed that the amount of WD-40 in a joint varied as the void volume and was not appreciably reduced by time or simulated condensate running over the seam.

SECTION 9

CONCLUSIONS

Detailed conclusions are at the end of each section. Conclusions that answer the initial objectives of the program are summarized here.

PHASE I

1. Radiographic, metallographic, and chemical analysis data were obtained that clearly show the corrosion defects observed to be due to pitting and stress corrosion cracking caused by the intrusion of sea salt, a humid environment, and residual welding stresses in a overlapping crevice joint.

2. After the evaporation of solvent the remaining 35% of WD-40 remains in the Atlas/Centaur seams and does not evaporate.

3. The static and fatigue properties of the corroded weld joints were determined and found to be above engineering requirements.

4. Extensive tests have shown WD-40 to be effective in preventing corrosion in Atlas/Centaur welded joints for over 18 months in a seacoast environment. They also show that WD-40 arrests previously initiated corrosion for over 18 months (Pt. Loma Tests).

5. The correlation between nine categories of defect images in radiographs with metallographic sectional evidence in resistance-welded, overlap joints in cold-worked 301 stainless steel sheet has been accomplished and is documented photographically in Figures 2-6 through 2-37. This group of photographs is considered to be a Standard, enabling improved interpretation of radiographs of similar material and joint configuration.

PHASE II ETR TESTS

1. The degree of undissolved carbide appears to have no effect on typical joint specimens, but the lack of significant corrosion on control specimens does not validate the data.

2. WD-40 appeared to give protection at initial, 30-day or 90-day application; however, again the control specimens did not corrode appreciably.

3. No further significant corrosion occurs on corroded specimens treated with WD-40 and exposed at ETR. The corroded control specimen also did not

develop significant additional corrosion. The Pt. Loma tests, however, show conclusively the effectiveness of WD-40 in preventing further corrosion of precorroded specimens.

SECTION 10

RECOMMENDATIONS

1. Based upon the results of this program it is recommended that the current corrosion protection requirements as outlined in Engineering Specification 0-79026J be continued without any relaxation for Atlas/Centaur vehicles.

2. Emphasis should be placed on the uniform application of WD-40 to the joints that are subsequently covered thus preventing renewal of the coating.

3. Specimens exposed at ETR on Complex 36A corroded only to a limited degree. As a result, definitive data on the required frequency of application of WD-40 and the effect of high undissolved carbides was not obtained. These specimens are available for continued test. It is recommended that they be exposed at Pt. Loma, unloaded, until meaningful data can be obtained.

4. The effect of hoop loads on the corrosion defects was not investigated. Metallurgical Specimen No. 3, containing defects which yielded slightly due to tanking loads, is available for static tensile or fatigue tests. This type of defect is shown in Figure 2-32.

   It is recommended that a specimen be designed and prepared from this material to determine the fatigue life of this type of defect at expected hoop loads.

SECTION 11

REFERENCES

1. "AC-33 Atlas Fuel Tank Leakage Investigation," General Dynamics Convair Aerospace Division Sales Order, Ref TD 094-105, 2 January 1975, p. 1.

2. D. D. Stenger, D-1 Centaur Unified Test Plan, GDC-BNZ69-007, General Dynamics Convair Division, 11 April 1975, Section 3.21.4.

3. Atlas 5013 (AC-33) Fuel Tank Leak Investigation, General Dynamics Convair Division, 13 November 1974.

4. NASA Malfunction Investigation Staff, MIS-064-74, 14 November 1974.

5. NASA Malfunction Investigation Staff, MIS-082-74, 10 February 1975.

6. W. M. Sutherland, Chemical Analysis of Corrosion Deposits Found Between the Faying Surfaces of Joints in Atlas Vehicle 5013, Report 643-3-75-12, General Dynamics Convair Division, March 1975.

7. James A. Crush, Radiographic Results Atlas Tank 5013, Revision No. 1, General Dynamics Convair Division, August 1975.

8. W. M. Sutherland, "Interim Status Report for Centaur 5013 Corrosion Investigation, Phase I," 631-2-76-51, General Dynamics Convair Division, 29 June 1976.

9. Corrosion Test Program Status Review, General Dynamics Convair Division, 17 January 1977.

10. G. W. Norris, "Modifications to Corrosion Procedures and Testing," Engineering Review Board Report, 670-0-77-ERB-415, General Dynamics Convair Division, 28 January 1977.

11. "Test Specimen - Corroded Tank," Drawing No. SK671-2-138, General Dynamics Convair Division, 11 November 1975.

12. "Test Specimen Tank Corrosion Test," Drawing No. SK671-2-120, General Dynamics Convair Division.

13. B. Floyd Brown, "Report to Lewis Research Center, March 22, 1975," General Dynamics Convair Division, 22 March 1975.

14. A. Hurlich, Memo to G. W. Norris, Reply to Report by B. Floyd Brown (Ref. 13), General Dynamics Convair Division, 2 May 1975.

15. B. Floyd Brown, "Second Interim Report on Corrosion," General Dynamics Convair Division, 10 May 1975.

16. G. W. Norris, Memo to R. H. Thomas entitled "Reply to Second Interim Report on Corrosion to Lewis Research Center by B. Floyd Brown, dated 10 May 1975," General Dynamics Convair Division, 16 September 1975.

17. W. M. Sutherland, The Effect of Corrosion on the Static and Fatigue Strength of Spotwelded Steel Joints at Cryogenic Temperatures, Memo ZZL-66-011, General Dynamics Convair Division, 22 April 1966.

18. Test Evaluation, Centaur Tank Corrosion Tests and X-Rays, GD/C-BNZ65-032, General Dynamics Convair Division, 1 August 1965.

19. L. D. Girton and C. J. Kropp, Metallurgical and Repair Weld Investigation Conducted on Defects in the Heat-Affected-Zones of Resistance Spotwelds in Centaur Aft Bulkhead, IR 816461, Memo ZZL-64-032, AR-504-1-535, General Dynamics Convair Division, 1 September 1964.

20. Tank Specimens Corrosion Test, Convair Procedure 55-30045-BK1, CTP-MECH-0002, 2 March 1976.

21. W. E. Witzell, Fracture Considerations for IUS Centaur, Memo M-39, General Dynamics Convair Division, 26 February 1975.

GENERAL DYNAMICS

Convair Division